NASA CONTRACTOR REPORT

NASA CR-62087

GEOS-II C-BAND SYSTEM PROJECT FINAL REPORT C-BAND RADARS AND THEIR USE ON THE GEOS-II PROJECT

STUDIES PERFORMED UNDER CONTRACTS NAS6-1467 AND NAS6-1628

By:
Wolf Research and Development Corporation
Range Engineering Department
Pocomoke City, Maryland
And:
RCA, Government and Commercial Systems
Missile and Surface Radar Division
Moorestown, New Jersey

Prepared for:
NATIONAL AERONAUTICS AND SPACE ADMINISTRATION
WALLOPS STATION
WALLOPS ISLAND, VIRGINIA 23337

October 1972

GEOS-II C-BAND
SYSTEM PROJECT

FINAL REPORT

C-BAND RADARS AND THEIR USE ON THE GEOS-II PROJECT

STUDIES PERFORMED
FOR
NASA/WALLOPS STATION
UNDER
CONTRACTS NAS6-1467 AND NAS6-1628
NASA Technical Monitor - H.R. Stanley

BY

WOLF RESEARCH AND DEVELOPMENT CORPORATION
Range Engineering Department
Pocomoke City, Maryland

and

RCA, GOVERNMENT & COMMERCIAL SYSTEMS
Missile and Surface Radar Division
Moorestown, New Jersey

October 1972

TABLE OF CONTENTS

1.0 INTRODUCTION 1

2.0 C-BAND RADAR PREPARATION FOR GEOS-II 4

2.1 ERROR MODEL DEVELOPMENT 4

2.1.1 Error Model Format 5
2.1.2 Real Time Data Correction Assumptions 14
2.1.3 Error Model Limitations 15

2.2 DEVELOPMENT OF CALIBRATION PROCEDURES 16

2.2.1 Mission By Mission Calibrations 17
2.2.2 Periodic C-Band Radar Calibrations 19

2.3 ESTABLISHMENT OF RADAR OPERATING PARAMETERS 20

2.3.1 General Operating Procedures 21
2.3.2 Servo Bandwidth Considerations 25

3.0 RADAR ERROR INVESTIGATIONS PERFORMED DURING THE PROGRAM 38

3.1 ANGLE ERROR INVESTIGATIONS 39

3.1.1 Pedestal Leveling Error 39
3.1.2 Boresight Null Shift Error 41
3.1.3 Dynamic Lag Angle Investigation 43
3.1.4 Use of GEOS as an Azimuth Calibration Aid 47
3.1.5 Elevation Angle Errors 47

3.2 RANGE ERROR INVESTIGATIONS 48

3.2.1 Effects of Miscellaneous Radar Operating Parameters 50
3.2.2 Range Zero Set Drift Effects 51
3.2.3 Range Calibration Atmospheric Propagation Error 54

TABLE OF CONTENTS (Continued)

	3.2.4	Reference Range Target Size Error	55
	3.2.5	Range Dynamic Lag Error	60
	3.2.6	Pulsewidth/Bandwidth Mismatch Error	61
	3.2.7	Track Propagation and Transit Time Range Error Corrections	71
	3.2.8	Beacon Delay Errors	73
	3.2.9	Summary of Range Error Computation/ Measurements	87
3.3	C-BAND RANGE RATE INVESTIGATIONS		88
4.0	SPECIAL GEOS-II TRACKING TESTS		93
4.1	SPECIAL TESTS - TEST PROCEDURES		94
4.2	SPECIAL TESTS - RESULTS		95
	4.2.1	Transponder Switching Results	95
	4.2.2	Polarization Sensitivity Test	95
	4.2.3	Angle Calibration Test	101
	4.2.4	Lag Angle Error Test	102
	4.2.5	Normal-Plunge Calibration Test	102
	4.2.6	Parameter Variations Tests	103
5.0	GEOS RELATED DEVELOPMENT PROGRAMS		120
5.1	LASER/MIPIR INTEGRATION AND LOOP LASER TRACKER		120
5.2	PASSIVE RADAR ENHANCEMENT DEVICES		123
6.0	SUMMARY AND RECOMMENDATIONS		127
	BIBLIOGRAPHY		131
	APPENDIX A	SPECIAL RADAR TEST PROCEDURES	A-1

LIST OF FIGURES

FIGURE		PAGE
1	FLOW DIAGRAM OF THE ERROR CORRECTION PROGRAM	13
2	TYPICAL GEOS-II RANGE VS TIME	27
3	TYPICAL RANGE RATE VS TIME	27-A
4	TYPICAL GEOS-B $\dot{A}$ VS TIME	28
5	TYPICAL GEOS-II $\ddot{A}$ VS TIME	29
6	TYPICAL GEOS-B $\dot{E}$ VS TIME	30
7	TYPICAL GEOS-B $\ddot{E}$ VS TIME	31
8	AZIMUTH DYNAMIC LAG ERROR FOR TYPICAL 79° ELEVATION GEOS-II PASS	32
9	AZIMUTH DYNAMIC LAG ERROR VS TIME FOR TYPICAL 55° ELEVATION GEOS-B PASS	33
10	ELEVATION DYNAMIC LAG ERROR FOR TYPICAL 79° ELEVATION GEOS-II PASS	35
11	AZIMUTH LAG ERROR FOR TEST NO. 24	46
12	ELAPSED TIME FROM RADAR TURN-ON (HOURS) RANGE DRIFT OF DIRAM	53
13	SIMPLE PULSEWIDTH EFFECT MODEL	63
14	EFFECTS OF MATCHED FILTER OPERATION	64
15	FILTERED PULSE RELATIONSHIP FOR $B\tau > 1.0$	66
16	FILTERED PULSE RELATIONSHIP FOR $B\tau < 1.0$	69
17	DELAY CURVE - SHORT DELAY TRANSPONDER SN*5 (BEACON 1)	75
18	DELAY CURVE - LONG DELAY TRANSPONDER SN*6 (BEACON 2)	

LIST OF FIGURES (CONTD.)

FIGURE		PAGE
19	RECEIVED SIGNAL STRENGTH VS RANGE	76
20	AN/FPQ-6 SKIN/BEACON #1 RANGE RESIDUALS DIFFERENCES	78
21	AN/FPQ-6 SKIN/BEACON #2 RANGE RESIDUAL DIFFERENCES	
22(a)	AN/FPQ-6 RANGE RESIDUALS FOR SPECIAL TEST A	96
22(b)	AN FPS-16 RANGE RESIDUALS FOR SPECIAL TEST A	97
23	RANGE RESIDUALS FOR TEST B (POLARIZATION SWITCHING)	98
24	AGC DATA FOR TEST B	100
25	VARIATION OF PARAMETERS TEST FOR AN/FPQ-6 TRACK OF BEACON #1	114
26	VARIATION OF PARAMETERS TEST FOR AN/FPS-16 TRACK OF BEACON #1	115
27	VARIATIONS OF PARAMETERS TEST FOR AN/FPQ-6 TRACK OF BEACON #2	116
28	VARIATIONS OF PARAMETERS TEST FOR AN/FPS-16 TRACK OF BEACON #2	117

LIST OF TABLES

TABLE		PAGE
1a	AZIMUTH SYSTEMATIC AND BIAS ERRORS WHICH ARE INDEPENDENT OF TRACK MODE	6
1b	AZIMUTH SYSTEMATIC ERRORS WHICH ARE TRACK MODE DEPENDENT	7
2a	ELEVATION SYSTEMATIC AND BIAS ERRORS WHICH ARE INDEPENDENT OF TRACK MODE	8
2b	ELEVATION SYSTEMATIC ERRORS WHICH ARE TRACK MODE DEPENDENT	9
2c	ELEVATION RANDOM ERRORS	9
3a	RANGE MEASUREMENT ERRORS (RADAR DEPENDENT)	10
3b	RANGE RANDOM ERRORS	11
4	RANGE RATE MEASUREMENT ERRORS (RADAR DEPENDENT)	12
5	ORIGINAL RADAR SETUP	22
6	REVISED RADAR SETUP (BEACON TRACK)	23
7	WALLOPS ISLAND AN/FPQ-6 RANGE CALIBRATION DATA	58
8	WALLOPS ISLAND AN/FPS-16 RANGE CALIBRATION DATA	59
9	RANGE CORRECTIONS TO BE APPLIED TO AN/FPQ-6 SKIN/BEACON TRACKING DATA	81
10	RANGE CORRECTIONS TO BE APPLIED TO AN/FPS-16 BEACON TRACKING DATA	83

LIST OF TABLES (CONTINUED)

TABLE		PAGE
11	RANGE CORRECTIONS TO BE APPLIED TO AN/FPQ-6 BEACON-ONLY TRACKING DATA	84
12	PRESENT DAY AN/FPQ-6 RANGE CORRECTIONS FOR WALLOPS ISLAND	89
13	PRESENT DAY AN/FPS-16 RANGE CORRECTIONS FOR WALLOPS ISLAND	90
14	TEST F1 DATA (AN/FPQ-6 BEACON #1)	105
15	AN/FPQ-6 BANDWIDTH MISMATCH ERROR WHEN TRACKING GEOS-II BEACON #1	106
16	TEST F2 DATA (AN/FPS-16/BEACON #1)	107
17	AN/FPS-16 BANDWIDTH MISMATCH ERROR WHEN TRACKING GEOS-II BEACON #1	108
18	TEST F3 DATA (AN/FPQ-6/BEACON #2)	109
19	AN/FPQ-6 BANDWIDTH MISMATCH ERROR WHEN TRACKING GEOS-II BEACON #2	110
20	TEST F4 DATA (AN/FPS-16/BEACON #2)	111
21	AN/FPS-16 BANDWIDTH MISMATCH ERROR WHEN TRACKING GEOS-II BEACON #2	113
22	SATELLITE CROSSECTION DATA	125

1.0 INTRODUCTION

This report, which is one of a series of six representing The Final Report of the results of the GEOS-II C-Band Radar System Project, contains a detailed description of how the C-Band instrumentation radars were used during the GEOS program.

The material presented covers all aspects of the radar's operation including

1) Pre-Program Planning
   a) Radar Error Source Identification
   b) Error Magnitude Predictions
2) Development of Standard Mission Operation Requirements.
   a) Pre- and Post-Mission Calibrations for Minimization of Systematic Errors
3) Revisions to the Orginal Operating Requirements Based upon Analysis of Tracking Data
4) Development and Analysis of Special Satellite Tracking Tests
5) GEOS Radar Related Programs.

The sequence in which these items are listed is approximately the same sequence in which they were performed. A similar sequence has therefore been followed for presentation of the material in this report. Thus, the pre-program planning effort is described in Section 2 as is the operating procedures development effort. Analyses of the tracking data and isolation of radar error sources are described in Section 3.

Although other reports of this series have been organized by mission requirements. This report has not been limited to the presentation of data which were gathered during any single portion of the GEOS-II project. Instead, the material presented covers the general topic of C-Band radars and their use throughout the GEOS-II C-Band Radar System Project and has direct application to the general problem of gathering accurate radar tracking data. The material is hardware oriented and all analyses and evaluations described pertain to the gathering of accurate data rather than to the application of the gathered data. The radar oriented investigations described herein formed a basic and necessary part of the overall C-Band experiment. The successful completion of these efforts led to the definition of how the radars were to be operated and calibrated. These hardware decisions directly affected the quality of the radar data and therefore played a large part in the successful application of these data to geodetic research.

The availability of the C-Band instrumented GEOS-II satellite presents the radar systems engineer with a unique radar test and calibration device. While the radar calibration aspects of the satellite were considered to be of secondary importance, special dynamic tracking tests performed during the program led both to a better quality of tracking data, and to a better understanding of the C-Band radar's dynamic capabilities and characteristics. These special radar tracking tests are discussed in Section 4.

Section 5 contains a description of two separate hardware studies which grew out of the GEOS-II C-Band Radar System Project. One of these studies called for application of radar range processing techniques to obtain Laser ranges. This study has subsequently led to the design of a new type

of Laser range measurement system which will form a part of an Integrated Laser/Radar System being developed at the NASA-Wallops Station. The second study investigated possible improvements which should be made to passive radar retro-reflectors such as the Van Atta array which has proved to be so useful during the GEOS-II project. The inclusion of such radar cross section enhancement devices as a part of future satellites would permit accurate orbit determination by C-Band radars while using passive tracking techniques.

The majority of the investigations were performed utilizing data from the Wallops Island AN/FPQ-6 and AN/FPS-16 radars. However, the acquired calibration knowledge has been applied successfully to the other radars of the C-Band Network. It is recommended that the described radar calibration techniques and general procedures be adopted as standards. Some caution is advised concerning the fact that considerable optimization was done to match the radar operating conditions to the tracking requirements of the GEOS-II satellite. New satellites, new orbits, new transponders, new radars, and different tracking dynamics may necessitate modification of the procedures, radar set-ups, or techniques employed, and certainly will alter the obtained accuracy and performance.

A set of conclusions and recommendations is included in Section 6.

A completed Bibliography of all referenced documents is included at the rear of this volume.

2.0 C-BAND RADAR PREPARATION FOR GEOS-II

Since the GEOS-II C-Band Systems Project had as its first goal the evaluation of the radar's geodetic support capabilities, the initial radar investigations dealt with:

a) Determination of the theoretical radar dependent errors and their expected magnitude during GEOS-II tracks;

b) Establishment of recommended radar calibration procedures and calibration schedules; and,

c) Establishment of recommended radar operating conditions to be used during all GEOS-II missions.

The importance and success of these systematic pre-program radar investigations and preparations is attested to by the consistently useful radar tracking data which have been obtained throughout the project. The following sub-sections provide a description of the procedures which were followed in arriving at the final set of standard C-Band radar operating (set-up) and calibration procedures used during the GEOS-II C-Band project.

2.1 ERROR MODEL DEVELOPMENT

The geodetic quality of the C-Band radar data was unknown during the initial days of the GEOS-II C-Band project. Therefore, it was decided that a complete radar error model should be developed so that the need for post mission data correction could be more fully evaluated. The complexity of the resulting error model[1] demonstrated how formidable such a correction program would have to be. However, the compilation of expected magnitudes for the various AN/FPQ-6 range

errors showed that the raw radar data should be directly useful with only a minimal amount of non-real time correction. This conclusion assumed that the AN/FPQ-6 radar would be properly calibrated and that a predetermined set of operating instructions would always be followed. The assumed calibration and operating conditions are mentioned in the discussion which is associated with the error model development and are discussed more fully in paragraphs 2.2 and 2.3. The original GEOS radar error model[1,2] contained error magnitude estimates together with supporting theoretical computations. An abbreviated form of the error model is provided below where only the form of the various errors is presented.

2.1.1 Error Model Format

An attempt has been made in the following tables to separate the radar dependent errors by coordinate (azimuth, elevation, range and radial range rate); by their frequency characteristics; and by their track mode dependency. For example, Tables 1a and 2a list those pure bias (zero frequency) and systematic (low frequency) error terms which must be considered during both beacon and skin tracking missions. Tables 1b and 2b provide a separate breakout of the azimuth systematic error terms which are track mode (beacon/skin) dependent. Tables 1c and 2c contain a listing of the angle track random errors. These latter errors are assumed to take the form of band-limited (by servo frequency) random noise.

A comparison of the tables containing the systematic and bias error terms points out that several similar error terms (e.g., zero set bias, dynamic lag error, etc.) appear in the tables for each radar coordinate. The same statement

TABLE 1a AZIMUTH SYSTEMATIC AND BIAS ERRORS WHICH ARE INDEPENDENT OF TRACK MODE

ERROR TERM (μ_{Ai}) AND FORM	ERROR SOURCE
μ_{A0} = Const.	μ_{A0} = Azimuth Zero Set Error
$\mu_{A1} = \Delta t\dot{A}$	μ_{A1} = Timing Error
$\mu_{A2} = -\frac{1}{C} R\dot{A}$	μ_{A2} = Transit Time Error
$\mu_{A3} = \frac{\dot{A}}{K_v} + \frac{\ddot{A}}{K_a} + \frac{\dddot{A}}{K_j} + \ldots$	μ_{A3} = Dynamic Lag Error
	K_v = Angle Servo Velocity Const.
	K_a = Angle Servo Acceleration Const.
	K_j = Angle Servo Jerk Const.
$\mu_{A4} = K_5 \mathrm{Sin}(A+\phi_A+180°0$	μ_{A4} = Transducer Nonlinearity
	K_5 = Nonlinearity Amplitude
	A = Azimuth Angle
	ϕ_A = Nonlinearity Phase Angle
$\mu_{A5} = K_1 \mathrm{Tan}(E)$	K_1 = Non-Orthogonality of Axis
	E = Elevation Angle
$\mu_{A6} = K_2 \mathrm{Sin}(A + K_3)\mathrm{Tan}(E)$	K_2 = Pedestal Tilt Phase
	K_3 = 270° Pedestal Tilt Phase
	A = Azimuth Angle
	E = Elevation Angle
$\mu_{A7} = K_4 \mathrm{Sec}(E)$	K_4 = Antenna distortion errors (Dynamic deflection and solar heating)
	E = Elevation Angle

TABLE 1b AZIMUTH SYSTEMATIC ERRORS WHICH ARE TRACK MODE DEPENDENT

ERROR TERM (μ_{Ai}) AND FORM	ERROR SOURCE	REMARKS
$\mu_{A8} = K_{as/ab}\,Sec(E)$	K_{as}/K_{ab} = Skin/Beacon collimation and boresight drift errors E = Elevation angle	Data Correction is assumed

TABLE 1c AZIMUTH RANDOM ERROR

ERROR TERM AND FORM	ERROR SOURCE	REMARKS
$\sigma_{A-A} = [(\sigma_{A-a})^2 + (\sigma_{a-b})^2 + (\sigma_{A-c})^2]^{1/2}$	σ_{A-a} = Azimuth Bearing wobble σ_{A-b} = Azimuth sero noise σ_{A-c} = Encoder quantizing error	Random error which is independent of trajectory and track mode
$\sigma_{A-B} = \sigma_{\theta t}\,Sec\ E$	E = Elevation angle $\sigma_{\theta t}$ = Angle thermal noise $= \frac{\theta}{k_m[S/Nf_r/\beta_n]^{1/2}}$ θ = 3dB Ant. Beamwidth k_m = Angle Error Slope Factor S/N = Signal to Noise Ratio f_r = PRF β_n = Servo Noise Bandwidth	

TABLE 2a ELEVATION SYSTEMATIC AND BIAS ERRORS WHICH ARE INDEPENDENT OF TRACK MODE

Error Term (μEi) and Form	Error Source
μ_{E0} = Constant	μ_{E0} = Elevation Zero Set Error
$\mu_{E1} = \Delta t \dot{E}$	μ_{E1} = Timing Error
$\mu_{E2} = \frac{1}{C} R\dot{E}$	μ_{E2} = Transit Time Error
$\mu_{E3} = \frac{\dot{E}}{K_v} + \frac{\ddot{E}}{K_a} + \frac{\dddot{E}}{K_j} + \ldots$	μ_{E3} = Dynamic Lag Error
	K_v = Angle Servo Velocity Const.
	K_a = Angle Servo Accel. Const.
	K_j = Angle Servo Jerk Const.
$\mu_{E4} = K_6 \sin (E + \phi_E + 180°)$	μ_{E4} = Transducer Nonlinearity
	K_6 = Nonlinearity Amplitude
	ϕ_E = Nonlinearity Phase Angle
$\mu_{E5} = K_0 \cos (E)$	K_0 = 0° EL Error due to droop
	E = Elevation angle
$\mu_{E6} = K_2 \cos (A + K_3)$	K_2 = Pedestal Tilt Amplitude
	K_3 = 270° - Pedestal Tilt Phase
μ_{E7} = Const. = K_4	Antenna distortion errors (Dynamic deflection and solar heating)

TABLE 2b ELEVATION SYSTEMATIC ERRORS WHICH ARE TRACK MODE DEPENDENT

Error Term (μEi) and Form	Error Source
μ_{E8} = const. = $K_{e\ s/b}$	$K_{e\ s/b}$ = Skin/Beacon Collimation and boresight shift errors

TABLE 2c ELEVATION RANDOM ERRORS

Error Term and Form	Error Source
Random error which is independent of trajectory and track mode $\sigma_{E-A} = \left[(\sigma_{E-a})^2 + (\sigma_{E-b})^2 + (\sigma_{E-c})^2\right]^{1/2}$ $\sigma_{E-B} = \sigma_{Et}$	σ_{E-a} = Elevation Bearing Wobble σ_{E-b} = Elevation servo noise σ_{E-c} = Encoder quantizing error σ_{Et} = Angle thermal noise $= \frac{\theta}{k_m\left[S/N f_r/B_n\right]^{1/2}}$

TABLE 3a RANGE MEASUREMENT ERRORS (RADAR DEPENDENT)

Error Term and Form	Error Source
$\mu_{R0} = \text{Const.} = \mu_{R0-1} + \mu_{R0-2} + \mu_{R0-3}$	μ_{R0-1} = Zero Set Error
	μ_{R0-2} = Discrim. drift
	μ_{R0-3} = Servo unbalance
$\mu_{R1} = \Delta t \dot{R}$	μ_{R1} = Timing Errors
$\mu_{R2} = -\frac{1}{C} R \dot{R}$	μ_{R2} = Transit time error
$\mu_{R3} = \frac{\ddot{R}}{K_a} + \frac{\dddot{R}}{K_j} + \ldots$	μ_{R3} = Dynamic Lag Error
	K_a = Range Servo Accel. Const.
	K_j = Range Servo Jerk Const.
$\mu_{R4} = \left[\mu_{R4-1} + \mu_{R4-2}\right] R$	μ_{R4-1} = Range Osc. Freq. Error
	μ_{R4-2} = Velocity of light error

TABLE 3b RANGE RANDOM ERRORS

Error Term and Form	Error Source
Random and independent of track geometry and track mode.	Range servo noise; range quantization; internal time jitter
$\sigma_{R-B} = \sigma_{Rt}$	σ_{Rt} = Range thermal noise $= \frac{\tau}{k_r \sqrt{(S/N)\, f_r/\beta_n}}$
	$\sigma_{Rt} = (\sigma_{Rt})_B$ for Beacon track
	$\sigma_{Rt} = (\sigma_{Rt})_S$ for Skin track

TABLE 4 RANGE RATE MEASUREMENT ERRORS (RADAR DEPENDENT)

Error Term and Form	Error Source
$\mu_{\dot{R}0} = \text{Const.} - \mu_{\dot{R}0-1} + \mu_{\dot{R}0-2}$	$\mu_{\dot{R}0-1}$ = Discriminator drift $\mu_{\dot{R}0-2}$ = Environmental effects upon components
$\mu_{\dot{R}1} = \Delta t \ddot{R}$	$\mu_{\dot{R}1}$ = Timing Error
$\mu_{\dot{R}2} = -\frac{1}{C} R \ddot{R}$	$\mu_{\dot{R}2}$ = Transit Time Error
$\mu_{\dot{R}3} = \frac{\dddot{R}}{K_a} + \frac{\ddddot{R}}{K_j} + \ldots$	$\mu_{\dot{R}3}$ = Dynamic Lag Error K_a = Range Rate Servo Accel. Const. K_j = Range Rate Servo Jerk Const.
$\sigma_{\dot{R}A} = \left[(\sigma_{\dot{R}A-1})^2 + (\sigma_{\dot{R}A-2})^2 + \ldots\right]^{1/2}$	$\sigma_{\dot{R}A-1}$ = Ref. Osc. stability error $\sigma_{\dot{R}A-2}$ = Transmitter noise and spurious effects $\sigma_{\dot{R}A-3}$ = Doppler granularity $\sigma_{\dot{R}A-4}$ = Granularity of Range readout
$\sigma_{\dot{R}B} = \sigma_{\dot{R}t}$	$\sigma_{\dot{R}t}$ = Range rate thermal noise $= \frac{(\lambda/2)\sqrt{3}}{\pi T^{2/3}\sqrt{2f_r \times S/N}}$ where T = Processing time

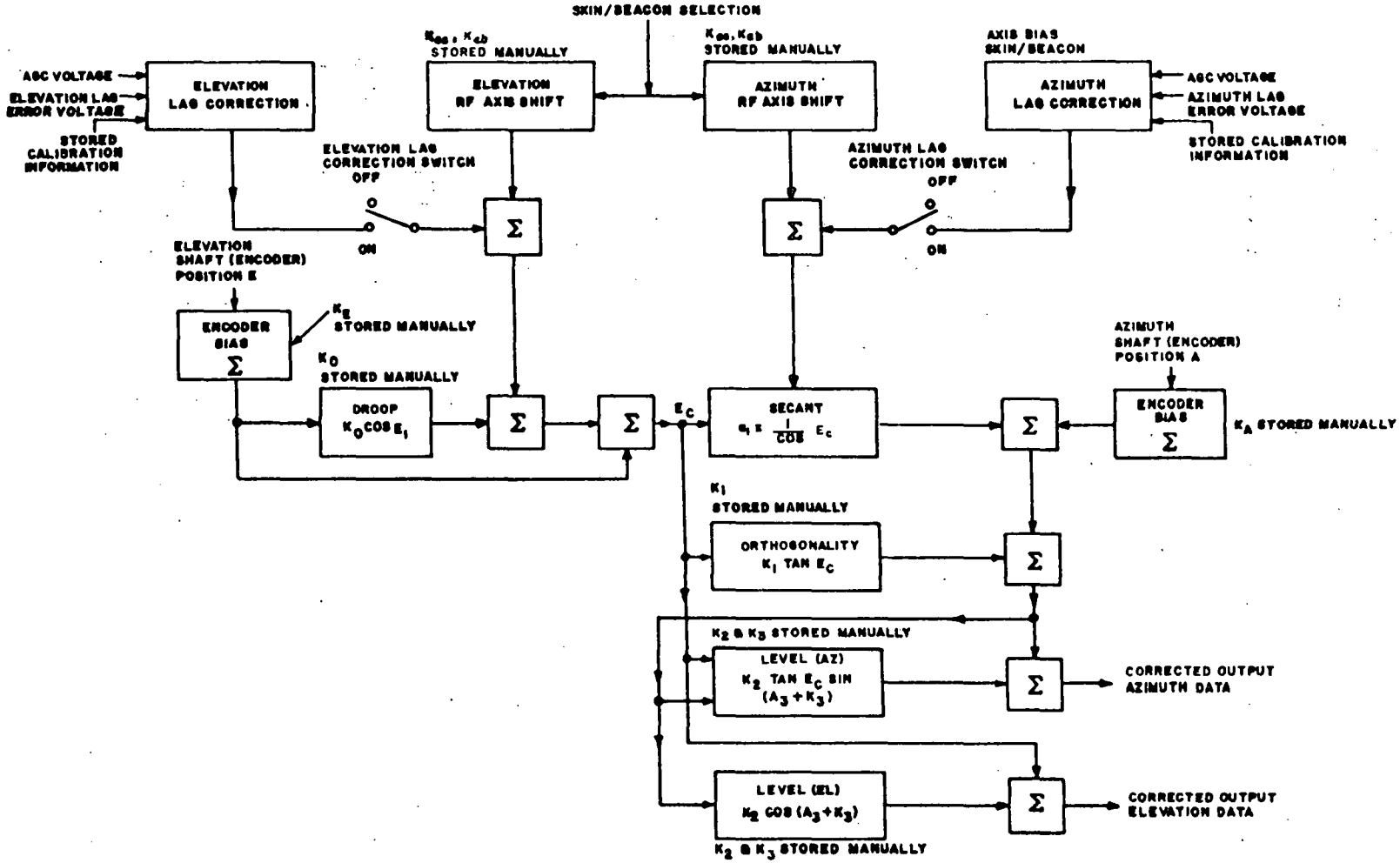

FIGURE 1

FLOW DIAGRAM OF THE ERROR CORRECTION PROGRAM

applies to the random error terms since quantizing and thermal noise error terms also appear in each radar coordinate. Having noted the similarity of the error terms in each coordinate, it becomes quite easy to switch between tables since relatively few unique error terms appear in any particular table.

2.1.2 Real Time Data Correction Assumptions

Real-time data correction capability has been programmed into the RCA 4101 computers which form an integral part of the AN/FPQ-6 and AN/TPQ-18 instrumentation radar systems. This real-time data correction capability normally is restricted to the correction of certain systematic angular errors. The standard correction program can apply corrections in real time for each of the following systematic errors:

Azimuth Errors	Elevation Errors
Zero Set Bias (μ_{A0})	Zero Set Bias (μ_{E0})
Dynamic Lag (μ_{A3})	Dynamic Lag (μ_{E3})
Non-Orthogonality (μ_{A5})	Droop ($_{E5}$)
Pedestal Leveling (μ_{A6})	Pedestal Leveling (μ_{E6})
Skin/Beacom Collimation (μ_{A8})	Skin/Beacon Collimation (μ_{E8})
Encoder Non-Linearity (μ_{A4})	Encoder Non-Linearity (μ_{E4})

The mathematical error models are used within the computer program (see Figure 1) are identical to the models presented in the accompanying tables. As stated above, no real-time corrections are applied to either the range or range-rate data in the standard program.

The real-time data correction program assumed that accurate calibrations are carried out to determine the magnitudes of the error coefficients for each applicable error teror terms. The accuracy of the corrections are, therefore, limited by the measurement uncertainties encountered during the calibration effort.

2.1.3 Error Model Limitations

The error model presented here has been based upon the following assumptions regarding the operational set-up of the radar and the dynamic characteristics of the mission.

First, that careful and accurate calibrations are performed to determine the error coefficient magnitudes for real-time data correction. This assumption implies that the applicable calibrations are performed on a pre- and post-mission basis for those errors which are known to be time dependent variables (e.g., range zero set error).

Second, that tracks are not performed at low (5°) elevation angles. Such low angle tracks will introduce an additional multipath error into the angle data.

Third, that certain prescribed radar operating conditions are followed and that all calibrations are performed with the radar set-up in its operational state. For example, assume that a transponder nominal 0.5 microsecond reply pulse width will be utilized. This will impose the requirement that all beacon-track range calibrations be performed with the radar set-up in the 0.5 microsecond pulsewidth mode even though a different pulsewidth may be used to interrogate the transponder. There is a secondary effect which will

be introduced by the 0.5 microsecond beacon pulsewidth since the AN/FPQ-6 has been designed to optimally process only a 0.75 microsecond beacon return pulsewidth. This will result in non-optimum processing which will show up primarily as a degradation in the dynamic response characteristics of the range servo. Specific effects of this mismatch are impossible to predict since they are greatly dependent upon operational set-up and adjustment procedures as well as upon the actual received beacon pulsewidth. Any differences between the 0.5 microsecond pulsewidth used for radar calibration and the actual pulsewidth received from the beacon will also introduce an apparent range zero set error.

Fourth, that a check and/or recalibration of the radar for dynamic angle lag error correction will be performed as often as necessary. Lag error calibration is affected by any adjustments which alter the relative gain and/or phase characteristics of the radar receiver's reference and angle error channels as well as by changes in the servo system's gain or bandwidth characteristics.

Fifth, that the target characteristics are such that the radar is operating within the linear portion of its dynamic response characteristics. Failure to maintain track at or near the antenna null could result in the introduction of unmodeled angle errors due to antenna dependent crosstalk and polarization effects.

2.2 DEVELOPMENT OF CALIBRATION PROCEDURES

The various radar error sources as itemized in the preceding section were reviewed to determine:

a) which errors were sufficiently large so as to require at least periodic calibration; and

b) which of these dominant radar errors were time dependent variables requiring mission by mission calibration.

Both a set of procedures and an associated calibration schedule were developed as a result of this review. The calibrations which were recommended are described in the following paragraphs.

2.2.1 Mission By Mission Calibrations

Static calibrations of the C-Band radars at Wallops Station are performed prior to, and immediately following each mission. Identical calibration procedures are followed in both of these pre- and post-mission calibrations. A detailed description of the mission calibration procedures is given in Reference 3) for the AN/FPQ-6 instrumentation radar and in Reference 4) for the AN/FPS-16 instrumentation radar.

The data obtained during these pre- and post-mission calibrations are recorded on magnetic tape using the standard sampling rate of 10 pps. The data recorded includes radar model number, ID word, time, range, azimuth, and elevation. Range rate and AGC voltage as well as V_a and V_e (lag error corrections) are also recorded when applicable.

It is assumed that the antenna is properly collimated prior to mission set-up. This means that the RF axis is aligned parallel to the optical axis and that the optical axis is aligned with the mechanical axis.

The calibration data is obtained for approximately 10 seconds (100 data points) in each of the following positions:

- Boresight tower normal - Electrically locked to the boresight tower (BST) in azimuth and elevation.
- Boresight tower plunged - Same set-up as for BST normal except antenna in plunged mode.
- Range target skin gate - The reference range target is locked onto using the skin L.O. The skin gate range displays should indicate surveyed range.
- Range target beacon gate - If a transponder track is planned, the proper delay compensation is set into the beacon gate range system.

In conjunction with the normal range and angle calibration procedures, an AGC step calibration is normally performed for each pre- and post-mission. The calibration is referenced to a zero db signal (i.e., one whose power is equal to that of the noise power). Although zero db is determined using a CW signal from the signal generator, the pulse mode is used for the actual recorder step-calibration. Basically, the method employs a power meter as an indicator, and a 3 db pad as the actual calibrating device. A measurement is taken on the power meter of the noise energy from the receiver without any signal applied. The 3 db pad is then inserted in the input to the power meter, and the CW signal applied to the receiver. A precision variable attenuator at the boresight tower is

adjusted until the power meter again indicates the same level measured on noise alone. Next a reference reading is taken of AGC voltage with the console digital voltmeter. The boresight signal generator is switched to pulse mode, and with the radar locked on to the pulsed signal, the attenuator at the boresight tower is adjusted to give the same AGC voltage as was obtained in CW mode. The resultant attenuator setting represents zero db, or S/N ≈ 1. The S/N is stepped-up in prescribed increments to 70 db.

It is also important to note that the AN/FPQ-6 class of instrumentation radar is equipped with a precision RF attenuator. This device provides the operator with the ability to perform the range zero-set calibrations at the receive S/N ratio which is always well within the linear operating range of the system (10 to 30 db), and should be approximately equal to the expected signal level during track. This attenuator should be utilized if the signal return from the range target is greater than 30 to 35 db. Range calibrations or tracking performed under very high S/N ratio conditions may be in error due to possible equipment saturation effects.

2.2.2 Periodic C-Band Radar Calibrations

Both the AN/FPQ-6 and the AN/FPS-16 C-Band radars at Wallops are periodically calibrated for the following errors:

a) Azimuth zero-set by observing polaris - (yearly)

b) Elevation zero-set by means of zero elevation target board - (yearly)

c) Pedestal leveling - (monthly) .

The following AN/FPQ-6 error correction coefficients are checked by periodic calibrations:

a) Lag error, linear fit coefficients (receiver gain calibration plus antenna error-pattern calibration) - (monthly)

b) Elevation droop - (yearly) .

The calibration procedures pertinent to each calibration are described in References 3 and 4. It is assumed that similar calibrations are performed by other agencies or other radars participating in the GEOS-II project.

2.3 ESTABLISHMENT OF RADAR OPERATING PARAMETERS

C-Band instrumentation radars such as the AN/FPS-16 and AN/FPQ-6 radars have been intentionally designed to fulfill the needs of a wide variety of users. As such, these instruments have been equipped with a great many selectable modes of operation. These various options were evaluated from the view point of the specific GEOS-II mission characteristics and requirements and a single recommended operating mode was established. As the project proceeded various minor changes were made to this initial procedure but a prescribed detailed operating mode always existed for each mission.

As will be discussed later, the establishment of a rigid set-up and operating mode did not necessarily result in optimum tracking mode for all missions. It did, however, greatly reduce the number of variables having an effect upon the radar's accuracy and thus insured that consistent tracking data would be obtained. Minor equipment

malfunctions, calibration errors, or deviations in the set-up procedures usually introduced obvious data changes. The ability to recognize and trace these changes back to their source proved to be an extremely valuable tool both in evaluating the radar's operation and in minimizing the time spent in analyzing faulty data.

Unfortunately, an associated set of set-up procedures was not initially established for use during the pre- and post-mission calibrations. This oversight was eventually corrected when it was found that the assumptions regarding a consistent calibrating mode were not valid. The need for an extremely detailed calibration set-up procedure became very apparent when data from the multi-station radar network were being reduced. Although steps were taken to minimize the allowable calibration mode variables, it was found that site operating personnel often followed their standard procedures rather than the recommended GEOS-II procedures. These site dependent operational idiosyncrasies were gradually recognized and eliminated as the project proceeded. Reference to some of these mode selection errors will be found both in Section 3 and 4.

2.3.1 General Operating Procedures

Table 5 presents the set of radar operating parameters which were originally established for GEOS-II tracks from Wallops Island. A comparison between this original set and the current set of parameters as specified in Table 6 will readily show how much more detailed and specific the recommended procedures became as the project progressed and other radars were included in the experiment.

ORIGINAL RADAR SETUP

TABLE 5

Term	Radar Setup for Transponder (Beacon Track)		Radar Setup for Passive Reflector (Skin Track)
	FPS-16	FPQ-6	FPQ-6
Peak Power	1.0 MW	2.0 MW	2.8 - 3.0 MW
Transmitter Frequency	5690 MHz	5690 MHz	5690 MHz
Receiver Frequency	5765 MHz	5765 MHz	5690 MHz
Pulse Width	1.0 μsec	1.0 μsec	1.0 or 2.4 μsec
Pulse Code	2 pulse 8 μsec spacing	2 pulse 8 μsec spacing	single pulse
Polarization	Linear Vertical	Linear Vertical	circular
PRF	160 or less	160	160 or 640
Beacon AFC	yes	yes	no
Beacon Delay Compensation	0, 0.07 or 5.0 μsec	0, 0.07 or 5.0 μsec	0

Table 6

REVISED RADAR SETUP (BEACON TRACK)

	MPS-26		CAPRI		FPQ-6 & TPQ-18		FPS-16 & MPS-25	
	Calibration	Mission	Calibration	Mission	Calibration	Mission	Calibration	Mission
Low Noise Amplifier (If available)	N.A.	N.A.	ON	ON	ON	ON	ON	ON
PRF	320	320	160	160	160	160	160	160
Pulse Width	0.75 usec	0.75 usec	.5 usec	.5 usec	.5 usec	.5 usec	.5 usec	.5 usec
Receiver Bandwidth	Optimum	Optimum	6 MHz	6 MHz	2.4 MHz	2.4 MHz	8 MHz	8 MHz
Attenuation (Tx.)	(STC)OFF	(STC)OFF	IN	OUT	IN	OUT	IN	OUT
Range Servo Bandwidth	5 Hz	5 Hz	4 Hz	4 Hz	4 Hz	4 Hz	4 Hz	4 Hz
Angle Servo Bandwidth	2.5 Hz	2.5 Hz	3 Hz	3 Hz	3 Hz	3 Hz	3 Hz	3 Hz
Data Corrector Bandwidth	N.A.	N.A.	N.A.	N.A.	2 Hz	2 Hz	N.A.	N.A.
Beacon AFC	ON	ON	ON	ON	ON	ON	ON	ON
Beacon Delay Compensation	800 yds	800 yds	800 yds	800 yds	800 yds	800 yds	800 yds	800 yds
Beacon Gate	ON	ON	ON	ON	ON	ON	ON	ON
Beacon L.O.	ON	ON	ON	ON	ON	ON	ON	ON
Skin AFC	OFF	OFF	ON	OFF	ON	OFF	ON	OFF
Skin Gate	ON	OFF	ON	OFF	ON	OFF	ON	OFF
Skin L.O.	OFF	OFF	ON	OFF	ON	OFF	ON	OFF
Polarization	Lin. Vert.	Lin. Vert.	Lin. Vert.	Lin. Vert.	Lin. Vert.	Lin. Vert.	Lin. Vert.	Lin. Vert.
Pulse Coder	ON	ON	ON	ON	ON	ON	ON	ON
Data Rate	10 PPS	10 PPS	10 PPS	10 PPS	10 PPS	10 PPS	10 PPS	10 PPS

The parameters specified in the original table were generally established by the operational characteristics and requirements of the satellite borne transponder[5]. The reason for the selection of these specific parameters is rather obvious when the GEOS-II C-Band transponder's characteristics are considered. It should be pointed out that a 1.0 microsecond interrogation pulsewidth was originally selected. As can be seen in Table 6, this transmit pulsewidth was later changed to 0.5 microseconds. There was also an interim period where the Wallops AN/FPS-16 used a 1.0 microsecond pulsewidth while the AN/FPQ-6 used the narrower mode. The effects of these pulsewidth changes upon the beacon track data are described in Sections 3 and 4.

A detailed discussion on radar receiver bandwidth considerations is contained in Section 3.2.8 and will not be repeated here. The wide bandwidths called out in Table 6 were intentionally selected to minimize beacon track mismatch effects.

All of the remaining parameters specified in Table 6 with the exception of the various servo bandwidths, were more or less arbitrarily specified to ensure consistency in the tracking data. The reasoning behind the selection of the various servo bandwidths is discussed in the next subsection. Specification of certain operating characteristics such as beacon L.O. "on" during beacon track mode may at first glance seem to be unnecessary. However, their inclusion together with a calibration mode requirement emphasizes that this operating mode must be identical during track and calibration. As stated previously, such detail was found to be necessary.

2.3.2 Servo Bandwidth Considerations

As shown in the error model presented in Section 2.1, the angle servo dynamic lag error is primarily a function of the target dynamics and the servo velocity and acceleration constants (K_v) and (K_a). The terminology "constant" when applied to these terms is somewhat of a misnomer since these parameters vary as a function of the servo gain and bandwidth settings. The angle servos have been designed so that the operations value of K_v remains quite constant regardless of the bandwidth selected. The value of K_a, however, is highly sensitive to the servo bandwidth setting. For the AN/FPQ-6 radar. The magnitude of K_a will typically vary from a maximum value of 20 to 25 sec^{-2} for the widest servo bandwidth (approx. 3 to 4 Hz), to a minimum value of 0.75 sec^{-2} at the narrowest normally used bandwidth. Therefore, since the dynamic lag error is an inverse function to K_a, the lag error will decrease with increasing bandwidth with the minimum lag associated with the widest servo bandwidth position.

Lag error considerations alone would tend to dictate that the radar should always be operated in its widest servo bandwidth position. However, reference to the random error portions of the error model will show that there is a thermal noise error which is directly proportional to the square root of this servo bandwidth. Thus, widening the servo bandwidth not only decreases the angle lag error effects, but also increases the random error. Therefore, it is necessary to investigate both the expected value of the lag errors and the thermal noise errors before an optimum bandwidth setting can be selected for operational use.

The first investigation performed for the GEOS-II project was to determine an expected magnitude for the dynamic lag errors. To accomplish this lag error evaluation it was first necessary that typical values for the expected angle velocity and acceleration tracking components be determined. Four types of satellite passes were chosen for analysis purposes and the angular tracking dynamics imposed upon the radar by each type of pass were computed. The passes selected for analysis were:

High Elevation Pass; max. El. = 79°

Medium Elevation Pass; max. El. = 55°

Low Elevation Passes; max. El. = 38.6° and 25°.

The radar dynamic tracking characteristics which were computed for these cases are plotted in Figures 2 through 7.

The azimuth lag errors were next computed based upon these azimuth velocities and acceleration components. Since the lag error is a function of servo bandwidth setting, the lag error was computed for each servo bandwidth. Theoretical azimuth lag errors for the high and medium elevation passes are presented in Figure 8 and 9. The lag errors for the lower elevation passes are not included due to their relatively small magnitudes.

The elevation angle lag errors for the sample cases were also computed. The errors associated with the high elevation pass have been included as Figure 10.

From the referenced figures it was concluded that significantly large angle lag errors could indeed be expected during certain GEOS-II satellite tracks if the servos were

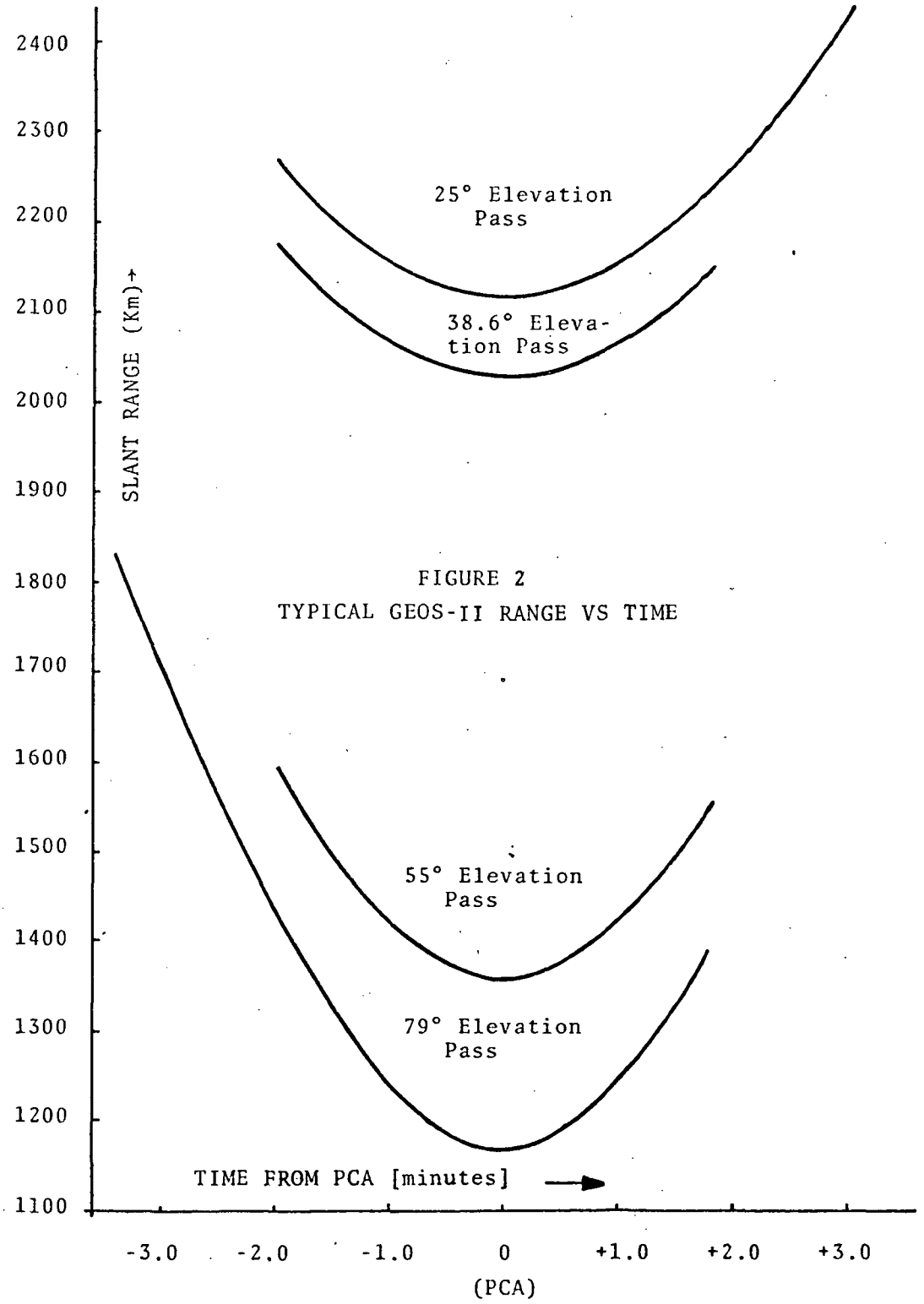

FIGURE 2
TYPICAL GEOS-II RANGE VS TIME

FIGURE 3

TYPICAL RANGE RATE VS TIME

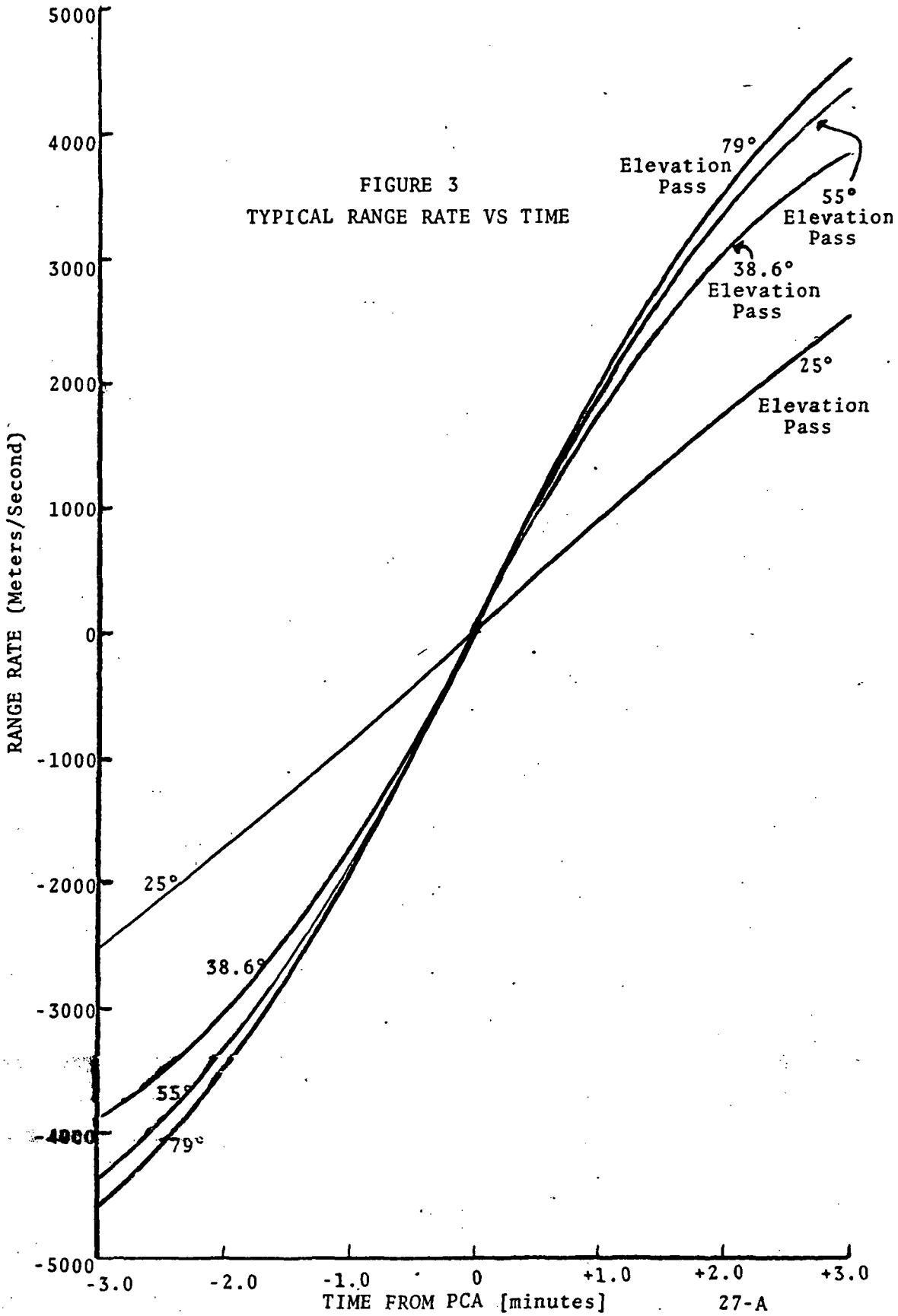

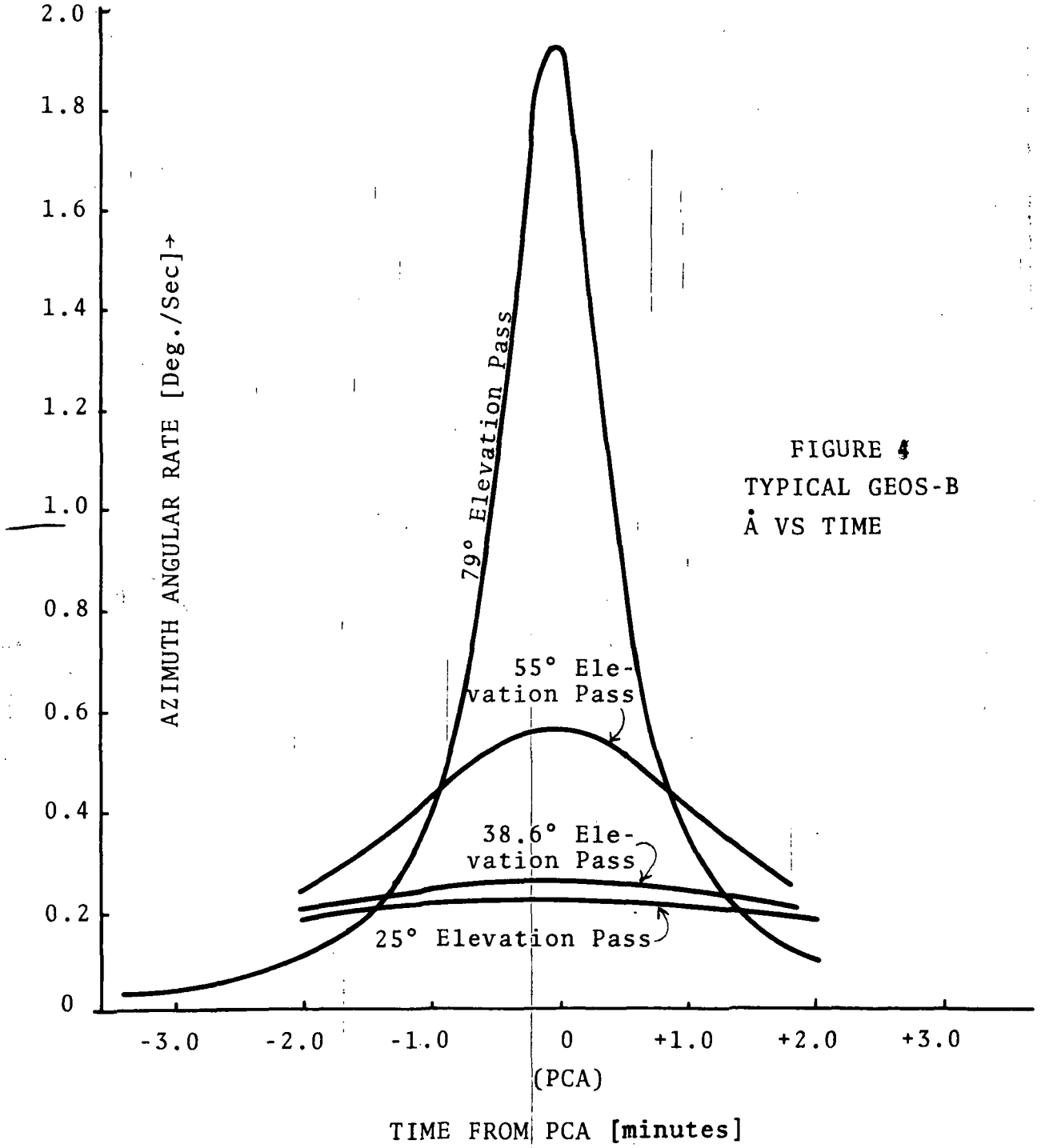

FIGURE 4
TYPICAL GEOS-B
$\dot{A}$ VS TIME

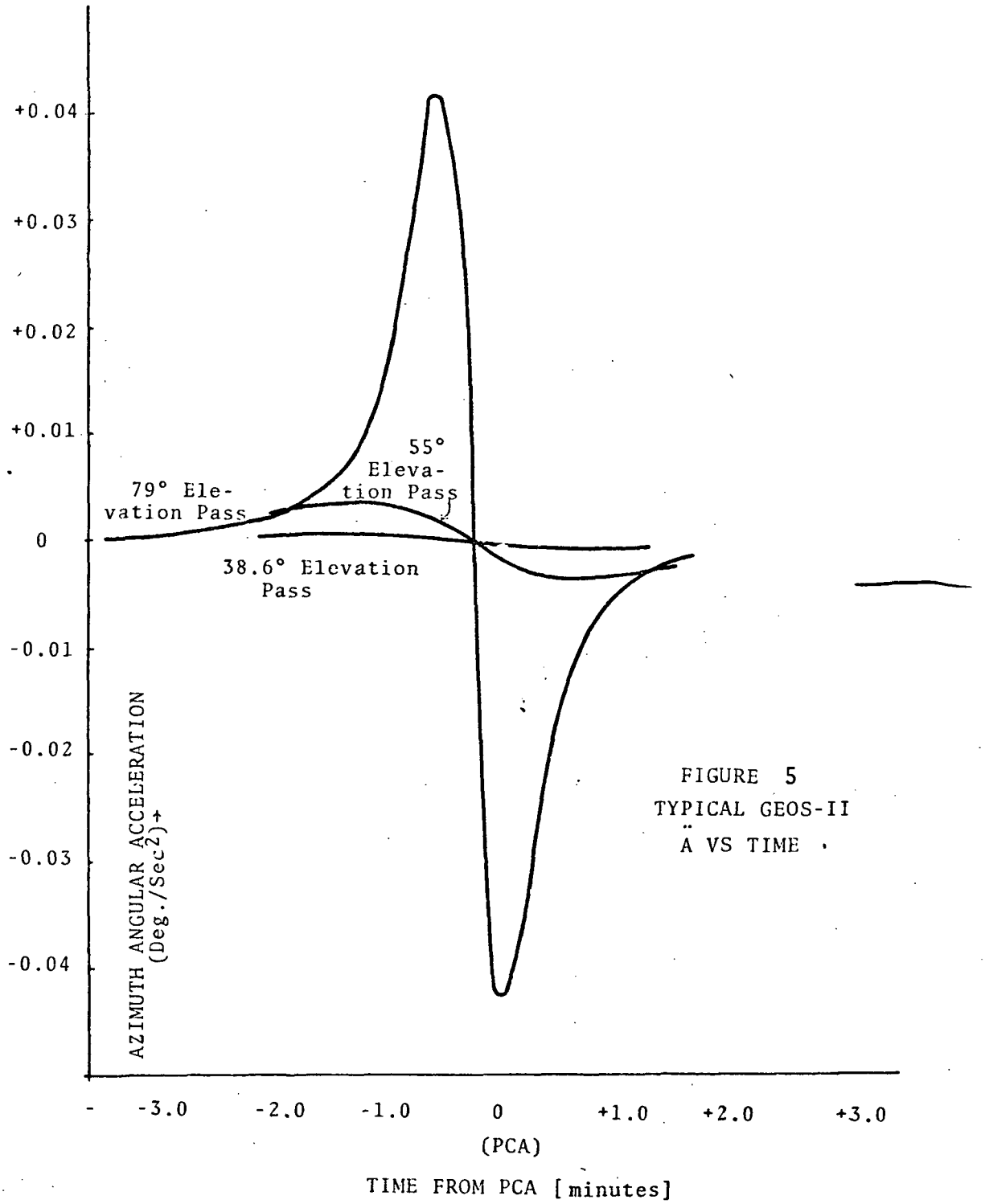

FIGURE 5
TYPICAL GEOS-II
$\ddot{A}$ VS TIME

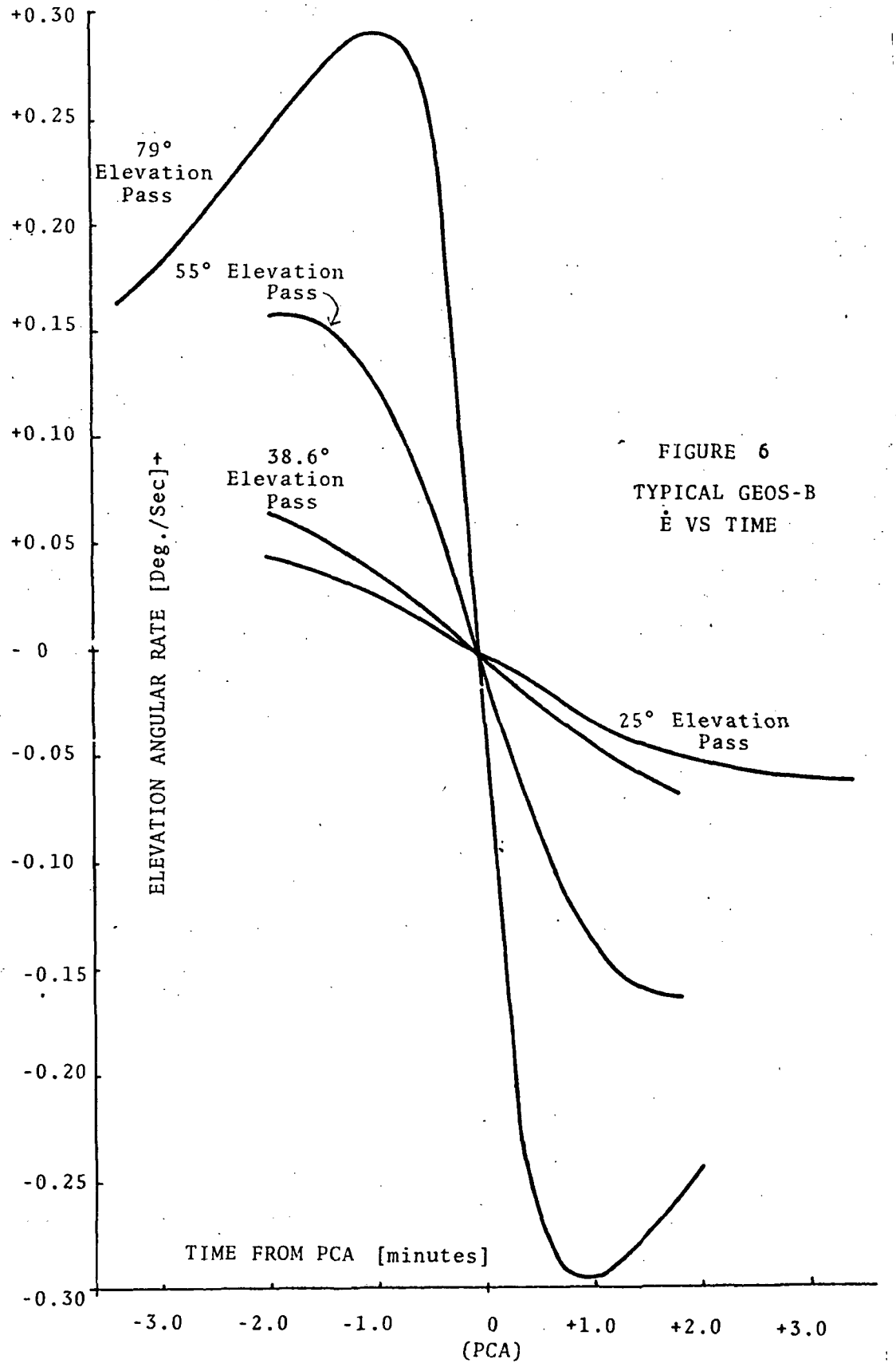

FIGURE 6

TYPICAL GEOS-B

$\dot{E}$ VS TIME

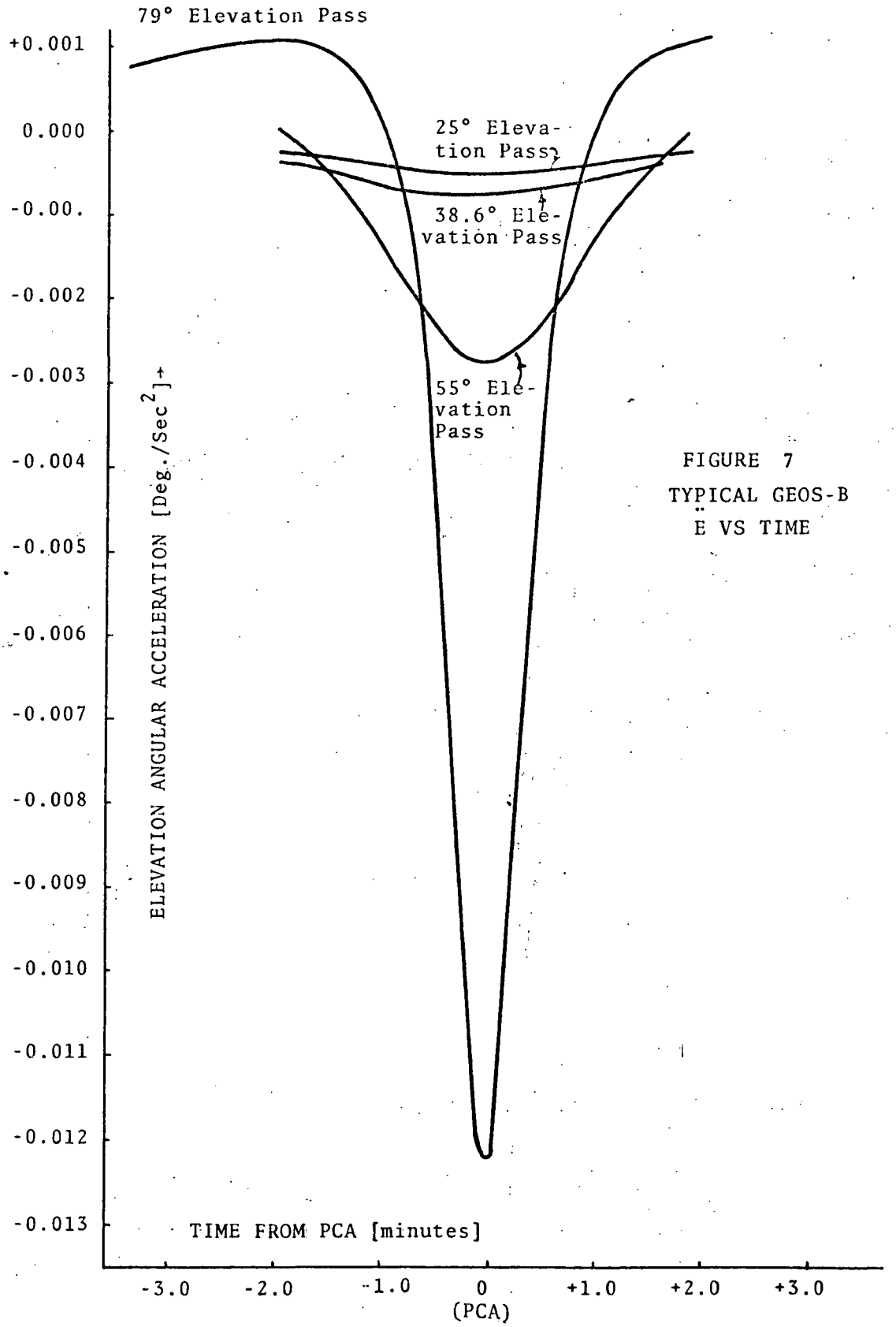

FIGURE 7
TYPICAL GEOS-B
$\ddot{E}$ VS TIME

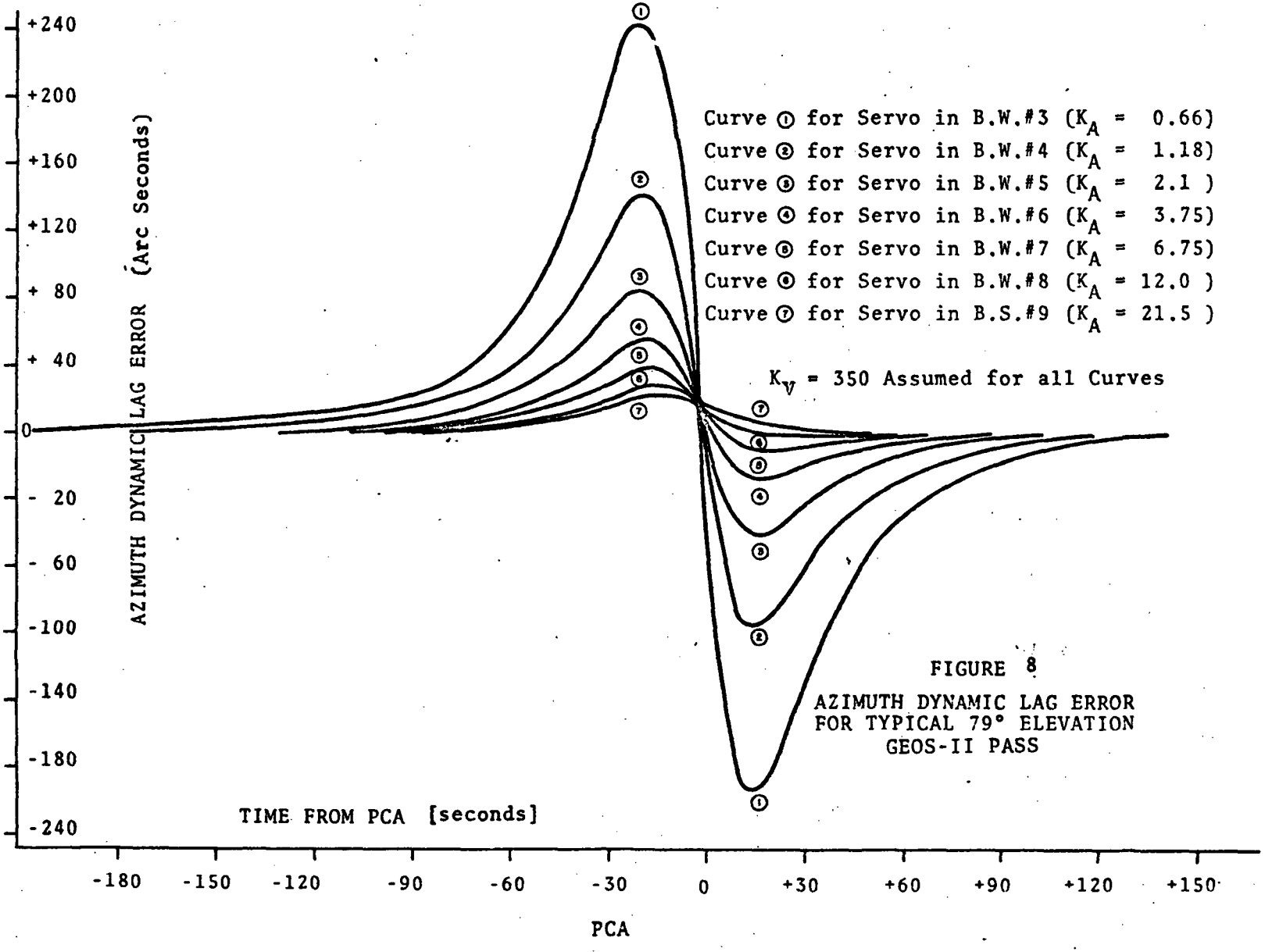

FIGURE 8

AZIMUTH DYNAMIC LAG ERROR
FOR TYPICAL 79° ELEVATION
GEOS-II PASS

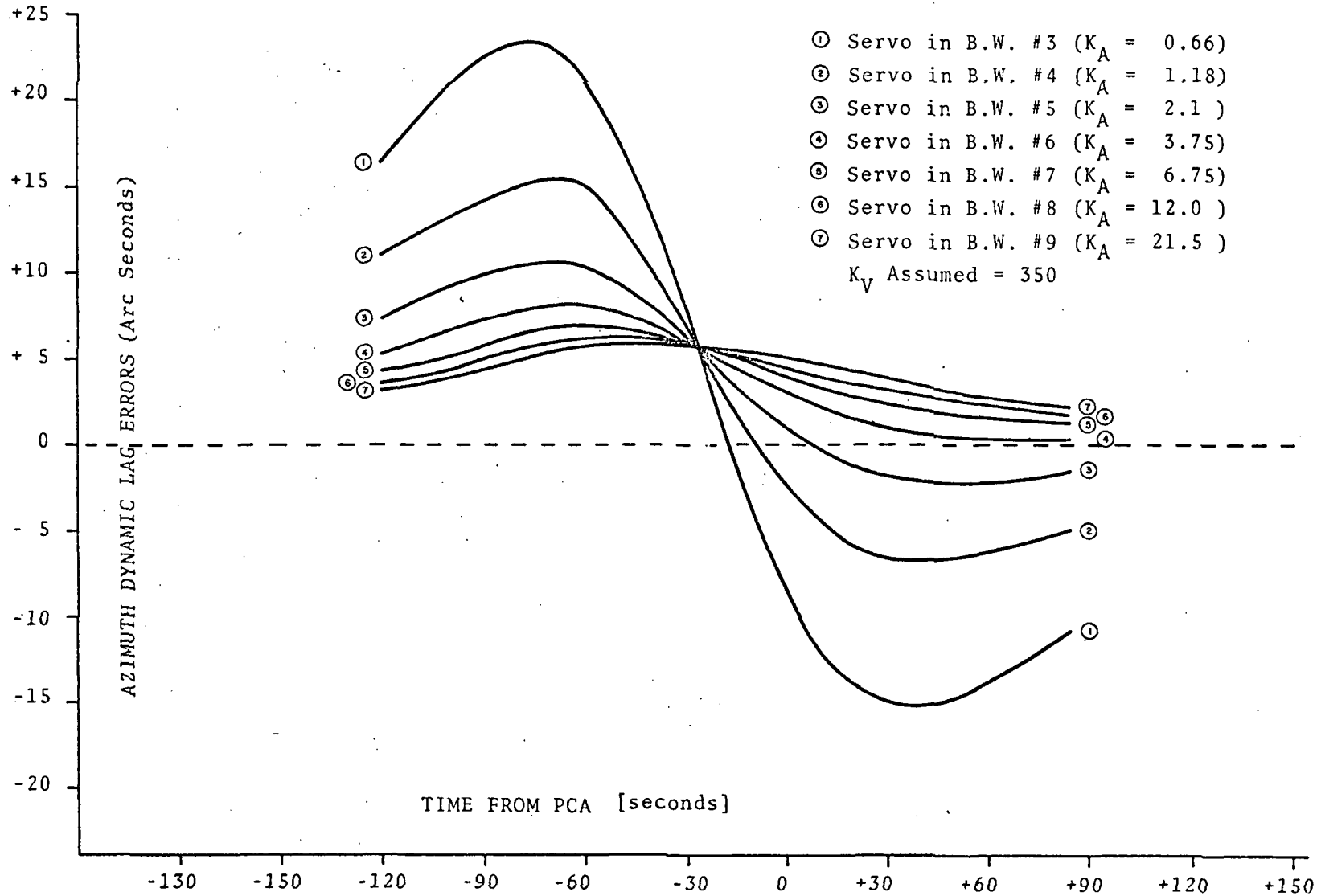

FIGURE 9

AZIMUTH DYNAMIC LAG ERROR VS TIME FOR TYPICAL 55° ELEVATION GEOS-B PASS

operated in their narrow bandwidth positions. It was further concluded that these angle lag errors would be negligibly small for all except the very high GEOS passes if the wider angle servo bandwidths were used.

Next, the published[5] values for the output power and the antenna gain for the satellite borne transponders were used to compute the expected radar receive S/N ratio for the beacon track case. It was found that a receive S/N ratio equal to at least 30 db could be expected even at the maximum expected satellite ranges (See Figures 2 and 19). Previous analyses which RCA has performed on other programs have determined that the widest AN/FPQ-6 servo bandwidth is optimum for the combined servo lag/random error case when the receive S/N $\geq$ 30 db. Therefore, using these results, it was concluded that the servo lag errors could be minimized for the beacon track case without introducing unnecessarily large thermal noise errors. As a result of this investigation it was recommended that both of the AN/FPQ-6 angle servos be operated always in their widest bandwidth (3.2 Hz) during GEOS beacon tracking missions.

The clear cut decisions reached during the beacon track investigation could not, unfortunately, be duplicated for the skin track case. An investigation to determine the expected receive S/N ratio when tracking the satellite borne Van Atta array (Passive C-Band retro-reflector) resulted in the conclusion that very low (< 10 db) S/N ratios could be expected during most skin tracks. This result indicated that servo bandwidth position #6 (approx. 1 Hz)

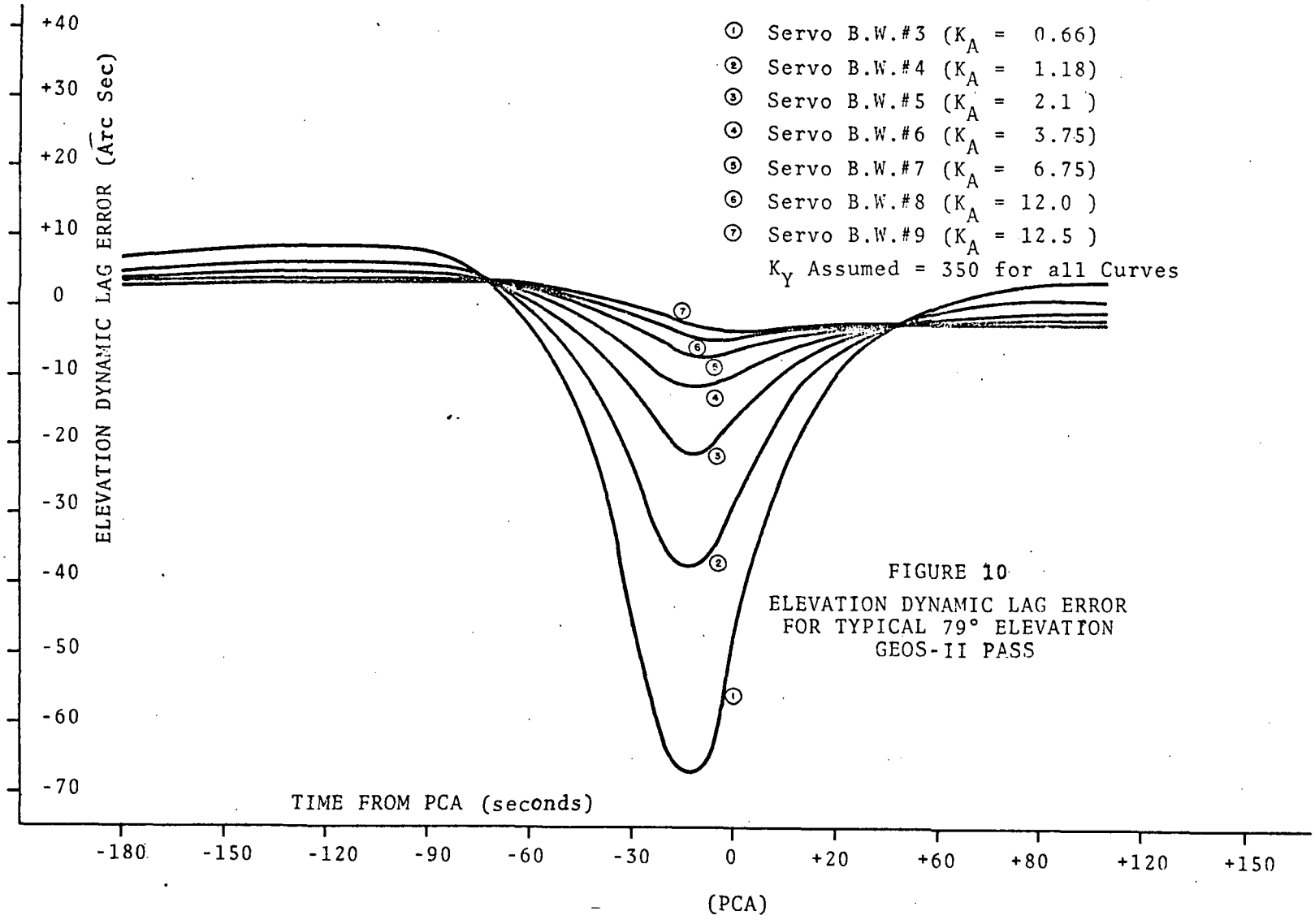

FIGURE 10

ELEVATION DYNAMIC LAG ERROR
FOR TYPICAL 79° ELEVATION
GEOS-II PASS

should be used for skin tracking missions if the combined lag and thermal noise errors were to be minimized. Reference to the curve for bandwidth #6 in Figure 8 (curve #4) shows that operation in the occurrence of large azimuth lag errors. (Note that skin tracks were only possible at the short ranges associated with high elevation passes). Further, it was recognized that the random thermal noise errors could, if necessary, be reduced during post-mission filtering (smoothing) while the systematic nature of the lag errors would be more difficult to remove once their effects were introduced. Based upon these considerations, as well as upon the desire to operate the radar in as consistent a fashion as possible, it was decided to risk the potentially large skin track thermal noise errors by always operating the radar in the widest angle servo bandwidth. Fortunately, it turned out that the actual skin track S/N ratio was higher than expected so that the deleterious aspects of the decision were minimized.

The decision to operate the range servo in its nominal 4 Hz position was also the result of optimal bandwidth computations. The range servo is a type two system having an acceleration constant of approximately 200 sec^{-2} in this intermediate bandwidth position. The expected low target radial range acceleration components coupled with the large beacon track receive S/N ratios indicated that the range servo should be operated in the 4 Hz bandwidth position.

A data correction bandwidth of 2 Hz was also recommended. This decision had relatively little impact upon the quality of the radar's data since the associated angle error data are only used for lag error correction computations. The decision not to correct for lag errors, therefore, made this

decision appear somewhat meaningless. The possibility of post-mission application of the lag corrections did exist, however, and because of this possibility it was felt that a specific operating mode should be established.

3.0 RADAR ERROR INVESTIGATIONS PERFORMED DURING THE GEOS-II PROGRAM

The material of this section of the report can be considered a natural extension of the radar dependent error model which was presented in Section 2. Descriptions are presented of detailed investigations which were performed to obtain a better estimate on the magnitude and stability of certain critical radar error terms. The investigations covered both angle and range errors.

It should be noted that these radar error investigations which were performed as a part of the GEOS-II project made maximum use of previously performed radar error evaluation programs. Reports issued under the MIPIR Test and Evaluation Program (Missile Precision Instrumentation Radar - i.e. AN/FPQ-6 and AN/TPQ-18 Radars) proved to be particularly useful[6,7] since the Wallops Island AN/FPQ-6 radar served as the test instrument for this evaluation program. Utililization of the data gathered during these past radar test programs permitted the GEOS-II effort to concentrate on those error terms which had not been thoroughly evaluated.

After reviewing existing data, a series of radar error investigations were undertaken which systematically evaluated the magnitude and stability of various radar angle and range errors. The calibration techniques, normally used to measure these error terms, were reviewed and either approved or changed.

The following paragraphs assume a familiarity with the material presented in Section 2. The angle error investigations and results are described first followed by a desciptions of the range error studies.

3.1 ANGLE ERROR INVESTIGATIONS

The following angle error discussion is presented in the same sequence in which the investigations were performed.

3.1.1 Pedestal Leveling Error

Previous radar evaluation programs[6] had noted that the Wallops Island AN/FPQ-6 radar exhibited an out of level error having a time varying amplitude and phase angle. Several possible reasons for this variation in the pedestal mislevel were proposed (i.e. tidal motion, solar heating etc.) but the referenced evaluation program had to be terminated before this mislevel error evaluation could be completed but recommended that the pedestal mislevel error be periodically measured and recorded. The hope at that time (1964) was that the MIPIR evaluation program would be resumed and, if so, an adequate amount of mislevel data would exist to permit correlation to be established between this error and at least one of the possible environmental causes. Therefore, when the GEOS radar error investigation began early in 1968, there were some four years of existing mislevel calibrations available for analysis and evaluation.

References 8) and 9) are unpublished reports which were issued based upon these Wallops data. These referenced reports both concluded that the pedestal mislevel error was subject both to gross long term drift effects (there were some data to indicate a cyclical variation with seasonal changes) and to smaller short term shifts (over intervals of several hours). The analysis also investigated the adequacy of the existing calibration procedure which calls for the manual gathering of calibration data.

The results of these investigations which were expanded upon and partially summarized in Reference 10) are as follows:

a) Long term changes in pedestal mislevel were noted where the peak to peak change in the amplitude of the error was on the order of 25 to 30 arc seconds together with an associated peak to peak variation in the measured error's phase angle of 20° to 25°.

b) Short term shifts of 4 to 6 arc seconds were noted in the amplitude of the error over time intervals as short as one to two hours.

c) An analysis of the data indicated that the precision with which the measurements were made (σ = 2 arc seconds) was adequate for calibration purposes if they could be performed immediately prior to or after a mission. The continued use of a manually read calibration instrument did not, however, appear to be consistent with this scheduling requirement. It was recommended that the possibility of automatic calibration be investigated and also that additional tests be performed in an attempt to arrive at some drift error model which would permit the error drifts to be predicted in advance.

Additional tests were performed at Wallops Island on 16 July, 1968 which established that the mislevel drift is at least partially dependent upon solar

heating effects. It was found that the peak to peak variation which occurred over an 18 hour interval was 7° in phase and 7 arc seconds in amplitude[11].

Finally as a part of the special tests described in Section 4.2 an attempt was made to obtain pre-and post-mission leveling calibrations for a high elevation GEOS track. This special test was performed in an attempt to obtain a better understanding of the large azimuth angle residual errors which occur during short arc orbital solutions for high elevation passes. The data from this special test have not, as yet, been fully reduced. However, based upon the leveling measurements it was possible to compute the leveling error which existed during this particular mission. It was found[12] that the mislevel errors (average of pre-and post-mission calibrations) were approximately 9.8° in phase and 2 seconds of arc in amplitude with respect to the actual computer constants used during this mission. It was computed that these uncorrected leveling error terms would have caused approximately 50 arc second azimuth error in the tracking at PCA (El = 84.5°). The test is more fully discussed in Reference 12.

3.1.2 Boresight Null Shift Error

As listed in the radar error model (see Section 2.1), the radar angle tracking data is subject to a track mode dependent systematic error which is referred to as the boresight null shift error. This error is functionally dependent upon the operating characteristics of the microwave, feed and antenna portions of the radar. Since it exhibits a frequency dependence, it is necessary

that it be redetermined each time the radar's operating frequency is changed. Since the radar receiver (including the receive microwave path) operates at a different frequency for the skin and beacon portions of a skin/beacon mission, it is necessary that separate correction constants be contained within the computer for each of these two operating modes.

The boresight null shift error affects the actual location of the RF antenna beam axes relative to the pedestal mechanical axes. If the necessary coordinate transformation is carried out to translate this beam error into azimuth and elevation errors, it is found that the error appears as a bias (non functional) error in elevation while a secant of elevation angle dependency is found for its effect upon azimuth.

The above discussion pertaining to the function form of the boresight null shift error has been included since an understanding of this relationship is necessary if the discussion which follows is to be understood.

One of the standard pre- and post-mission calibrations which were performed throughout the GEOS project is commonly referred to as a normal-plunge calibration. This simple test merely requires that the radar be successively locked onto the boresight tower target in normal and plunge track modes. (Plunge mode refers to the situation where the radar is locked onto the tower after first being "plunged" 180° in elevation and rotated 180° in azimuth). By properly manipulating the resultant angle data it is possible to obtain a measure of the radar's boresight null shift error.

An analysis of these normal-plunge boresight calibrations was carried out to determine the approximate magnitude of the boresight null shift or skew errors. It was found that this error source did not appear to be as stable as had been anticipated. Having established the apparent mean skew error from the calibrations, a check was made to determine the value of the error coefficient being used in the Wallops radar' 4101 computer. It was found that no separate boresight null-shift error coefficients were being inserted into the program. Instead, angle bias correction coefficients were being selected so that the proper corrections were achieved relative to the known location of the boresight tower. This bias correction approach is legitimate for elevation null shifts but, since the azimuth skew error is a function of the elevation angle, the use of this approach in azimuth resulted in improper skew correction. Since the mean value of the null-shift error was known to be on the order of 20-arc-seconds, the misuse of the correction program was introducing approximately a 200 arc-second error in azimuth at an elevation angle of 84° (20 X secant · 84°). The radar operating procedures were changed after this error was found and the proper boresight null shift corrections are now being applied to the angle data.

3.1.3 Dynamic Lag Angle Investigation

One of the earliest tasks performed as a part of the GEOS-II program was an evaluation of the expected angle lag errors. This investigation, which is discussed in Section 2.4 was necessary so that decisions could be reached regarding optimum radar operating parameters. All of the pertinent decisions were made including the decision not to apply lag angle corrections in real time. This lag angle correction decision was based upon three factors:

a) The predicted target dynamics are sufficiently low so that only very small lag errors are expected if the radar is operated in the wide servo bandwidth mode as recommended.

b) The existing AN/FPQ-6 lag angle correction computation is based upon a linear approximation to the antenna off-axis error gradient which is of limited use in correcting very small lag errors.

c) The receiver gain characteristics are not adequately stable to ensure proper lag correction unless special calibrations are performed on a daily routine basis. (Such a calibration schedule was found to be unrealistic from a scheduling point of view.)

As the project proceeded, large azimuth error residuals began to appear in the short arc solutions associated with high elevation passes. Since the lag-errors translate into the azimuth coordinate as a function of the secant of elevation, the lag angle error assumptions were reviewed to reestablish their validity.

The predictions regarding the expected magnitude of the lag errors were checked by making use of actual tracking data[13]. Based upon assumed values for the servo velocity and acceleration gain constants (K_v) and (K_a), the theoretical lag error was computed for some actual GEOS missions. These theoretical lag curves were then compared to the actual lag errors as computed in real time by the 4101 computer.

(Note that the lag errors were computed and recorded in real time but not actually applied to the tracking data.) As a result of this investigation, it was found that the lag error model being used could indeed predict realistic values for the lag errors (See Figure 11). Based upon this result, there appeared to be no reason to change the original decision not to apply lag error corrections.

Even though the small nature of the lag errors was verified, there would be no reason not to apply a correction if confidence existed in the correction technique. The effects of the linear error pattern approximation were investigated again. Actual error pattern calibration data were reduced and analyzed and it was concluded[14] that the original decision was indeed valid. An interesting outcome of this investigation however was the conclusion that a significant improvement in lag error correction for small lag errors could be achieved merely by changing the calibration so that only small offset angles were measured. It was suggested that such a calibration change be performed for subsequent GEOS tracks but this suggestion was never actually carried out. Based upon these GEOS results and upon other considerations, RCA's newest line of C-Band radars (AN/MPS-36) make use of an improved lag correction technique. This revised procedure approximates the antenna error pattern with two straight line segments rather than only one. One of the two segments covers only the nearly linear portion of the error pattern so that corrections can realistically be applied for small lag errors.

A final investigation was conducted to determine whether or not the expected equipment stability problem was a valid factor to take into consideration in reaching the lag error decision. An analysis of receiver gain calibrations

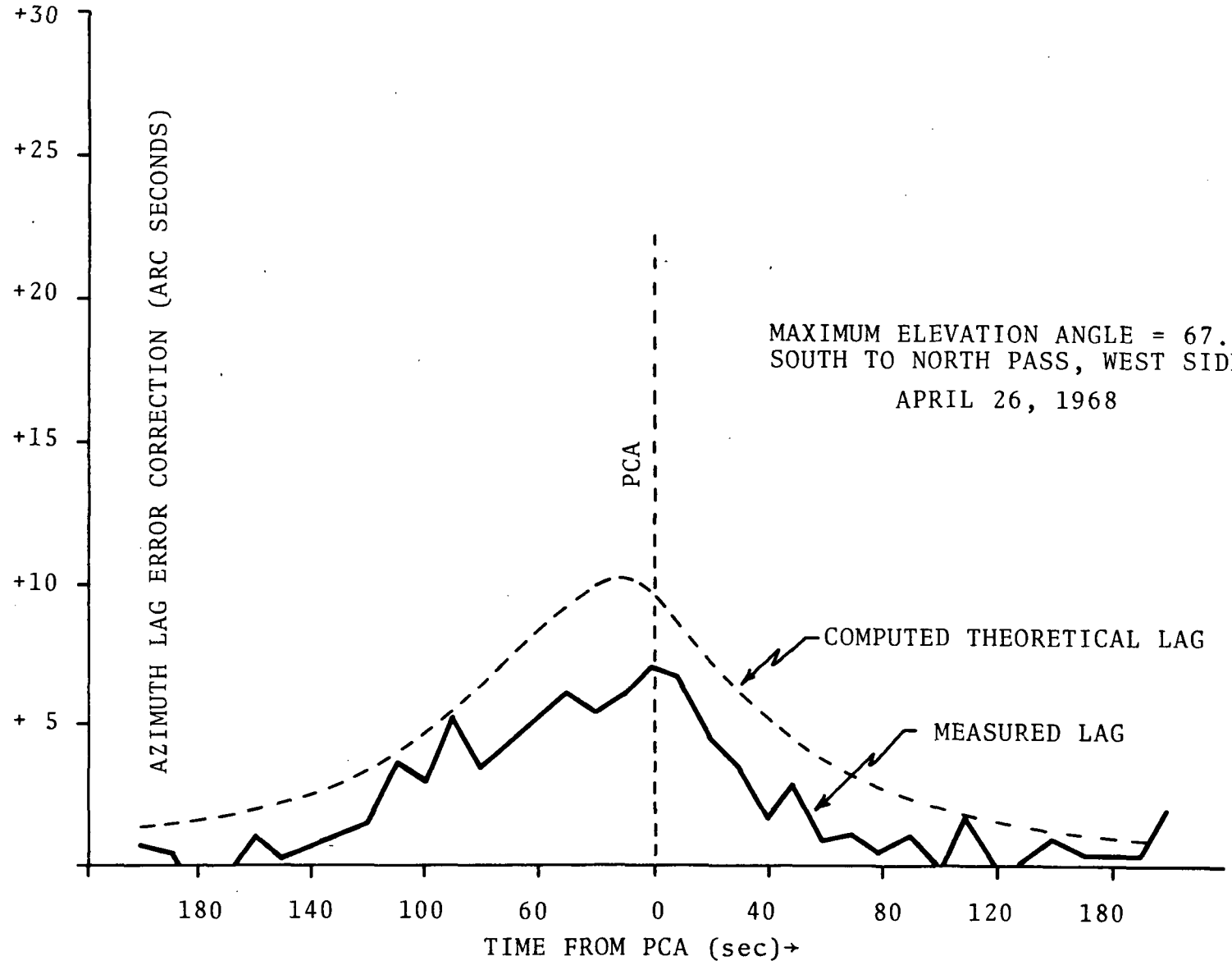

FIGURE 11

AZIMUTH LAG ERROR FOR TEST NO. 24

was performed which showed that the equipment did not exhibit the expected drift characteristics. Therefore, it was concluded that lag error calibrations would not have to be performed on a daily basis as had previously been assumed.

As a result of all the lag error investigations, it was decided that real time lag error corrections would not be applied to GEOS tracking data unless and until the calibration program is changed to limit the measurements to only small (< 1.0 MIL) off axis angles. Lag error corrections should be carried out if such a calibration change is made and if periodic (at least once a month and after every receiver realignment) calibrations are performed.

3.1.4 Use of GEOS as an Azimuth Calibration Aid

As mentioned previously, large azimuth angle errors continued to show up in short arc orbital solutions for high elevation tracks. Since it was difficult to pinpoint the cause of this apparent error based upon standard equipment calibrations, it was decided to use long arc orbital solutions in an attempt to separate the error into its bias and systematic components. A separate investigation had previously established the fact that long arcs (especially multi-station) solutions should be useful for this purpose[15].

3.1.5 Elevation Angle Errors

From the radar error model presented in Section 2.1, it can be seen that the form of the various elevation angle

errors would be relatively small. Analyses carried out on early GEOS-II tracks using short arc techniques showed this expectation to be true[18,19,20]. The use of long arc techniques resulted in an estimate of the Wallops Island AN/FPQ-6 elevation bias error (30 to 40 arc seconds) for the radar configuration utilized throughout most of the GEOS-II project. Recent modifications of the Wallops Island radar (installation of a new antenna feed and subreflector assembly and new angle encoders) have, however, now made these previously valid results obsolete. It is expected that new elevation error estimates will result as new tracking data become available for analysis. Preliminary investigations indicate that the magnitude of the residual droop error term has significantly changed as a result of the antenna feed/subreflector modification. Additional analyses of long arc orbital solutins or an analysis of the special droop test data (see Section 4) should provide an up-to-date estimate of the magnitude for the droop error coefficient.

3.2 RANGE ERROR INVESTIGATIONS

Data gathered during the GEOS-II C-Band Systems project were split into two main categories:

a) Beacon-Only Tracks - Since this target contained two C-Band beacons, the beacon-only tracks could be further subdivided into Beacon #1 (Short delay) tracks and Beacon #2 (Long delay) tracks. The nominal beacon delay used was 112.47 meters for Beacon #1 and 739.48 meters for Beacon #2. Due to uncertainties in these beacon delay times as well as possible differences in beacon output pulse widths, a separate range error evaluation was carried out for tracking data from each of the two transponders.

b) Skin/Beacon Tracks - Due to the presence of a satellite borne passive Van Atta Array, the AN/FPQ-6 was able to skin track the GEOS-II satellite. Therefore, a number of missions were carried out where the AN/FPQ-6 radar performed a beacon track during the initial and final stages of a satellite pass with switchover to skin (echo) track occurring near the point of closest approach (PCA). Since the AN/FPS-16 radar was incapable of skin tracking the vehicle, it performed simultaneous beacon-only tracks while the AN/FPQ-6 carried out its skin/beacon mission.

Due to the different mission modes employed, it was desirable to subdivide the potential radar range errors into those errors which affect both skin and beacon tracking data, and into those errors which affect only the beacon track data.

Errors which affect both skin and beacon data are:

Range Target Survey Errors
Propagation Errors
Drift Errors
Transit Time Errors
Dynamic Lag Errors
Miscellaneous Set-Up Dependent Errors (PRF mode, L.O. mode)
Radar Dependent Random Errors

Errors which affect only the beacon track data are:

Bandwidth/Pulse Width Mismatch Error
Beacon Delay Error
Beacon Delay Jitter

The effects of each of these range errors were evaluated during the project. The evaluation employed, and the results of the evaluations are discussed in the following sections.

3.2.1 Effects of Miscellaneous Radar Operating Parameters

The status of each of the following selectable radar operating modes was found to affect the radar's range zero-set error. In most cases this mode dependent error was eliminated by simply making sure that the radar was set up in an identical operating state during both the pre-mission calibrations and the actual tracking missions.

In some cases it was necessary to switch from one mode to another during a mission. These unusual cases were taken into account by obtaining a measure of the radar's sensitivity to each of the variable parameters. These measurements were obtained by varying the operating parameters in a prescribed manner while locked onto a reference range target. Analysis of the resulting range data permitted the effects of each parameter change to be computed.

The set-up parameters which were investigated and the results of the evaluation are:

Radar Parameter	Radar Change Measured
a. Beacon Code (switched from "off" to "on")	
FPQ-6 (0.5μ second pulse)	+ 1.9 meters
FPQ-6 (1.0μ second pulse)	+ 4.3 meters
FPS-16 (0.5μ second pulse)	+ 0.9 meters
b. PRF (switched from 640 to 160)	
FPQ-6 (0.5μ second pulse)	+ 0.9 meters
FPQ-6 (1.0μ second pulse)	+ 1.0 meters
FPQ-6 (2.4μ second pulse)	+ 1.5 meters
FPS-16 (0.5μ second pulse)	+ 0.9 meters
FPS-16 (1.0μ second pulse)	- 0.6 meters

3.2.2 Range Zero Set Drift Effects

There are various types of radar tracker configurations represented by the world-wide network of C-Band radars. The two C-Band radars at the NASA Wallops Island Station contained different models of digital range machines. The AN/FPQ-6 radar contains a DIgital RAnge Machine (DIRAM) which is the earliest in a family of RCA digital range trackers. The AN/FPS-16 radar at Wallops Island has been modified and its electro-mechanical ranging system has been replaced by an Advanced Digital RANger (ADRAN). The ADRAN, which is also built by RCA, is an advanced version of the older DIRAM. The main physical difference between the two trackers is the completely solid-state nature of the circuits used in ADRAN while DIRAM made use of a combination of transistor and vacuum tube circuitry. This difference in construction is mentioned since the use of tubes in the DIRAM meant that significantly more heat is dissipated in DIRAM than in the subsequent all solid state

RCA range trackers such as ADRAN and IDRAN (Integrated Circuit Digital RANge). It was recognized that a range zero-set thermal dependent drift might exist in the DIRAM. Therefore, tests were conducted to obtain a measure of the gradient of this thermal drift and to determine the warm up time which would be needed to ensure equipment stability prior to track. The tests simply consisted of locking the radar onto the reference range target and observing the change in the range measurement as the equipment warmed up. The results of this test are depicted in Figure 12.

From the Figure, it can be seen that warm up times of from four to six hours would be necessary if this drift effect were to be reduced to the point where less than a 1 meter error is to occur during a 1 hour tracking mission. Further reference to the measured drift curve will show that the drift error will be less than three meter over a one hour interval as long as the radar is allowed at least two hours for warm up. If pre-and post-mission range calibrations are performed and if the average value between these two readings is used during post mission data reduction, the DIRAM drift error can be limited to approximately 1 meter. The alternative is to allow the equipment to stabilize prior to calibration. The pre and post mission calibration procedure was followed at NASA Wallops Island throughout the GEOS-II project.

Similar tests performed on the ADRAN type of range machine did not indicate that thermal drift was a significant factor in the calibration of these trackers. However, similar pre-and post-mission measurements were also taken by the Wallops Island AN/FPS-16 radar.

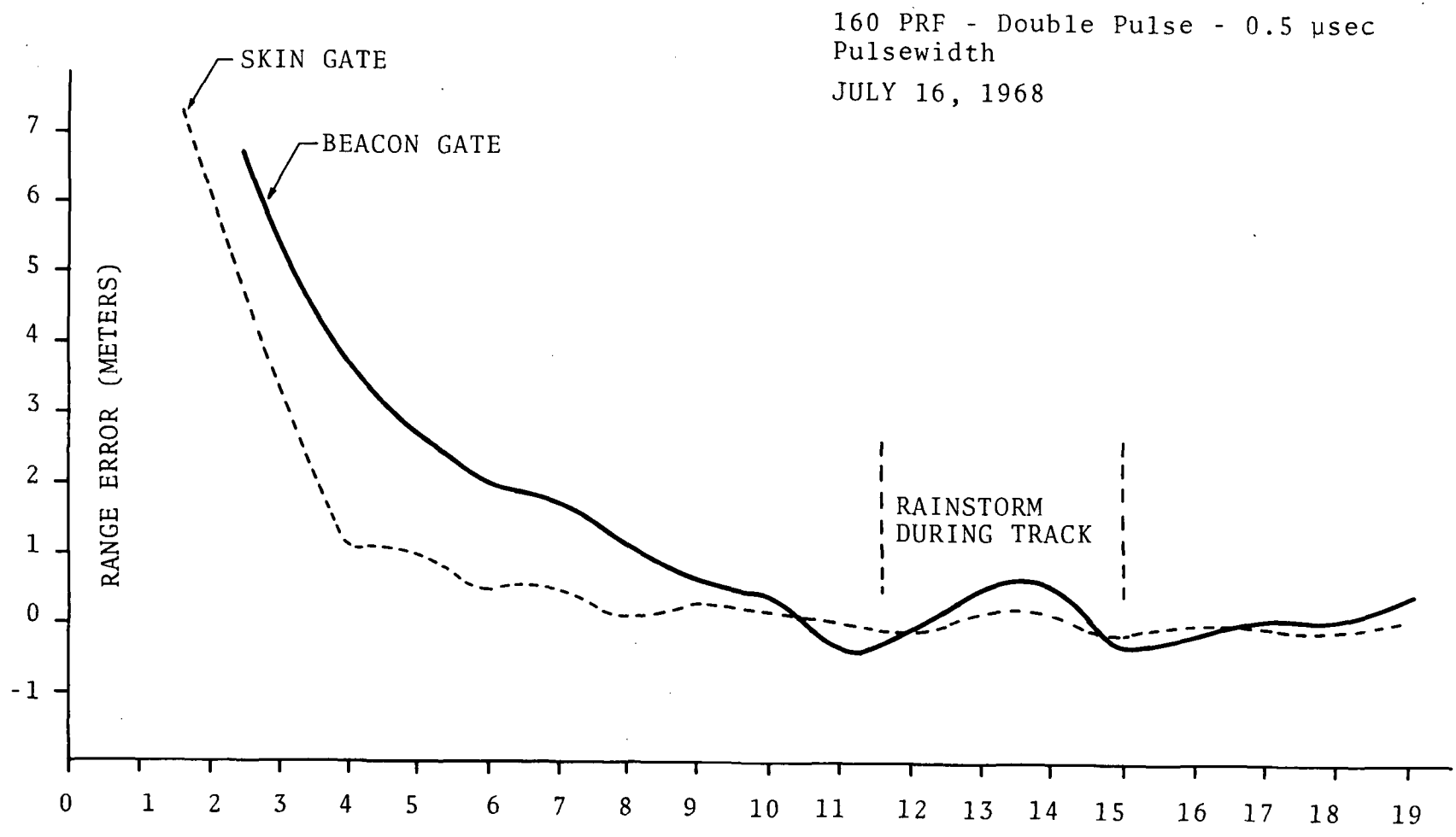

RANGE DRIFT OF DIRAM

FIGURE 12

3.2.3 Range Calibration Atmospheric Propagation Error

It is common practice for radar data users to apply a correction factor to radar elevation and range tracking data to compensate for effects of the earth's atmosphere. In the case of range data the presence of the atmosphere tends to reduce the velocity of propagation relative to that which would occur in a vacuum. Since the radar's range measurement is based upon an assumed vacuum condition, the uncorrected range readings obtained during the tracking mission are long and a range propagation correction must be subtracted from the measured range reading. The amount of correction depends upon the atmospheric path length and is, therefore, a function of the radar-to-target geometry. Section 3.2.7 provides a discussion of the post-mission corrections performed on the GEOS tracking data to remove this propagation error.

Unfortunately, the effects of the non-vacuum propagation medium are often neglected when the radar is being calibrated against a reference range target. Figure 12 shows the effect of a rainstorm on the calibration range measurements. This atmospheric correction factor attains significance only when the reference target is located at long distances from the radar. The distances to the reference targets at Wallops Island are given below for each of the C-Band radars. Using an average value for the ground level index of refraction, it is possible to compute the nominal propagation error which will result if the propagation effects are ignored during calibration. These computed values are also given below:

Target	Radar	Survey Distance to Range Target	Nominal Propagation Error
Kennedy Tower	AN/FPQ-6	8193.02 meters	.2438 meters
FSR	AN/FPQ-6	3544.82 meters	.9144 meters
NAOTS Tower	AN/FPS-16	10,910.30 meters	3.2004 meters
FSR	AN/FPS-16	1733.40 meters	.4572 meters

Wallops Island is currently using the FSR (Frequency Shift Reflector) as its reference range target and, therefore, the effects of this propagation error during calibration is quite small. However, the Kennedy and NAOTS Towers were used during the early part of the GEOS project (i.e., during the WICE) and, therefore, the WICE data contains range propagation zero-set errors having a magnitude as indicated above.

3.2.4 Reference Range Target Size Error

The radar's range is zero set by forcing the output range data to agree with some a priori reference range while the radar is locked onto a reference range target. The actual method of range adjustment varies from radar to radar but the end result is always the same. The range to the reference target which is used as the zero set value is usually obtained by accurate survey techniques. However, the validity of the zero set method requires that the radar be locked onto the exact point on the target which was used during the survey. Such an exact correlation is extremely difficult to achieve in practice unless specially fabricated reference targets are used for range calibration purposes. One such reference range target is a Frequency Shift Reflector (FSR). Wallops Island procured and installed an FSR early in 1969. Unfortunately, this point-source

target was unavailable during the WICE tests. Therefore, the WICE range data contained a zero set bias error which was introduced during calibration by making use of physically large reference range targets. The later installation of the FSR permitted the magnitude of WICE zero-set range error to be evaluated. The evaluation procedure was quite straight forward and consisted of measuring the range to the previously used range target after first zero setting the radar against the FSR. The difference between this range and the previously used survey distance would then be a measure of the WICE target size error. The evaluation procedure was, however, somewhat complicated by the fact that the new FSR was located quite near the radars while the previously used WICE range target was located at a greater distance. This difference in range meant that the analysis had to take propagation effects into account. As a specific example, a large water tank had been used to calibrate the Wallops Island AN/FPS-16 radar during the WICE. This tower was located almost 10,910 meters away from the radar. A normal propagation error on the order of 3.2 meterscould be expected over such a large range. This large propagation effect had to be compared to a much smaller propagation error of only.4572 meters which would be expected at the 1676 meter FSR ranges. Thus, a 2.74 meter range error would be introduced into the water tank measurements due to the differences in propagation effects. This propagation range difference was taken into account during the evaluation of the target size effects.

Tables 7 and 8 contain a listing of calibration data which were gathered using both the FSR and the previously used range targets. Table 7 contains AN/FPQ-6 range calibration data. The second target referred to as the Kennedy

tower was the target used by the FPQ-6 during WICE. Table 8 contains similar data from the AN/FPS-16 radar.

The apparent target size error can be computed from these data as follows:

a) Compute a propagation corrected value for the target's beacon gate survey range as follows:

	Original Survey Range (meters)	+	Prog. Corr.	-	Beacon Delay Setting (Meters)	=	Corrected Range (meters)
FPQ-6 to FSR	3544.82		.9144		731.52		2,814.2184
FPQ-6 to Kennedy Tower	8193.02		2.4380		731.52		7,463.9420
FPS-16 to FSR	1733.39		.457		731.52		1,000.1824
FPS-16 to NAOTS Tower	10,910.32		3.20		731.52		10,181.8440

b) Compute the expected difference in range between the FSR and the appropriate tower:

For FPQ-6: DR = 7,463.9424 - 2,814.2184 = 4,649.724 meters
For FPS-16: DR = 10,181.9964 -1,002.3348 = 9,179.662 meters

c) Compute the average difference in measured range from the radar to each target (see Tables 7 and 8).

From FPQ-6 to Kennedy Tower $\overline{R}$ = 7,462.7536
From FPQ-6 to FSR $\overline{R}$ = 2,813.6697
Measured R(FPQ-6) = 4,649.0839

From FPS-16 to NAOTS Tower $\overline{R}$ = 10,174.8336
From FPS-16 to FSR $\overline{R}$ = 1,003.0968
Measured R(FPS-16) = 9,171.7368

TABLE 7

WALLOPS ISLAND
AN/FPQ-6 RANGE CALIBRATION DATA

Rev. #	FSR Measurement (meters)	Kennedy Tower Measurement (meters)
4917 Pre	2813.91	7460.59
4917 Post	2813.30	7463.33
4973 Pre	2813.30	7464.25
4973 Post	2813.39	7460.59
5025 Pre	2814.83	7463.03
5025 Post	2814.52	7462.11
5046 Pre	2814.52	7464.55
5046 Post	2814.22	7463.33
5057 Pre	2814.52	7458.15
5057 Post	2814.83	7465.77
5089 Pre	2813.61	7462.92
5089 Post	2813.30	7461.81
5102 Pre	2813.30	7463.03
5102 Post	2813.00	7463.64
5108 Pre	2813.00	7464.55
5108 Post	2812.39	7463.03

TABLE 8

WALLOPS ISLAND

AN/FPS-16 RANGE CALIBRATION DATA

Rev.	FSR Beacon Gate Measurement (meters)	Water Tank Beacon Gate Measurement (meters)
8170 Pre	1001.57	10174.53
8170 Post	1001.57	10173.61
8222 Pre	1003.71	10173.00
8222 Post	1004.93	10171.45
8311 Pre	1003.40	10173.31
8311 Post	1001.27	10172.09
8324 Pre	1002.79	10172.40
8324 Post	1001.88	10172.70
8326 Pre	1002.98	10173.92
8326 Post	1001.57	10172.40
8350 Pre	1003.10	10176.66
8350 Post	1003.40	10176.36
8363 Pre	1004.93	10176.66
8363 Post	1005.54	10178.19
8351 Pre	1004.32	10176.05
8351 Post	1003.40	10173.92
10746 Pre	1002.18	10175.44
10746 Post	1003.10	10176.05
10502 Pre	1003.40	10177.58
10502 Post	1003.71	10177.27
10495 Pre	1003.10	10176.66
10495 Post	1003.10	10175.75
10823 Pre	1002.18	10175.14
10823 Post	1003.10	10173.92
10836 Pre	1002.49	10173.92
10836 Post	1002.49	10174.53

d) Compute the apparent target size error by subtracting the measured differences of c) from the expected differences of b):

Apparent Kennedy Tower Size error =

4649.72 - 4649.08 = 64 meters

Apparent NAOTS Tower Size error =

9,179.66 - 9171.74 = 7.92 meters

Therefore, the pre FSR FPS-16 radar ranges should be corrected for a Kennedy Tower size error by subtracting 0.6 meters from the measured ranges. The pre FSR FPS-16 radar ranges should be corrected for a NAOTS tower size error by subtracting 7.9 meters from the measured ranges.

3.2.5 Range Dynamic Lag Error

The digital range trackers which are used by most radars which participated in the GEOS-II C-Band Systems project are closed loop trackers and as such have a finite response time to changes in target dynamics. The range servos used in the RCA range trackers are referred to as type 2 servo loops which means that two integrations occur within the servo loop. This in turn means that only range acceleration and higher order dynamic errors will build up in the loop. For an orbiting object such as GEOS-II, the range acceleration is the only dynamic term which might introduce a significant range servo lag error. For the range servo bandwidth chosen (approximately 4 Hz) the range servo's acceleration constant (K_a) is approximately 210 $sec.^{-2}$.

Therefore, assuming a maximum GEOS-II range acceleration value of 50 meters/sec^{-2}, the magnitude of the range servo lag error can be computed to be

$$E(\text{range lag}) = \frac{50}{200} = 0.25 \text{ meters}.$$

This is considered to be a negligibly small range error.

3.2.6 Pulsewidth/Bandwidth Mismatch Error

The term pulsewidth/bandwidth mismatch error has been originated to describe the range bias error which occurs in a centroid type of range tracker due to the use of a different pulsewidth during calibration than is received during the actual mission. This situation obviously existed whenever the C-Band radars performed a beacon (transponder) track of the GEOS-II satellite. The pulsewidth effects are easily visualized and will, therefore, be discussed first. The simple pulsewidth dependent error model is subsequently extended to cover the more general case of where both pulsewidth and bandwidth effects are modeled.

The pulsewidth mismatch effects arise due to the centroid tracking technique which is used by modern day digital range trackers. The effect os using a different pulsewidth during calibration and track is such as to introduce a range bias error. If an infinite bandwidth receiver is assumed (i.e., the bandwidth effects neglected for the moment), the range bias error introduced will be directly proportional to one-half the difference in pulsewidths.

For discussion purposes, consider the situation shown in Figure 13 which depicts a pulsewidth with the mismatch condition. The top waveform represents the return pulse received when the radar's own pulse is reflected from a reference target. The lower waveform might represent the return from a zero delay transponder located at exactly the same distance from the radar. Since the zero set range calibration is assumed to occur with the radar receiving its own pulse, the centroid of the top waveform represents the zero error condition after calibration. If this zero set condition exists and if the range tracker then locks onto the transponder pulse, the range readout will change to a new value as represented by the centroid of the lower waveform. This range change for the simple case being considered is obviously:

$$\Delta R = (\Delta t)(C/2) = (\Delta \tau/2)(C/2)$$

where C represents the velocity of propagation; Δt represents the time difference in the occurrence of the centroids; and $\Delta \tau$ represents the difference in pulse widths. The range would read long for the situation depicted where the transponder reply pulse is assumed to be wider than the radar calibration pulsewidth.

To extend this simple model to the finite bandwidth case, refer to Figure 14, which depicts the effects of an ideal matched filter upon an ideal radar pulse. As depicted, the filter charges linearly throughout the time when the pulse is present. When the pulse disappears the filter discharges. The charge and discharge characteristics are assumed identical for the ideal case being considered.

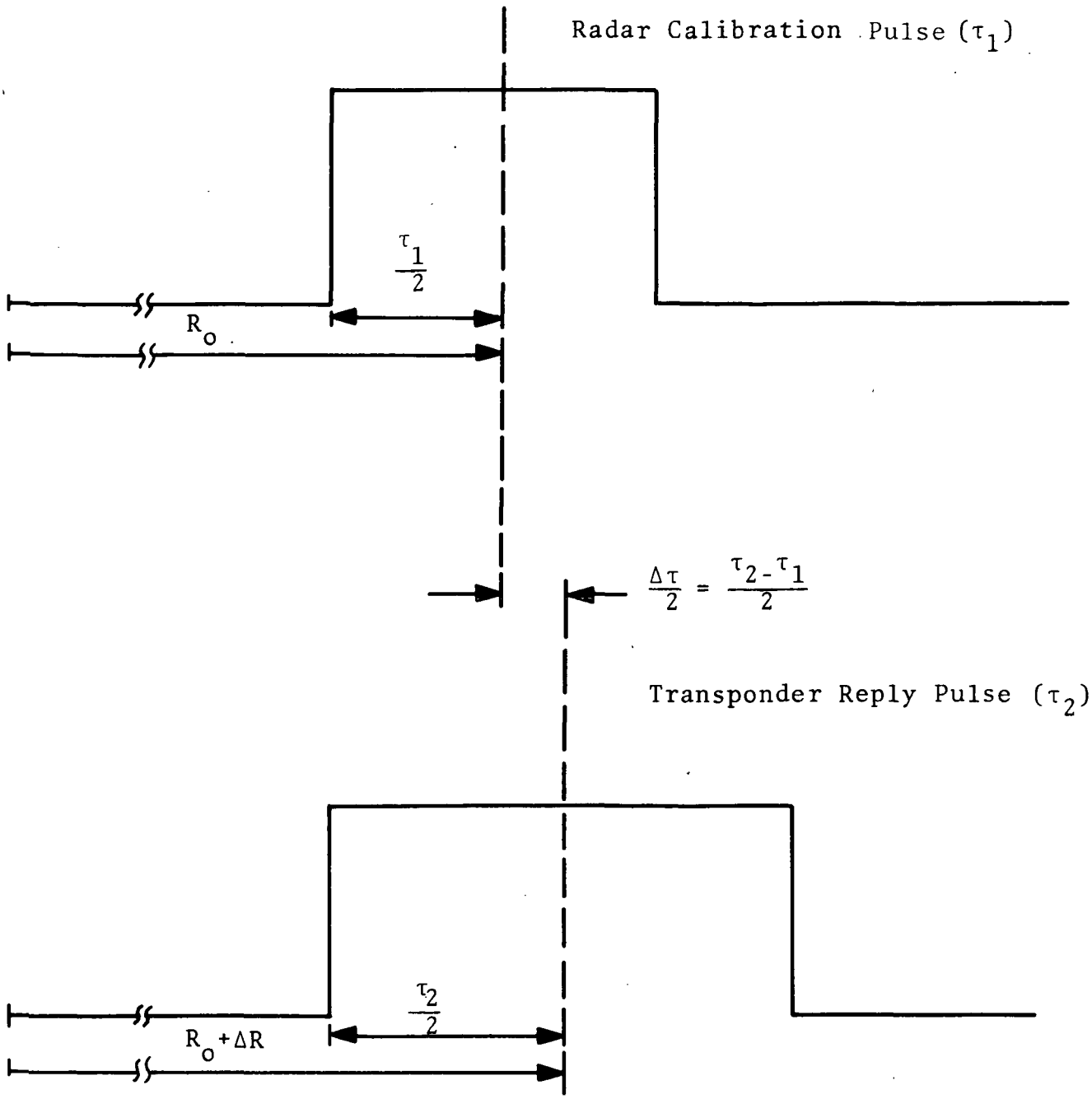

FIGURE 13

SIMPLE PULSEWIDTH EFFECT MODEL

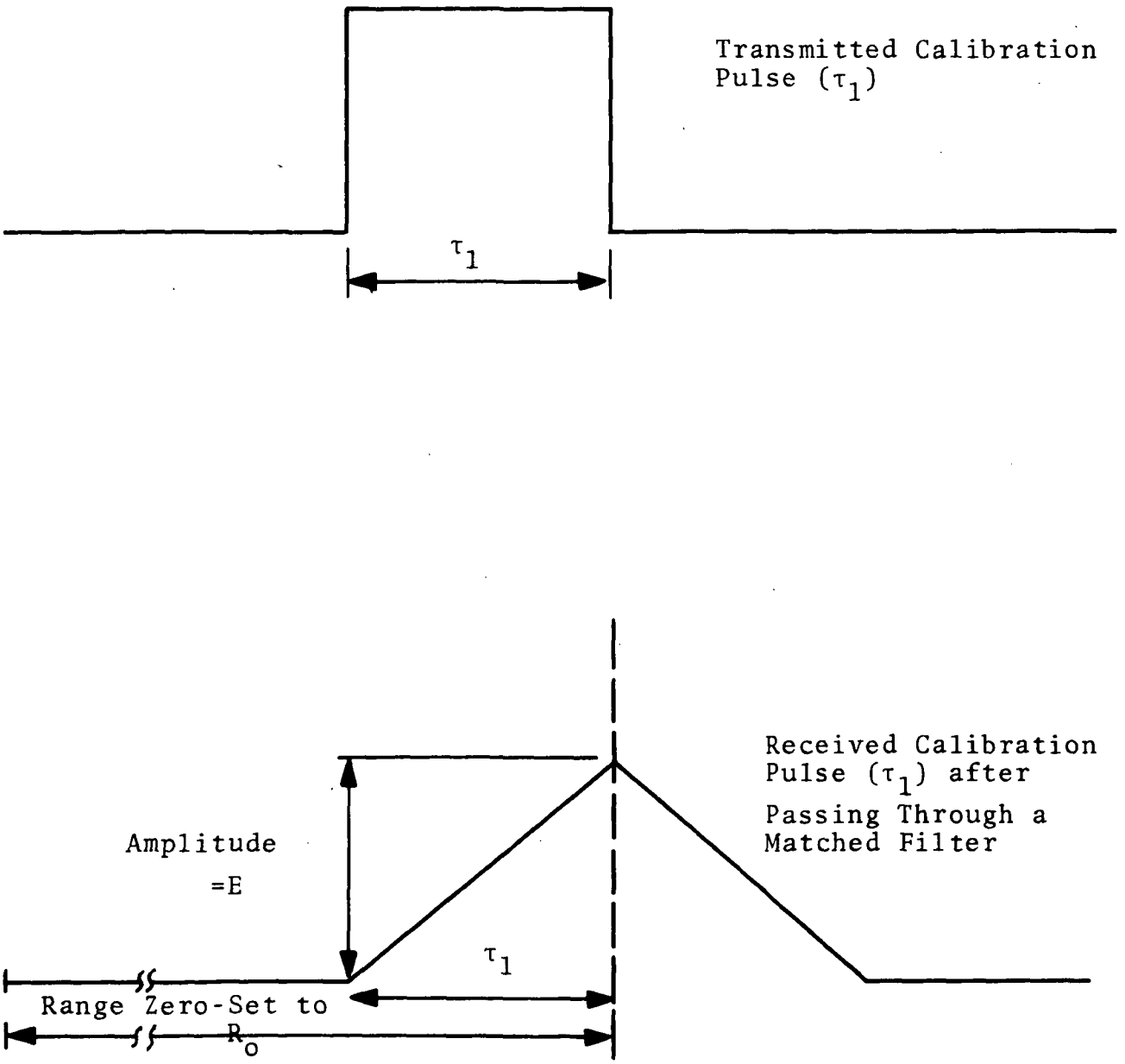

FIGURE 14

EFFECTS OF MATCHED FILTER OPERATION

The term "matched filter" is used here to mean the situation where the ideal filter's charge time and the pulse duration are identical. The effective bandwidth of this hypothetical filter will then be defined to be

$$B = \frac{1}{\tau}$$

Before proceeding with the mismatch error model, it is necessary to establish one final characteristic of the filtering action. It must be noted that the triangular filtered and detected waveform is the input signal which is seen by both the range tracking and AGC circuits. The effects of variations in the received signal's pulse amplitude must, therefore, be considered. The present model will assume that the AGC action is such as to force the detected receiver output to some preset level regardless of the amplitude of the input pulse. This AGC action thus has the effect of causing the ideal filter to always charge to the voltage (E) regardless of the amplitude or duration of the input pulse. The importance of this assumed AGC action will become apparent later in this discussion when mismatched conditions having $B\tau < 1$ are considered.

The interrelationship between pulsewidth, receiver bandwidth and AGC action can now be further investigated.

First, the previously discussed situation where the tracked pulse is wider than the calibration pulse will be reconsidered for the more practical finite receiver bandwidth condition. The filtering action of the receiver can be seen by referring to Figure 15. The top waveforms shown

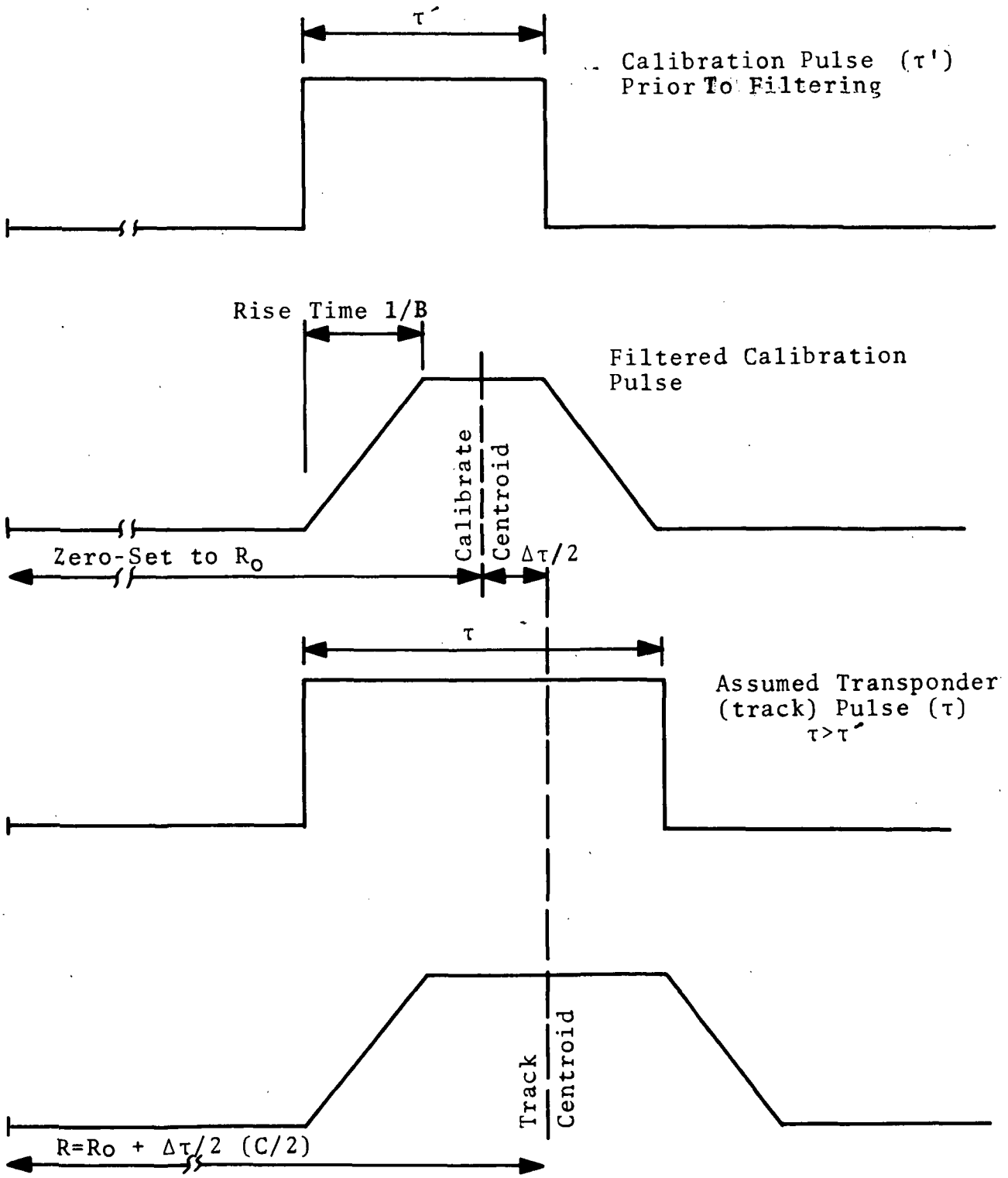

FIGURE 15
FILTERED PULSE RELATIONSHIP FOR
$B\tau > 1.0$

depict the filtered calibration pulse. Therefore, the indicated pulse centroid would be tracked and the range tracker's output would be zero-set at the survey range based upon the time occurrence of this centroid. It should be noted that the calibration pulsewidth is assumed to be greater than the rise time of the idealized receiver bandwidth. This assumption is in accord with normal radar design practices which generally meet the relationship

$$B\tau \geq 1.2$$

For example, the AN/FPQ-6 radar uses a nominal 2.4 MHz bandwidth for receipt of a nominal 0.5 μ second calibration pulsewidth (i.e. $B\tau = 0.5 \times 2.4 = 1.2$). If the equipment had been designed to exactly meet the $B\tau = 1$ condition then matched filter operation would exist as previously discussed.

Now, referring again to Figure 15, note that the difference in the centroid for the two pulses is equal to 1/2 the difference in pulsewidth. This is the identical result which was obtained for the more simple infinite bandwidth receiver model discussed previously. Thus, the simple and the more complex mismatch error models give identical results for mismatch conditions

$$B\tau > 1.0$$

This result is not unexpected and is in fact the reason why the radars are designed to have bandwidths slightly wider than matched filter operation would call for.

As a generalization then, the following rule can be given:

The range mismatch error will be proportional to 1/2 the difference in the calibrate/track pulsewidths for the condition where the width of the tracked pulse is such that the $B\tau > 1.0$ condition is met. (Note that it is assumed that the calibrate pulse also met this criteria during the range zero set calibration).

Figure 16 depicts the as yet undiscussed situation where the transponder (track) pulse is narrower than the calibration pulse. The depicted waveforms represent the case where the track pulsewidth is such that the previously established $B\tau > 1.0$ criteria is violated.

The most important thing to note is that the filtered track waveform has (due to the assumed AGC action) the same peak amplitude as all previously depicted waveforms. If this condition is to exist, it is necessary that the effective charging time of the receive filter be different. That is, the filter now fully charges in a time $t < 1/B$ where previously (i.e. for $B\tau > 1.0$) the fully charged condition always occurred in a time $t = 1/B$.

The next thing to note is the assumption that the discharge time of the filter remains unchanged. This assumption must be true since the discharge takes place after the pulse ends and therefore, must be independent of any receiver AGC action.

The change in the filter charge time is represented by a new slope on the leading edge of the filtered waveform. This slope is now (for $B\tau < 1.0$) only a function of the recieve pulse width. The AGC action is such that a fully

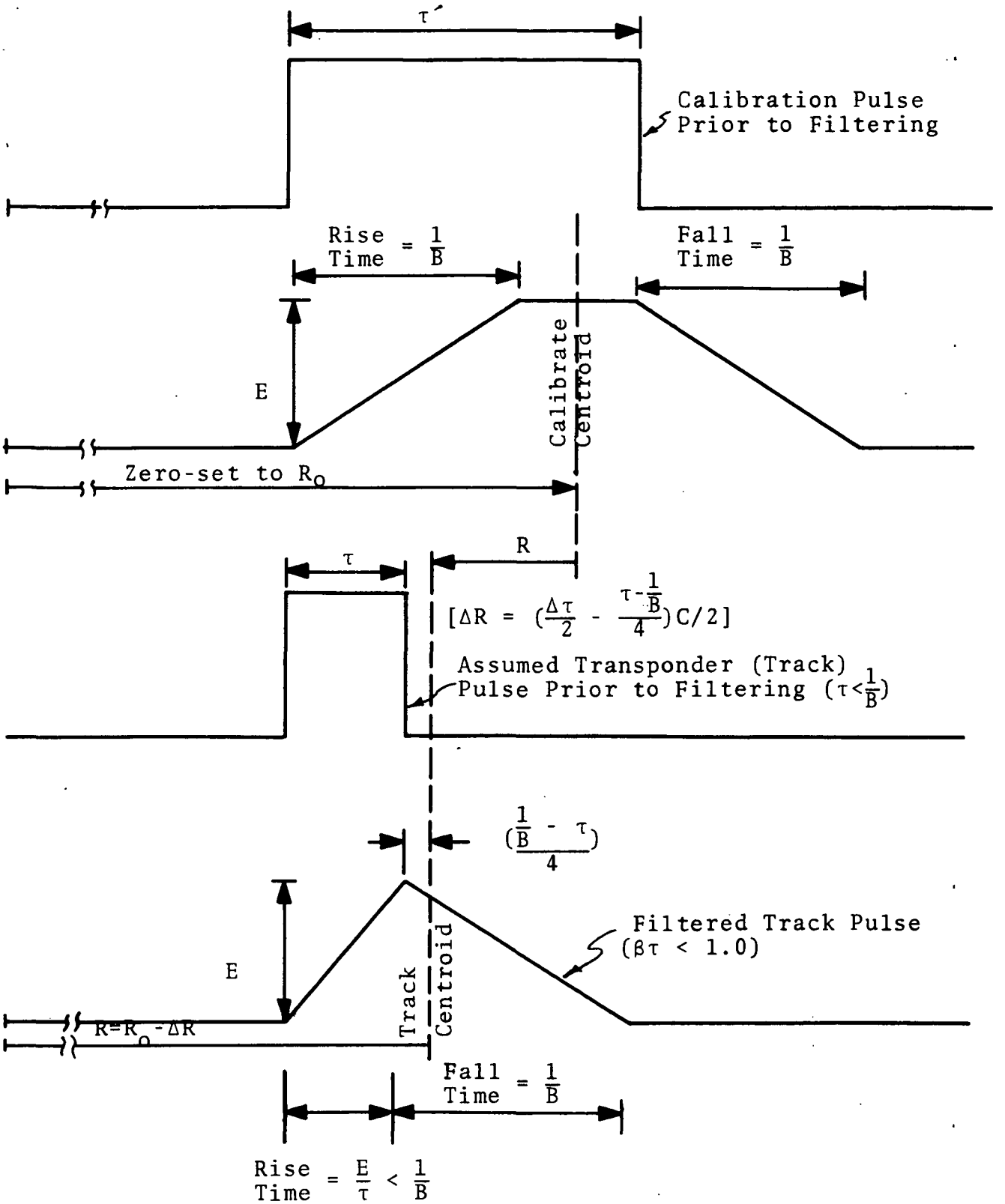

FIGURE 16

FILTERED PULSE RELATIONSHIP FOR

$B\tau < 1.0$

charged condition is reached at the end of the pulse. The trailing edge of the pulse follows the same slope as previously assumed (i.e., slope = $\frac{1}{\tau}$).

The result of the AGC action is to generate a filtered pulse which is no longer symmetric about its maximum amplitude point. As shown in Figure 16, the centroid of this filtered pulse occurs at a point which to a first approximation is equal to:

$$t(\text{centroid}) = t_o + \tau + \frac{1/B - \tau}{4}$$

where

t_o = time at start of the pulse

τ = width of the pulse

B = nominal receiver bandwidth

Since the calibration centroid occurs at:

$$t = t_o + \frac{\tau' + 1/B}{2}$$

where τ' = width of calibration pulse it is possible to arrive at a mathematical expression for the shift in the centroid as a function of pulsewidth (for $B\tau < 1.0$):

$$\Delta t \text{ (in centroid)} = \frac{\tau - \tau'}{2} + \frac{\tau - 1/B}{4}$$

Upon comparison it can be seen that the first term is identical to the expression obtained for the case where $B\tau > 1$ (i.e. error of 1/2 the difference in pulsewidths). The second term is an expression which takes the AGC effects into account (non symmetry).

From the foregoing discussion it is apparent that a range bias error arises whenever a difference in width exists between the pulse used in zero setting the range tracker and the pulse which is received during the mission. In addition, it can be seen that the magnitude of the resulting mismatch error is dependent upon the receiver bandwidth as well as upon the actual pulse width difference. The error model developed above permits the error to be calculated knowing the pulsewidth difference and bandwidth. More importantly, the availability of this model presents the radar user with the ability to obtain measurements of mismatch error by using the radar itself as the test instrument. This self-calibration technique removes the measurement uncertainties which would otherwise exist. A series of mismatch error measurements were carried out using the Wallops Island radars. The technique and results are discussed in Section 4.1. Tables 14 to 21 list the measured values of this range mismatch error for various radar operating conditions.

3.2.7 Track Propagation and Transit Time Range Error Corrections

The GEOS-II range tracking data were automatically corrected for both propagation and transit time errors as a part of the post mission pre-processing program[2]. The corrections which were applied to the data were computed as follows:

a) Refraction Correction

The tropospheric refraction correction applied to Wallops radar data during pre-processing used a measured surface index of refraction and a cosecant dependence upon elevation angle.

The refraction index, μ, for radar is computed as follows:

$$\mu - 1 = \left[\frac{103.49\ (P-e)}{T} + \frac{86.26}{T}\left(1 + \frac{5748}{T}\right)e\right] \times 10^{-6},$$

where

P = total atmospheric pressure (mm Hg),
e = partial pressure of water vapor (mm Hg),

and

T = absolute (K) temperature

If temperature, pressure, and relative humidity are not known, a nominal value of 0.2919×10^{-3} (see reference 10 and 11) for μ-1 is pre-set in the program.

The refraction corrected ranges are computed by:

$$R_c = R_o - [(\mu - 1)(s)/(\sin E_c + .026)]$$

where

E_c = corrected elevation angle measurement
$= E_o - (\mu-1)/[.01644+.93(\tan E_o)]$
E_o = observed elevation angle measurement
R_c = corrected range measurement
R_o = observed range measurement
s = scale height of the atmospheric refractive index, μ, approximately 7.6 km

b) Transit Time Correction

The measurement time tags are corrected to the time the radar pulse left the satellite by the relationship:

$$T_c = T_o - R_c/C$$

where

T_c = corrected observation time (seconds)

T_o = sampled time at radar

C = velocity of light = 299792.5 km/sec.

3.2.8 Beacon Delay Errors

Any error in the assumed value for the internal delay of the beacon will appear as a bias error in the range tracking data. The GEOS-II satellite carried two C-Band transponders having the following nominal transponder delays:

Beacon #1: Delay = 112.47 meters

Beacon #2: Delay = 739.25 meters

These values for the delays are the result of bench calibrations and apply only for specific transponder operating conditions (e.g.: receive pulsewidth 0.5 μsec, rise time of less than 0.1 μsec) and were therefore considered to be only nominal values. It was recognized that there would be at least some minor variations under actual operating conditions.

One operating parameter which certainly effects the transponder delay is the signal strength of the interrogating radar pulse as received at the transponder. An attempt was made to minimize this signal strength dependence

of the delay during the design of the transponder. Subsequent test data indicated that the variation was reduced to a very small value. Figures 17 and 18 show measured (bench test) response curves for transponder delay as a function of receive signal strength. Figure 19 shows theoretical curves for receive signal strength at the transponder for each of the Wallops Island radars. Based upon these curves it is possible to predict that the range error resulting from this delay variation with signal strength should be no greater than approximately $\pm$ 1.0 meters. Analysis of tracking data seems to bear out these predictions.

The transponders have been found to exhibit a delay dependence upon interrogation pulsewidth. This seems to be a negligible effect when only expected variations in the nominal receive pulsewidth (0.5 μsec) are considered. However, changes in the interrogation pulse from the nominal to other widths such as 1.0 μsec have been found to noticeably effect the transponder's delay. The tests performed to verify this pulsewidth dependence are described in Section 4.1. The delay change has been found to result in a + 2.0 meter range change when Beacon #1 is interrogated with a 1.0 μsec pulse. Beacon #2 was found to be slightly more sensitive to pulsewidth change since a range change of + 2.2 meters was measured as its interrogation pulsewidth was switched from 0.5 μsec to 1.0 μsec.

A major uncertainty in the beacon track data is associated with the assumed value for the nominal beacon delay. A series of beacon/skin tracks were carried out in an attempt to obtain a better estimate of the actual beacon delay. These beacon/skin tracks were performed only by the

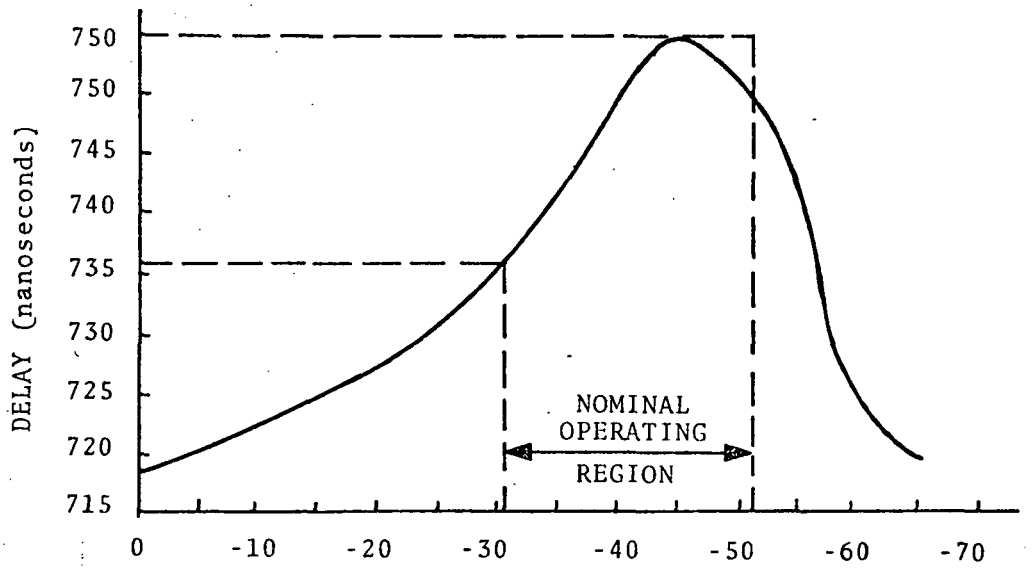

DELAY CURVE - SHORT DELAY TRANSPONDER SN*5 (Beacon 1)

FIGURE 17

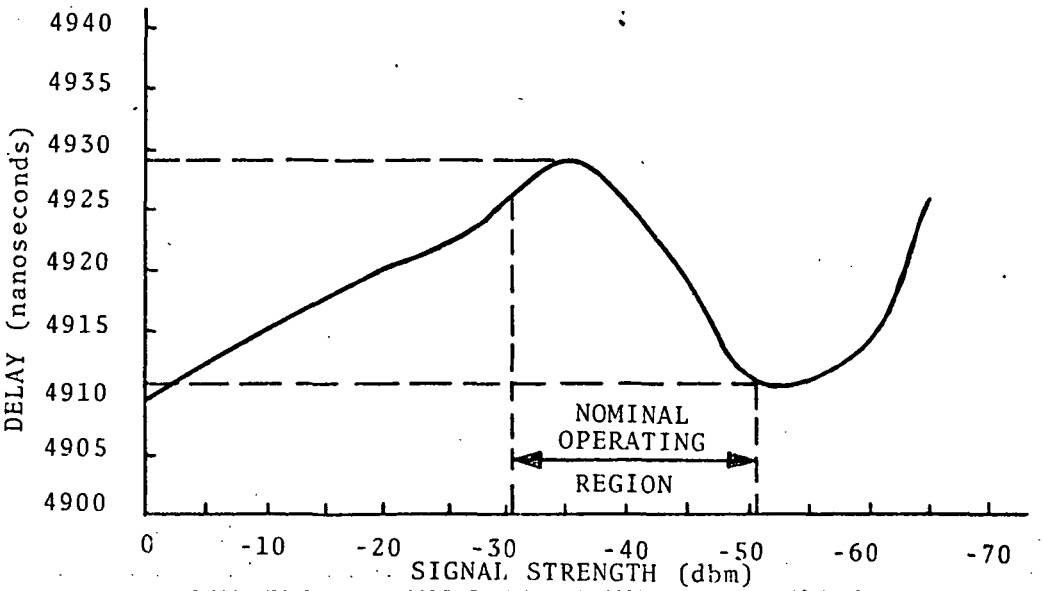

DELAY CURVE - LONG DELAY TRANSPONDER SN*6 (Beacon 2)

FIGURE 18

RECEIVED SIGNAL STRENGTH VERSUS RANGE

FIGURE 19

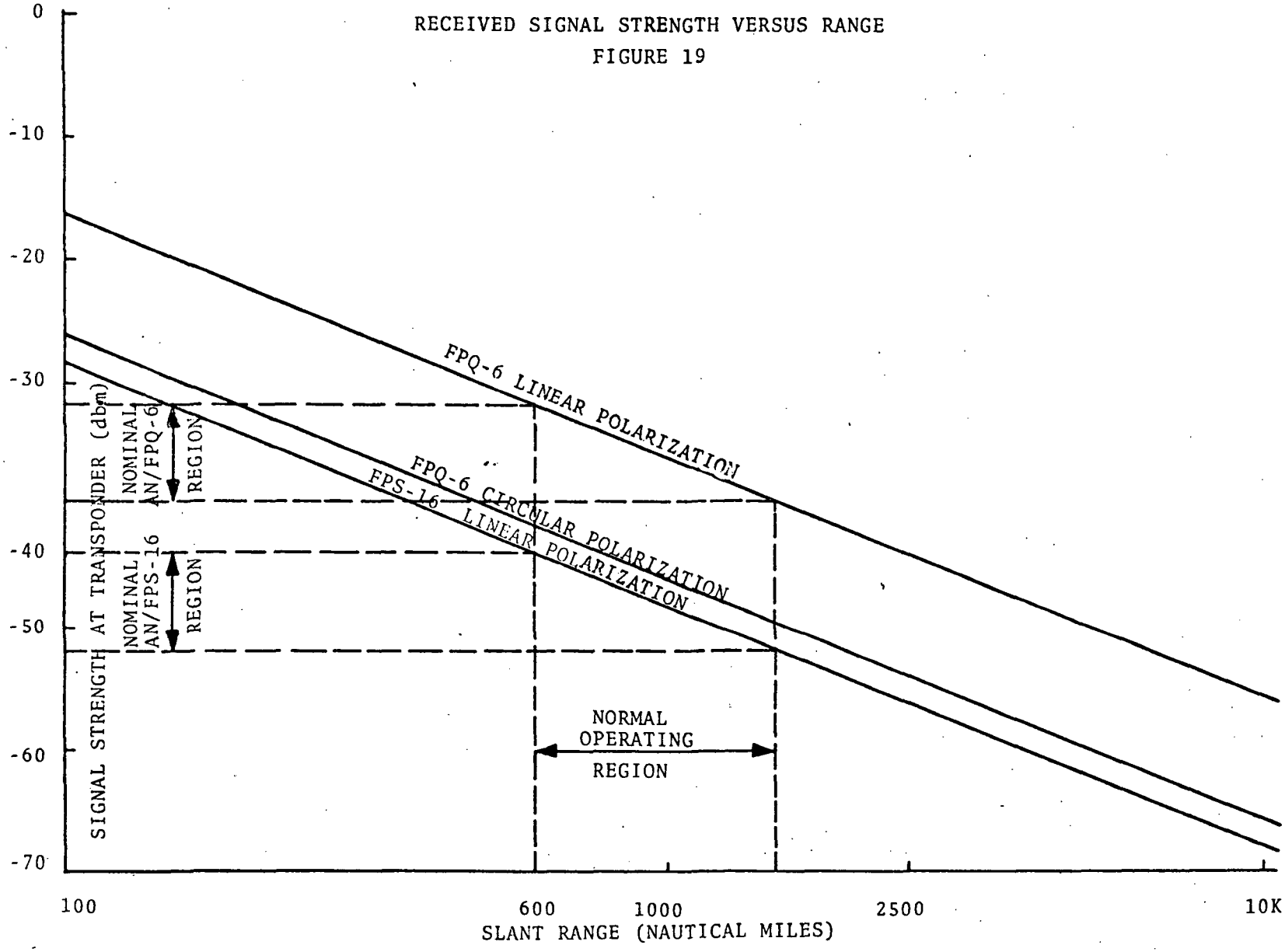

AN/FPQ-6 radar since the satellite's radar cross-section was too small to permit skin track by the AN/FPS-16 radar. Since the AN/FPQ-6 radar's operating parameters had to be switched during these skin/beacon tracks (acquisition was carried out in beacon track mode and the switchover to skin track was made as the satellite approached PCA), it was decided that simultaneous and uninterrupted beacon tracks should also be carried out by the Wallops Island AN/FPS-16 radar. As shall be seen, the availability of these AN/FPS-16 beacon track data provides a convenient method for verifying the beacon delay correction computations.

The first step taken in the beacon delay investigation was to compute the mean difference between the AN/FPQ-6 skin and beacon range residuals. (Short arc solutions based upon AN/FPS-16 beacon track data were used as a common reference for comparison of these data.) It was found that the following skin to beacon range differences existed in the AN/FPQ-6 tracking data:

Beacon #1: + 19.8 meters

Beacon #2: + 25.5 meters

where the positive sign indicates that the skin track residuals were above the beacon track residuals (i.e., the skin track ranges were longer.) These residual differences are shown in Figures 20 a) and 21 a) respectively.

The computed residual difference cannot be used directly as a measure of the beacon delay error. Instead, it is necessary to correct these residuals for all those known

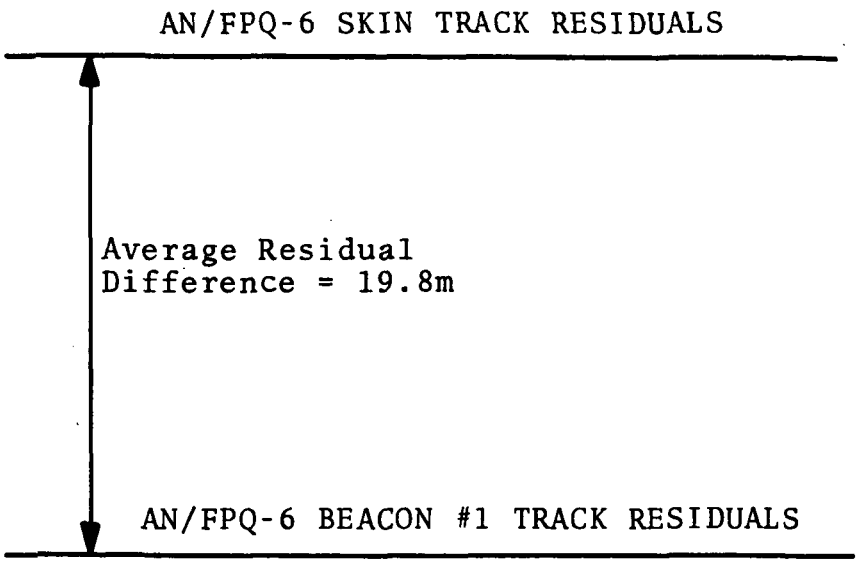

(a) Original Residual Difference

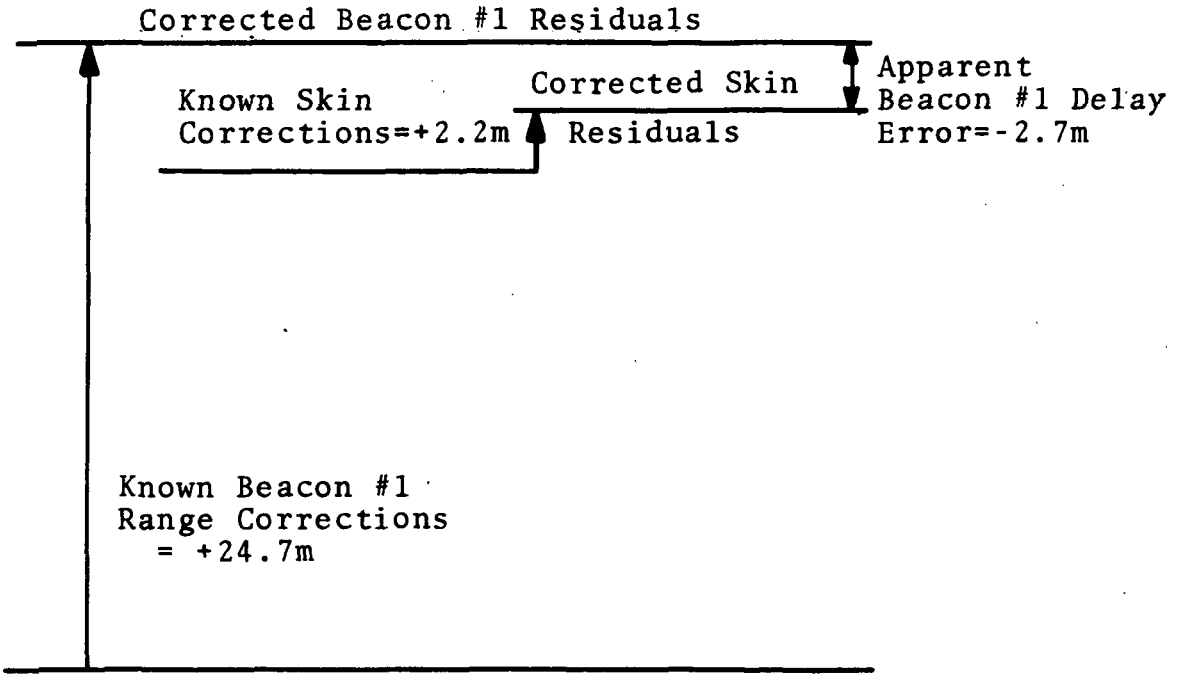

(b) Corrected Residuals

FIGURE 20

AN/FPQ-6 SKIN/BEACON #1 RANGE
RESIDUAL DIFFERENCES

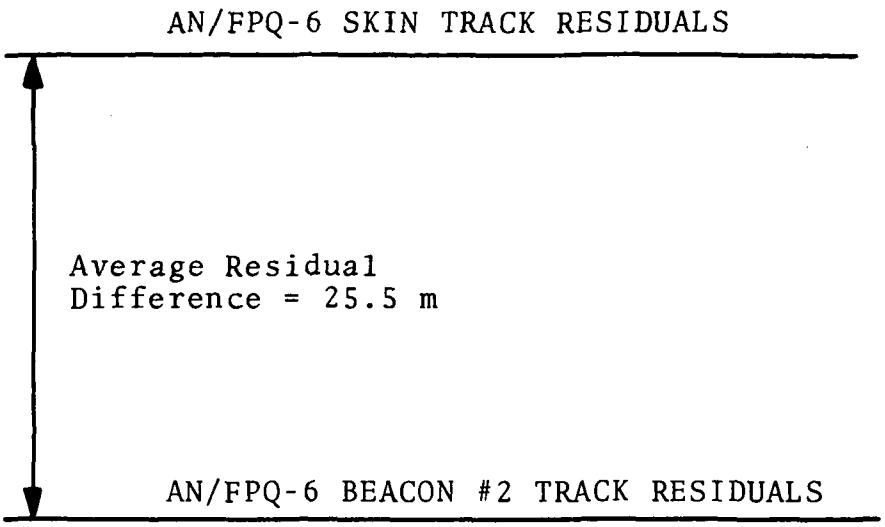

(a) Original Residual Differences

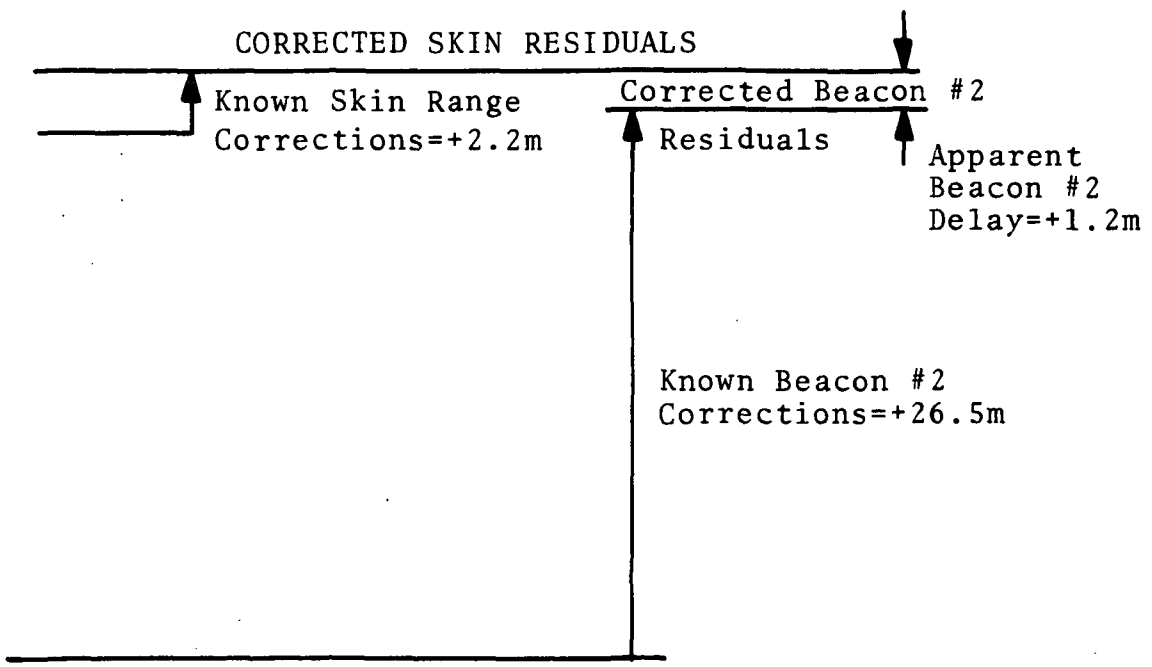

(b) Corrected Residuals

FIGURE 21

AN/FPQ-6 SKIN/BEACON #2 RANGE
RESIDUAL DIFFERENCES

range errors which formed the basis for the discussions found in the previous sections of this report. A tabular listing of the corrections to be applied to both the skin and beacon data for skin/beacon missions is provided in Table 9. These corrections apply for all such missions performed during the WICE. The corrections for the first four error sources are quite straight forward and have already been discussed in detail. The value given for the beacon track mismatch error is based upon the analysis provided in Section 4.1. This error was exceptionally large during these skin/beacon missions since the AN/FPQ-6 radar was erroneously calibrated in the 1.0 μsec pulsewidth mode. Fortunately this large calibration error only occurred during these skin/beacon missions. The values for beacon delay pulsewidth dependent error as listed in the table are also based upon results presented in Section 4.1. These beacon pulsewidth dependent errors affect the AN/FPQ-6 data only during the skin/beacon missions. This is due to the fact that the AN/FPQ-6 transmitted a 1.0 μsec pulsewidth only during these types of missions but the proper 0.5 μsec value was used during beacon-only missions. The AN/FPS-16, however, had a similar error associated with its beacon track data throughout the WICE since it always utilized a 1.0 μsec beacon interrogation pulsewidth.

The total corrections for the FPQ-6 data are:

Total Skip Track Range Correction = +2.2 meters
Total Beacon #1 Track Range Correction = +24.7 meters
Total Beacon #2 Track Range Correction = +26.5 meters.

Shifting the appropriate residuals by the amount indicated will result in a corrected set of skin/beacon residuals which are separated by:

TABLE 9

RANGE CORRECTIONS TO BE APPLIED TO

AN/FPQ-6 SKIN/BEACON TRACKING DATA

Range Error Source	Skin Track Correction (Meters)	Beacon #1 Correction (Meters)	Beacon #2 Correction (Meters)
L.O. Mode Selection (Dual/Single)	-0.9	-0.9	-0.9
Range Target Size (Survey Error)	-0.6	-0.6	-0.6
Propagation Error (Calibration)	+2.2	+2.2	+2.2
PRF Selection (160/640)	+1.5	-	-
Beacon Track Mismatch (Calib. in 1.0 usec., 1.6 MHz)	-	+26.0	+28.0
Beacon Pulsewidth Dependent Error (1.0 usec. pulse)	-	-2.0	-2.2
Totals	+2.2	+24.7	+26.5

Skin to Beacon #1: 19.8 + 2.2 - 24.7 = -2.7 meters

Skin to Beacon #2: 25.5 + 2.2 - 26.5 = +1.2 meters.

These results are depicted in Figure 20 b) and 21 b) respectively. From these results, it is apparent that an additional range correction must be applied to each set of residuals if the resulting skin and beacon tracking data are to agree. The only known uncorrected range error is the beacon delay error. If the remaining range residual difference is attributed to this error source, the beacon delays for the two beacons must be 109.73 - 738.56 meters instead of the assumed values of 112.97 and 739.75 meters.

The fact that these complex beacon delay computations result in fairly small delay errors is encouraging.

There are two independent data sets which were not used in the beacon delay computations which can be used to verify the derived results.

First of all, the AN/FPQ-6 beacon/skin data were associated with simultaneous AN/FPS-16 beacon tracking data. The average difference between these AN/FPS-16 range residuals and the corrected AN/FPQ-6 range residuals have been computed to be:

Beacon #1 AN/FPS-16 to AN/FPQ-6 = +20.4 meters

Beacon #2 AN/FPS-16 to AN/FPQ-6 = +9.3 meters.

If the AN/FPS-16 range residuals are corrected for known errors (see Table 10), the corrected residual differences become:

TABLE 10

RANGE CORRECTIONS TO BE APPLIED TO

AN/FPS-16 BEACON TRACKING DATA

Range Error Source	Beacon #1 Correction (Meters)	Beacon #2 Corrections
Range Target Size (Survey Error)	-7.9	-7.9
Propagation Error (Calibration)	+3.2	+3.2
PRF Selection	-	-
Beacon Pulsewidth Dependent Error (1.0 μsec. Interrogate)	-2.0	-2.2
Computed Beacon Delay Error	-2.7	+1.2
TOTALS*	-9.4	-5.7

*NOTE: These totals do not include a value for AN/FPS-16 beacon track mismatch error.

TABLE 11

RANGE CORRECTIONS TO BE APPLIED TO

AN/FPQ-6 BEACON-ONLY TRACKING DATA

Range Error Source	Beacon #1 Correction (Meters)	Beacon #2 Correction (Meters)
L.O. mode Selection (Dual/Single)	0	0
Range Target Size (Survey Error)	-0.6	-0.6
Propagation Error (Calibration)	+2.2	+2.2
PRF Selection (160/640)	0	0
Beacon Track Mismatch (Calibration 0.5 μsec., 1.6 MHz)	-9.3	-7.5
Beacon Pulsewidth Dependent Error	0	0
Computed Beacon Delay Error	-2.7	+1.2
TOTALS	-10.4	-4.7

Beacon #1: AN/FPS-16 to AN/FPQ-6 = + 11.0 meters

Beacon #2: AN/FPS-16 to AN/FPQ-6 = + 3.6 meters.

Since these corrections have taken all errors into account except the AN/FPS-16 beacon track mismatch error, these remaining range differences can presumably be attributed to this range error source. Making this assumption, it is now possible to compute a complete set of corrections for each radar which would apply to the final unused set of data. These data were obtained from the beacon only tracking missions. Since the AN/FPS-16 was always operated in a consistent manner, the previously applied corrections plus the computed mismatch correction can be directly applied to the AN/FPS-16 beacon-only range data:

Beacon #1: Corrected AN/FPS-16 = Measurements -20.4 m

Beacon #2: Corrected AN/FPS-16 = Measurements - 9.3 m.

The AN/FPQ-6 beacon track data, however, was obtained under different operating conditions than existed during the beacon track portion of the skin/beacon test. The AN/FPQ-6 radar used a 0.5 μsec pulsewidth and a 1.6 MHz bandwidth during both the calibration and track portions of these beacon/only missions.

Referring to the discussion of Section 4.1 it is found that these operating conditions result in AN/FPQ-6 beacon track mismatch errors of:

Beacon #1 mismatch error = + 9.3 meters

Beacon #2 mismatch error = + 7.5 meters

rather than the +26.0 meter and +28.0 meter mismatch errors associated with the skin/beacon missions. A second difference in AN/FPQ-6 errors results from the fact that the beacon delay pulsewidth dependent error of +2.0 meters and +2.2 meters no longer apply to beacons #1 and #2 since the property interrogation pulsewidth (0.5 μsecond) was used during these missions. The final difference in corrections arises from the fact that the local oscillator mode dependent error does not apply to the beacon-only tracking data. Only one L.O. was turned on during both the tracking and calibration portions of these beacon-only missions. Taking these differences into account, it is calculated that the AN/FPQ-6 beacon only residuals should be corrected by the following amounts (see tabulation in Table 11):

Beacon #1: Corrected AN/FPQ-6 = Measurements -10.4 m

Beacon #2: Corrected AN/FPQ-6 = Measurements - 4.7 m.

Residual data were used from approximately 25 beacon-only tracks of each GEOS-II beacon. These data obtained during WICE have been analyzed and the following uncorrected AN/FPS-16 to AN/FPS-16 residual differences exist:

Beacon #1 tracks: (FPS-16) - (FPQ-6) = +8.9 meters

Beacon #2 tracks: (FPS-16) - (FPQ-6) = +5.9 meters.

After correcting both sets of residuals:

For beacon #1:

(Corrected FPS-16)-(Corrected FPQ-6)= +8.9 - 20.4 + 10.4 = -1.1 meters.

For beacon #2:

(Corrected FPS-16)-(Corrected FPQ-6) = +5.9 - 9.3 + 4.7 = -1.3 meters.

It is felt that these results provide quite a high level of confidence both in the approach taken in arriving at the various errors and in the completeness of the error model used. The consistent and unexplained difference still remaining may very well be due to the beacon delay being different for the lower signal strength available at the beacon from AN/FPS-16 interrogations.

3.2.9 Summary of Range Error Computation/Measurements

A range zero-set error model was developed and each of the various error terms were systematically investigated. Actual measurements were obtained for all error terms and these corrections were applied to 3 separate and different sets of C-Band radar range tracking data. As a result of these corrections, a single interchangeable set of measurements has resulted where all data agree to within 1.5 meters. Since 109 tracks from each of two radars are contained in the data sets, including data gathered while tracking different beacons and under varying radar operating conditions, it is felt that this is a significant accomplishment.

It should be noted that most of the rather large error terms discussed above no longer affect the Wallops Island radar data. The operating/calibration procedures were changed as the sources of these errors were recognized. As a result of these changes the current Wallops Island

GEOS-II range tracking data need only be corrected by the amounts indicated in Table 12 and 13.

3.3 C-BAND RANGE RATE INVESTIGATIONS

The Wallops Island AN/FPS-6 radar contains a coherent signal processing modification which permits the radar to coherently process the C-Band data to obtain doppler frequency shift measurements. The resulting data after proper scaling becomes a direct measurement of the targets radial range rate.

The availability of C-Band radar range rate data offered several advantages over data available from other doppler measuring systems. First of all, assuming equal frequency measurement capabilities for all systems, the C-Band system should be more precise since the magnitude of the doppler shift is greater at C-Band than at lower frequencies such as are used for Tranet or the GRARR.

Secondly, the C-Band frequency is well above the frequencies which are subject to noticeable tropospheric doppler refraction effects.

Next, there is no need for a satellite borne ultra - stable frequency source nor for an active transponder if a satisfactory cross section is available for skin tracking.

Finally, the simultaneous reception of both range and range rate data at the single site offers a previously unavailable opportunity to directly convert the extremely

TABLE 12

PRESENT DAY AN/FPQ-6 RANGE CORRECTIONS

FOR WALLOPS ISLAND

Range Error Source	Skin Track Corrections (Meters)	Beacon #1 Corrections (Meters)	Beacon #2 Corrections (Meters)
L.O. Mode Select	0	0	0
Range Target Size (FSR assumed)	0	0	0
Propagation Error (FSR assumed)	+0.9	+0.9	+0.9
PRF Select	0	0	0
Beacon Track Mismatch (Cal. in 0.5 usec, 2.4 MHz; and track in 2.4 MHz)	0	-6.2	-5.0
Beacon Pulsewidth Dependent Error (Interrogate with 0.5 usec.)	0	0	0
Computed Beacon Delay Error	0	-2.7	+1.2
Total Track Correction	+0.9	-8.0	-2.9

TABLE 13

PRESENT DAY AN/FPS-16 RANGE CORRECTIONS

FOR WALLOPS ISLAND

Range Error Source	Beacon #1 Corrections (Meters)	Beacon #2 Corrections (Meters)
Range Target Size (FSR)	0	0
Propagation Error (FSR)	+1.4	+1.4
Beacon Track Mismatch Error (Cal. in 0.5 usec, wide BW, track in Wide BW)	+7.6	+8.2
Beacon Pulsewidth Depedent Error (1.0usec, Interrogate)	-2.0	-2.2
Computed Beacon Delay Error	-2.7	+1.2
Total Track Corrections	+4.3	-8.6

precise range rate data into range data. An investigation into this conversion possibility was performed[21,22,25] (Also Reference for Volume IV) as a part of the GEOS project.

The method used to accomplish the range rate integration was extremely straightforward and consisted in merely solving the standard formula:

$$R = R_o + \int [\dot{R} + \int \ddot{R} dt] dt$$

or,

$$R_W = R_o + \sum_{k=1}^{N-1} \dot{R}_k \Delta t + \sum_{k=2}^{N} \frac{\dot{R}_k - \dot{R}_{k-1}}{2} \Delta t$$

where: Δt = radar data sampling rate.

The problem of obtaining the initial range R_o was solved by arbitrarily selecting the radar skin track range associated with the initial range rate measurement (the two sets of data are synchronously sampled). Since this R_o could be in error, the resulting set of doppler ranges were compared on a point by point basis with the skin track range data. The average difference between the two sets of data was computed and a bias correction then applied to the doppler ranges so as to eliminate this bias.

While no claim is made that this simple approach to utilization of range rate data provides an optimum solution, it does provide an easily visualized and readily obtainable solution. It is planned that the results obtained by this technique will be used as a reference in establishing figures of merit for more sophisticated solutions.

It is recommended that this investigation be continued to determine whether or not more optimum methods can be found for using the C-Band doppler data. Additional investigations should also be carried out into the uses of integrated doppler range data.

A final comment which is applicable is that the data gathered to date were obtained with the radar's coherent signal processor (CSP) operating in the fine line track mode. This means that the normal radar tracking loops were operating in their normal fashion (i.e. closed through the Gross spectrum receiver). The Wallops Island radar also has the capabilitity of carrying out a so called "Fine Line Position Track Mode" (i.e., the radar's angle and range servos closed through the fine line receiver). This latter mode has not been used to obtain any of the data presented in this report. Future investigations are recommended to evaluate the effects of operating the radar in a completely closed loop CSP mode.

4.0 SPECIAL GEOS-II TRACKING TESTS

One of the goals of the GEOS-II C-Band systems project was to evaluate the possibility of using the satellite as a radar calibration aid. This goal was consistent with the primary goal of obtaining geodetic radar data since any improvement in radar calibration would result in improved tracking data.

The project did not attempt to replace normal calibration techniques. Instead, the satellite calibration effort was oriented so as to augment the information which could be obtained from the purely ground based measurements.

The special tests portion of the project as discussed below was performed initially only at the Wallops Island Station. Later the NASA Bermuda Station also performed the various tracking tests, but these non-Wallops Island data were not reduced in time for inclusion in this report. The evaluation of this Bermuda data is, however, still planned since it is important that the general nature of the Wallops results be established. This is particularly true of the parameter variations test (also referred to as tests F-1 through F-4). The usefulness of previously discussed pulsewidth mismatch model requires verification that various radars react to pulsewidth changes in the same predictable fashion. If this can be shown, the technique will provide a simple method for eliminating the remaining dominant source of range bias error. Elimination of this error would, in turn, permit accurate world-wide geodetic quality data to be obtained on future programs without resorting to complex error evaluation techniques.

4.1 SPECIAL TESTS - TEST PROCEDURES

A set of special test procedures was generated early in 1970 which when implemented fully evaluate the ability of the satellite to act as a calibration aid. It should be noted that these tests were originally developed for use at those sites where more than one radar exists. This multi-radar configuration allows one radar to be evaluated while the second radar acts as the data source for the reference orbit.

The actual detailed test procedures are included in Appendix A. The list below provides a summary of the procedure by numbers and titles:

TEST PROCEDURES FOR SPECIAL PURPOSE
GEOS-II C-BAND RADAR TRACKING MISSIONS

Test	Title	Req'd Radar(s)	Required Transponder	
A	Transponder Switching	FPS-16 & FPQ-6	1 and 2	STADAN Switching FPQ-6 Skin/Beacon
B1	Polarization	FPS-16 & FPQ-6	1	FPQ-6 Skin/Beacon
B2	Polarization	FPS-16 & FPQ-6	2	FPQ-6 Skin/Beacon
C	Angle Calibration	FPS-16 & FPQ-6	Either	Pass Elev. > 70°
D1	Lag Angle Error Correction	FPQ-6	Either	Pass Elev. > 80°, Servo BW #4
D2	Lag Angle Error Correction	FPS-16 & FPQ-6	Either	Pass Elev. > 80°, 4101 Mod, Servo BW #4
D3	Lag Angle Error Correction	FPS-16 & FPQ-6	Either	Pass Elev. > 80°, 4101 Mod, Servo BW Normal
E	Normal Plunge	FPS-16 & FPQ-6	Either	Pass 70°$\geq$Elev $\leq$84°
F1	Range Calibration	FPQ-6 Prime w/ FPS-16 Normal	1	
F2	Range Calibration	FPS-16 Prime w/ FPQ-6 Normal	1	
F3	Range Calibration	FPQ-6 Prime w/ FPS-16 Normal	2	
F4	Range Calibration	FPS-16 Prime w/ FPQ-6 Normal	2	

4.2 SPECIAL TESTS - RESULTS

4.2.1 Transponder Switching Results

Figures 22 (a) and (b) provide the results of the transponder switching test (Special Test A). Note that a split scale has been used in these figures so that both beacon #1 and Beacon #2 residuals can be shown in a single figure.

As was stated previously, the GEOS transponders have nominal delays of 112.47 meters (Beacon #1) and 739.72 meters (Beacon #2). Therefore, if these nominal delays are exact there should be a range residual difference of 739.72 - 112.47 = 627.25 meters when Test A is performed. Any result other than this would indicate that at least one transponder has a delay which differs from its nominal value.

The residual plots shown in Figures 22 (a) and 22 (b) show a residual difference which is certainly close to the hoped for value of 627 meters. The trending of the residuals together with the range noise will not permit a more exact measurement to be made. This test appears to corroborate the theoretical calculations described in Section 3.2.8 and establishes that either both transponders have delays close to their nominal value or that both have an approximately equal delay bias error. The nominal delay possibility is the more probable condition. Based upon this test it is highly improbable that any large beacon delay errors exist in the GEOS-II beacon track data.

4.2.2 Polarization Sensitivity Test

The residual range data from this test is plotted in Figure 23 (a). The main point to be noted from these range

TEST A NWALI3 RANGE RESIDUALS

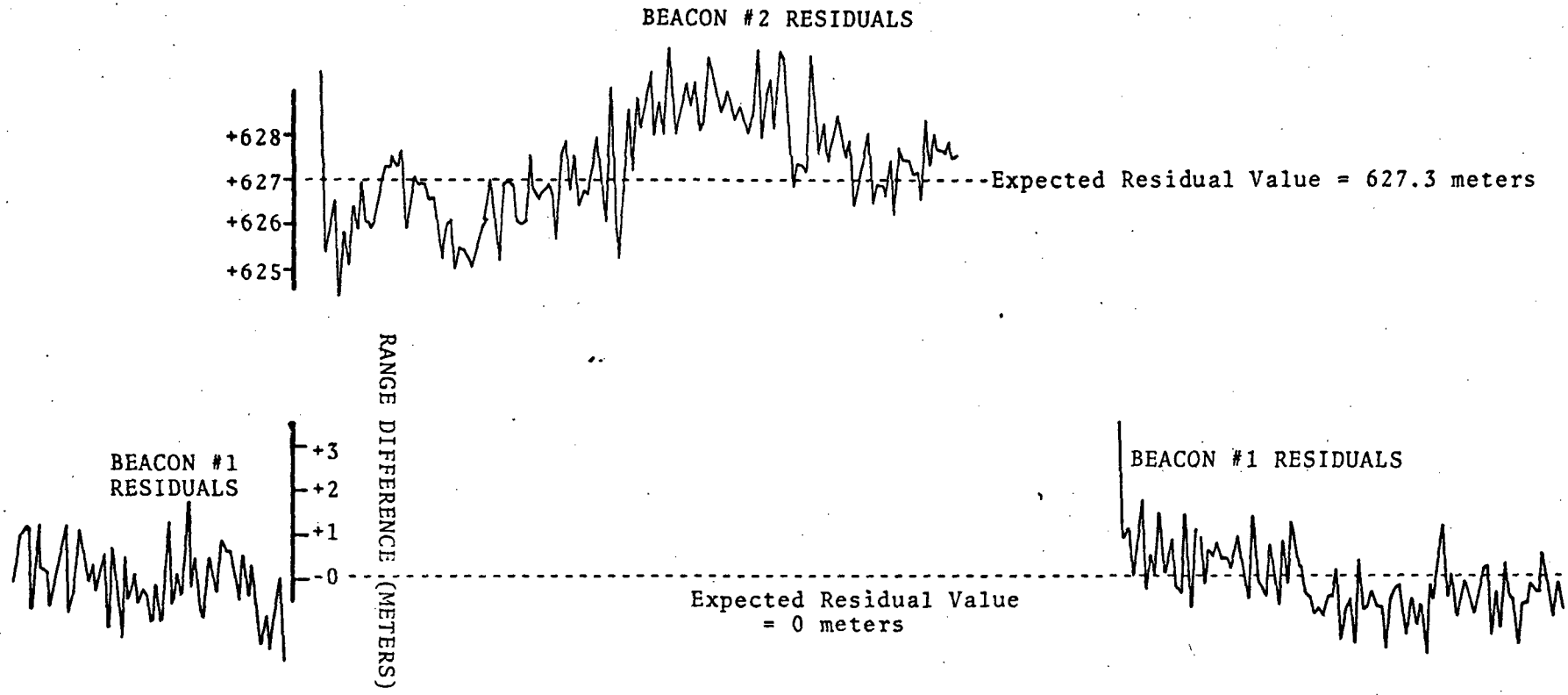

FIGURE 22(a)

AN/FPQ-6 RANGE RESIDUALS
FOR SPECIAL TEST A

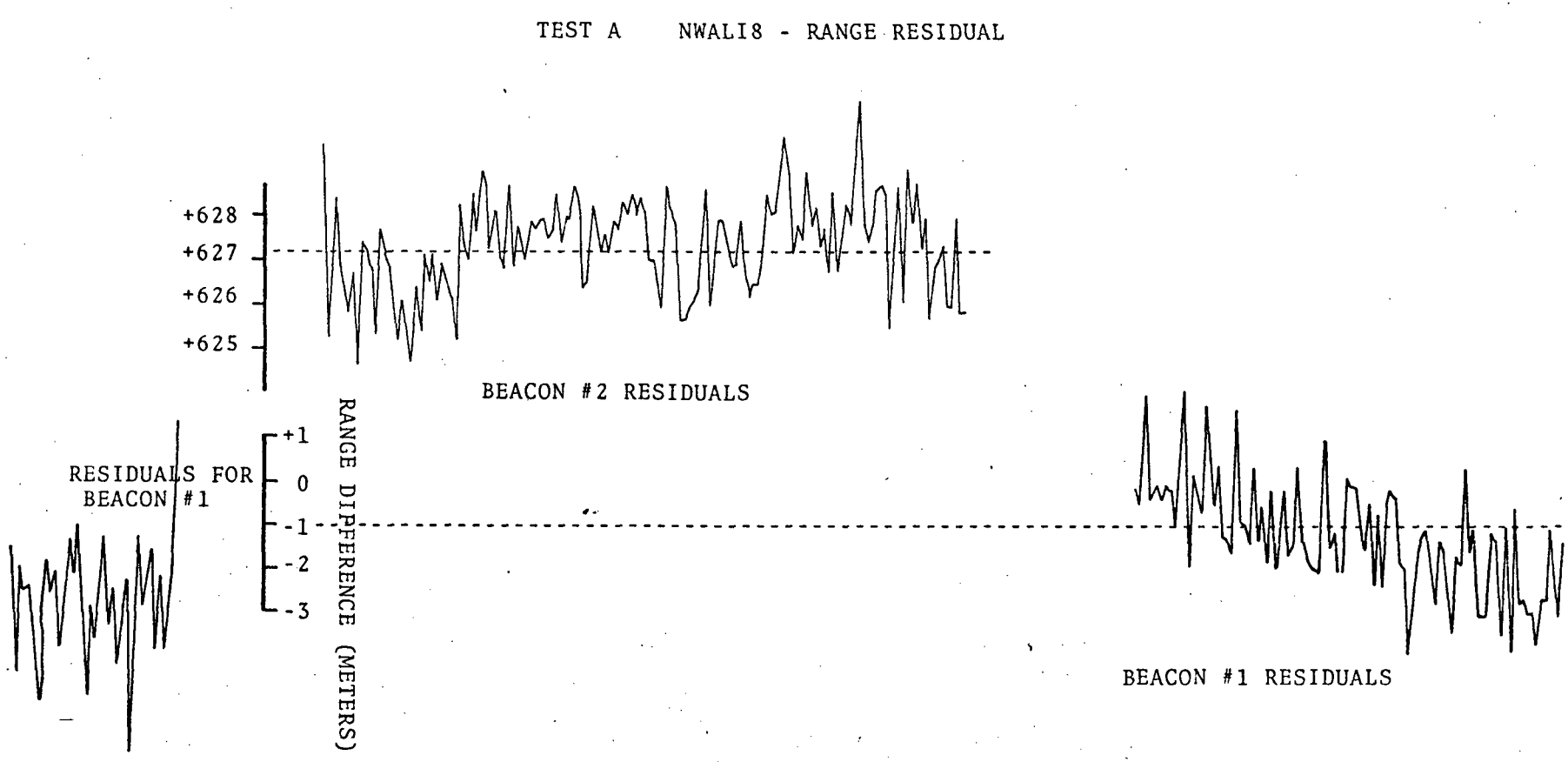

FIGURE 22(b)

AN FPS-16 RANGE RESIDUALS
FOR SPECIAL TEST A

FIGURE 23

RANGE RESIDUALS FOR TEST B
(POLARIZATION SWITCHING)

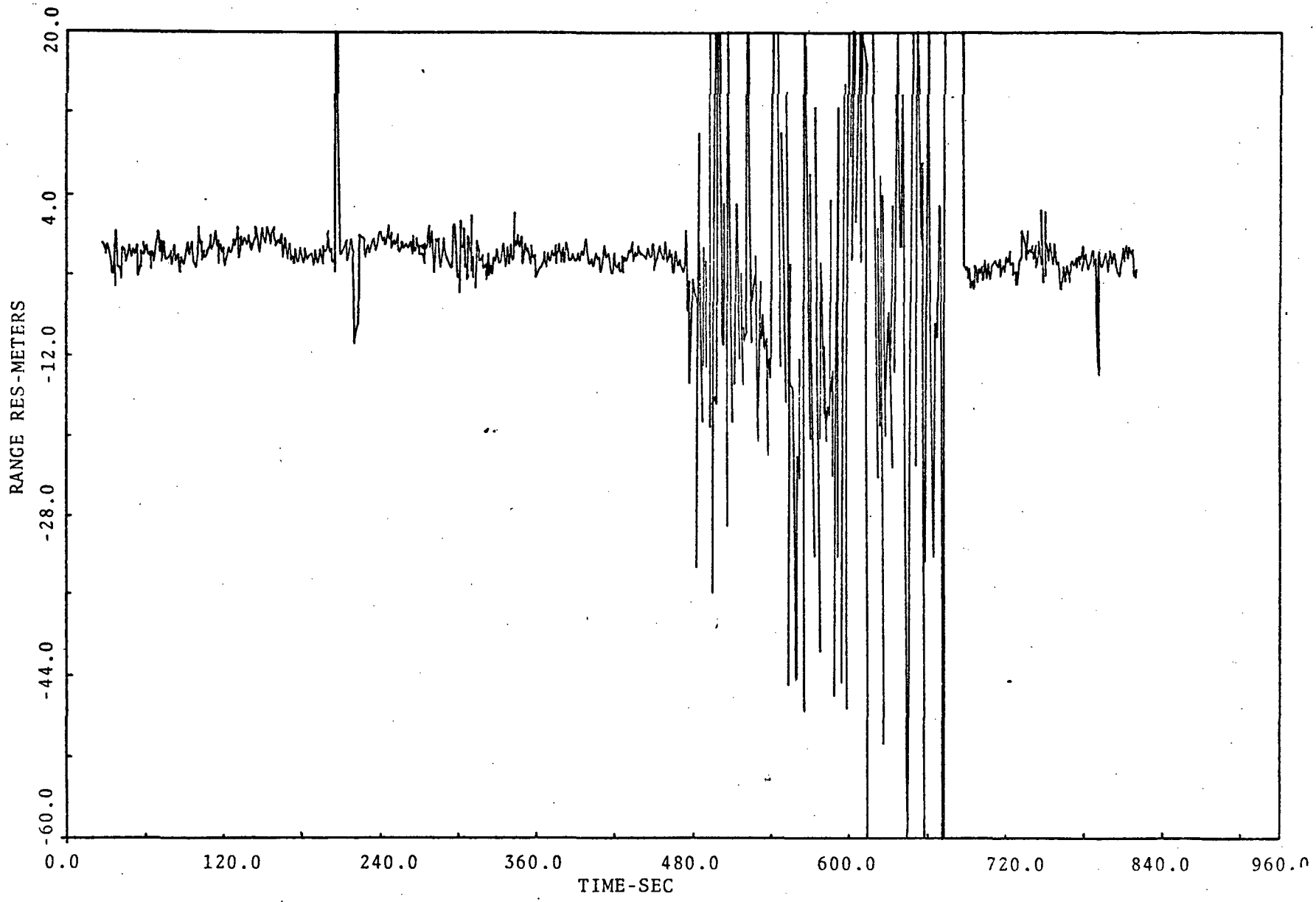

data is that there are no apparent polarization dependent range variations. The change in range which occurred between beacon and skin track (switchover was initiated at approximately 450 seconds and was completed by 480 seconds) is explainable by other non-polarization dependent means. In fact it is of interest that the apparent 6 to 12 meter range difference between the skin track data and beacon track data agrees very well with the tabulation of necessary current range corrections given in Table 12. This tabular data predicts that uncorrected Beacon #1 residuals will lie 8.9 meters above uncorrected skin residuals. This prediction is borne out in Test B1 data.

Figure 23 (b) provides a somewhat odd looking plot of the digitized AGC voltage. Since the more negative numbers indicate a greater gain reduction and, therefore, a stronger signal strength, the plot as shown is an inverted indication of signal strength. Each AGC bit represents a known value of AGC voltage (a complete listing of the radar output data words with bit weights can be found in reference 1) and can, by making use of the pre- and post-mission calibration data, be associated with a specific value of S/N ratio. This scaling from bits to S/N has not been carried out since an evaluation of the data shown in Figure 23 (b) indicates that there are no large variations of AGC with polarization change. The large spikes appearing in this plot occur each time the mode of the radar is switched. Thus, these spikes can be used to identify the times at which polarization switching occurred. A comparison between these switching times and the range residuals indicates that there is no correlation between the polarization changes and changes in the range data. No changes at all occurred during the

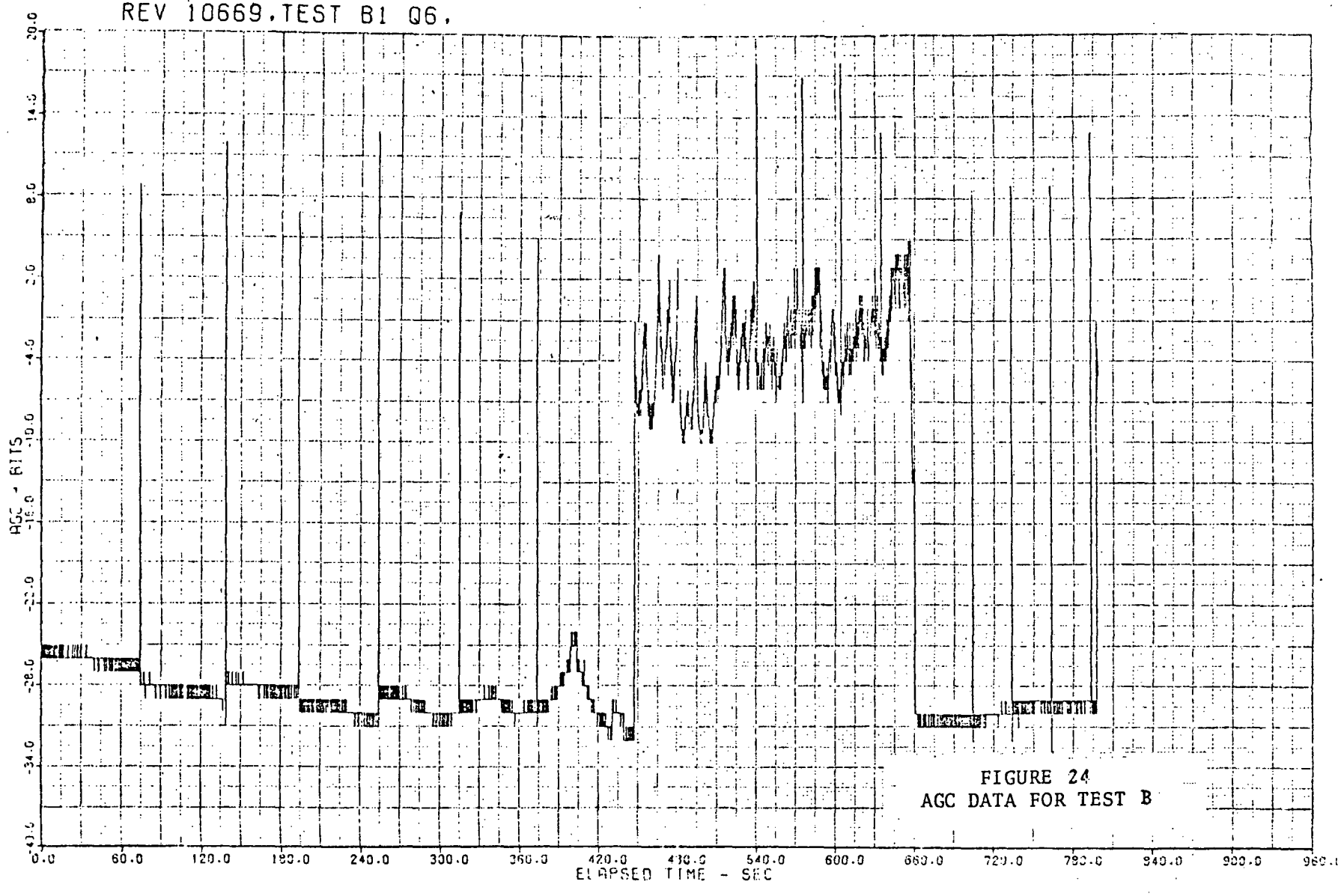

FIGURE 24
AGC DATA FOR TEST B

Beacon track portion and, although there appears to be some distinguishably different levels of range error during the skin track portion, the skin track variations appear to be uncorrelated with polarization changes.

The original purpose of the test was to determine whether a stable tracking phase center was being obtained during skin tracks of the satellite. It was feared that the gravity stabilization boom plus end-mass might be tracked rather than the desired Van Atta array. Since it was felt that the boom's apparent crossection would be much more sensitive to polarization changes than the Van Atta array, it was hoped that variations in AGC voltage or range occurring during this test would indicate which point was being tracked.

While additional analysis could remove all remaining uncertainties, it is felt that the existing results from this test greatly strenghten the belief that a stable point on the satellite such as the Van Atta array is indeed being tracking during skin tracks. Future efforts which could be carried out would be to convert the AGC data into receive S/N data and to smooth the skin track range data. Smoothed range data would provide a better basis for evaluating possible correlation between polarization switching and radar range residual changes.

4.2.3 Angle Calibration Test

This test was carried out in the hopes that it would permit identification of the source of the large azimuth residuals which occur during most high elevation passes. It was recognized that long arc results could provide a better estimate of angle error magnitudes but it was felt

that the possibility of using single station short arc solutions for angle calibration should also be investigated.

Unfortunately, the data reduction and analysis efforts required to obtain useful evaluation results were found to be excessive. However, the data were gathered and a preliminary analysis was performed. This analysis showed that a large azimuth residual would remain even after data corrections had been applied for leveling errors and lag errors. Pre- and post-mission data exists for computation of boresight null shift error and removal of the effects of this error source is also possible. Time did not permit completion of this effort, however, the data is being saved so that the analysis can be completed at some future date.

4.2.4 Lag Angle Error Test

This test which is given in Appendix A as Special Test D was intended as a method for verifying the angle lag error analysis which were carried out on normal tracking and calibration data (see reference 13 and 14). The test was divided into two parts one of which required that programming changes be made ot the 4101 computers calibration and real-time error correction programs. Unfortunately, the Wallops Island operations schedule did not allow for radar shutdown while new programs were being checked out. Therefore, no tracks were carried out specifically to obtain data in accordance with Special Test D.

4.2.5 Normal-Plunge Calibration Test

It has always been recognized that an accurate measurement of the droop error is extremely difficult to obtain using normal calibration techniques. There have been

various previously proposed methods for obtaining better droop calibration data by tracking special targets such as balloon borne spheres, aircraft or helicopters borne beacons, and satellites with flashing lights. It was hoped that a plunge/normal track of the GEOS satellite (See Test E procedure in Appendix A) would provide a relatively simple method of obtaining such data.

The tests were carried out and tracking data were obtained. However, the analysis of this data required the generation of new data analysis/reduction computer programs. It was felt that the limited manpower available on the GEOS-II C-Band systems project could be utilized more effectively on other more urgent tasks. Therefore, the test data has been filed for possible future reduction and analysis.

4.2.6 Parameter Variations Tests

This series of tests (one test involving each of the two Wallops C-Band radars and each of the two GEOS transponders) was originated in an attempt to gain a better understanding of the dependency between range errors and certain radar operating parameters. In particular, the bandwidth/pulsewidth mismatch error which was previously discussed in Section 3.2.6 was to be investigated. It was hoped that the results of these tests could be used to explain the range residual differences which existed in the radar data gathered during WICE. These early GEOS-II tracking results not only exhibited different range residuals for the two radars but also exhibited a residual dependence upon radar operating mode.

The discussion of Section 3.2 provides a detailed model for the mismatch error effects. The parameter variations tests required the operators to vary certain of the radar's operating parameters in a specific fashion during both the calibration and track phases of a mission. The mode changes were selected so that data would be available which would enable the mismatch error to be computed. Thus, it was planned that the radar itself act as the test equipment for obtaining accurate measurements on the effects of bandwidth and pulsewidth changes.

The data obtained during the AN/FPQ-6 calibrations for tests F(1) (Beacon #1 track) and F(3) (Beacon #2 track) are given in Tables 14 and 18 respectively. Similar data for the AN/FPS-16 radar are included in Tables 16 and 20.

The (a) and (b) sections of each of these tables contain pre and post-mission range measurement data obtained while the radar was locked onto a reference range target. These calibration data are summarized in the range difference values listed in the (c) sections of the tables. These summaries include the effects of both the pre- and post-mission data. It should also be noted that the range readings provided in Sections (a) and (b) of the tables are themselves the average of at least 100 range measurements. The granularity shown indicates that these data are computed rather than single range measurements which would a granularity of only 1.83 meters.

TABLE 14

TEST F1 DATA

(AN/FPQ-6 BEACON #1)

(a) PREMISSION CALIBRATIONS

F1 CAL STEP #	RADAR OPERATING MODE PULSEWIDTH	BANDWIDTH	RANGE READING (meters)
9	0.5 μsec;	2.4 MHz	7463.11
10	1.0 μsec;	2.4 MHz	7494.29
11	1.0 μsec;	1.6 MHz	7508.88
12	0.5 μsec;	1.6 MHz	7473.21
13	0.5 μsec;	2.4 MHz	7463.35

(b) POSTMISSION CALIBRATIONS

9	0.5 μsec;	2.4 MHz	7461.71
10	1.0 μsec;	2.4 MHz	7492.13
11	1.0 μsec;	1.6 MHz	7506.32
12	0.5 μsec;	1.6 MHz	7471.43
13	0.5 μsec;	2.4 MHz	7461.45

(c) AVERAGE DIFFERENCES BETWEEN CALIBRATIONS

$\Delta R_{1c} = \bar{R}$ (step 10) - $\bar{R}$ (step 9) = +30.8 meters

$\Delta R_{2c} = \bar{R}$ (step 11) - $\bar{R}$ (step 9) = +45.2 meters

$\Delta R_{3c} = \bar{R}$ (step 12) - $\bar{R}$ (step 9) = + 9.9 meters

(d) AVERAGE BEACON TRACK RANGE CHANGES

$\Delta R_{1T} = \overline{\Delta R}$ (Bandwidth only switched) = $R_{1.6} - R_{2.4}$ = +13.0 m

$\Delta R_{2T} = \overline{\Delta R}$ (Pulsewidth only switched) = $R_{1.0} - R_{0.5}$ = +2.0 m

AN/FPQ-6 BANDWIDTH MISMATCH ERROR WHEN TRACKING

GEOS-II BEACON #1

CALIBRATION MODE				RADAR (BEACON #1) TRACK BANDWIDTH MISMATCH ERROR	
1.6 MHz B.W.	2.4 MHz B.W.	0.5 μSec P.W.	1.0 μSec P.W.	TRACK MODE BANDWIDTH = 2.4 MHz	TRACK MODE BANDWIDTH = 1.6 MHz
	X	X		$\varepsilon_1 = 2(\Delta R_{1T} - \Delta R_{3c})$ $= 2(13.0 - 9.9) = +6.2$ m	$\varepsilon'_1 = \varepsilon_1 + \Delta R_{1T}$ $= 6.2 + 13.0 = +19.2$ m
	X		X	$\varepsilon_2 = \varepsilon_1 - \Delta R_{1c}$ $= 6.2 - 30.8 = -24.6$ m	$\varepsilon'_2 = \varepsilon_2 + \Delta R_{1T}$ $= -24.6 + 13.0 = -11.6$ m
X			X	$\varepsilon_3 = \varepsilon_1 - \Delta R_{2c}$ $= 6.2 - 45.2 = -39.0$ m	$\varepsilon'_3 = \varepsilon_3 + \Delta R_{1T}$ $= -39.0 + 13.0 = -26.0$ m
X		X		$\varepsilon_4 = \varepsilon_1 - \Delta R_{3c}$ $= 6.2 - 9.9 = -3.7$ m	$\varepsilon'_4 = \varepsilon_4 + \Delta R_{1T}$ $= -3.7 + 13.0 = +9.3$ m

NOTES: 1. See tabulation of Test F1 Data for computation of ΔR's

2. Mismatch Error During WICE $= \varepsilon'_4 = +9.3$ m

3. Post WICE Mismatch Error $= \varepsilon_1 = +6.2$ m

TABLE 15

TABLE 16
TEST F 2 DATA

(AN/FPS-16/BEACON #1)

(a) PREMISSION BEACON CALIBRATIONS

F 2 TEST STEP #	RADAR OPERATING MODE PULSEWIDTH	BANDWIDTH	RANGE READING (meters)
5	0.5 μSec	Narrow	10,178.16
6	1.0 μSec	Narrow	10,214.73
7	1.0 μSec	Wide	10,214.95
8	0.5 μSec	Wide	10.178.77

(b) POST MISSION BEACON CALIBRATIONS

5	0.5 μSec	Narrow	10,176.39
6	1.0 μSec	Narrow	10,213.88
7	1.0 μSec	Wide	10,214.03
8	0.5 μSec	Wide	10,178.49

(c) AVERAGE DIFFERENCES BETWEEN CALIBRATIONS

$\Delta R_{1c} = \bar{R}$ (Step 7) - $\bar{R}$ (Step 8) = +35.9 meters

$\Delta R_{2c} = \bar{R}$ (Step 6) - $\bar{R}$ (Step 8) = +35.7 meters

$\Delta R_{3c} = \bar{R}$ (Step 5) - $\bar{R}$ (Step 8) = - 1.3 meters

(d) AVERAGE BEACON TRACK RANGE CHANGES

ΔR_{1T} (Bandwidth only switched) = R (Narrow) -R(Wide) = -5.1 m

ΔR_{2T} (Pulsewidth only switched) = R (1.0 μSec) -R (0.5 μSec) = +3.2 m

AN/FPS-16 BANDWIDTH MISMATCH ERROR WHEN TRACKING

GEOS-II BEACON #1

CALIBRATION MODE				RADAR (BEACON #1 TRACK) BANDWIDTH MISMATCH ERROR	
NARROW B.W.	WIDE B.W.	0.5 μSec	1.0 μSec	TRACK MODE BANDWIDTH = WIDE	TRACK MODE BANDWIDTH = NARROW
	X	X		$\varepsilon_1 = 2(\Delta R_{1T} - \Delta R_{3c})$ $= 2\left[(-5.1) - (-1.3)\right] = -7.6$ m	$\varepsilon_1' = \varepsilon_1 + \Delta R_{1T}$ $= (-7.6) + (-5.1) = -12.7$ m
	X		X	$\varepsilon_2 = \varepsilon_1 - \Delta R_{1c}$ $= (-7.6) - (+35.9) = -43.5$ m	$\varepsilon_2' = \varepsilon_2 + \Delta R_{1T}$ $= (-43.5) + (-5.1) = -48.6$ m
X			X	$\varepsilon_3 = \varepsilon_2$	$\varepsilon_3' = \varepsilon_2'$
X		X		$\varepsilon_4 = \varepsilon_1$	$\varepsilon_4' = \varepsilon_1'$

NOTES: 1. See tabulation of Test F2 Data for source of ΔR's

TABLE 17

TABLE 18

TEST F3 DATA

(AN/FPQ-6/BEACON #2)

(A) PREMISSION BEACON CALIBRATIONS

F 3 CAL STEP #	RADAR OPERATING MODE PULSEWIDTH	BANDWIDTH	TIME Hr: Min: Sec	RANGE READING (meters)
9	0.5 μSec;	2.4 MHz	21:43:22.44	7462.80
10	1.0 μSec;	2.4 MHz	21:44:20.04	7494.92
11	1.0 μSec;	1.6 MHz	21:45:24.54	7509.35
12	0.5 μSec;	1.6 MHz	21:45:46.44	7472.65
13	0.5 μSec;	2.4 MHz	21:46:01.84	7462.85

(b) POSTMISSION BEACON CALIBRATIONS

9	0.5 μSec;	2.4 MHz	22:22:53.84	7461.61
10	1.0 μSec;	2.4 MHz	22:23:16.94	7493.23
11	1.0 μSec;	1.6 MHz	22:23:39.04	7505.47
12	0.5 μSec;	1.6 MHz	22:24:01.04	7471.02
13	0.5 μSec;	2.4 MHz	22:24:17.94	7461.29

(c) AVERAGE DIFFERENCES BETWEEN CALIBRATIONS

$\Delta R_{1c} = \bar{R}$ (Step 10) - $\bar{R}$ (Step 9) = +31.9 meters

$\Delta R_{2c} = \bar{R}$ (Step 11) - $\bar{R}$ (Step 9) = +45.3 meters

$\Delta R_{3c} = \bar{R}$ (Step 12) - $\bar{R}$ (Step 9) = + 9.8 meters

(d) AVERAGE BEACON TRACK RANGE CHANGES

$\Delta R_{1T} = \overline{\Delta R}$ (Bandwidth only switched) = $R_{1.6} - R_{2.4}$ = 12.3 meters

$\Delta R_{2T} = \overline{\Delta R}$ (Pulsewidth only switched) = $R_{1.0} - R_{0.5}$ = 2.2 meters

AN/FPQ-6 BANDWIDTH MISMATCH ERROR WHEN TRACKING

GEOS-II BEACON #2

CALIBRATION MODE				RADAR (BEACON TRACK) BANDWIDTH MISMATCH ERROR	
1.6 MHz B.W.	2.4 MHz B.W.	0.5 μSec P.W.	1.0 μSec P.W.	TRACK MODE BANDWIDTH = 2.4 MHz	TRACK MODE BANDWIDTH = 1.6 MHz
	X	X		$\varepsilon_1 = E_{2.4} = 2\,(\Delta R_{1T} - \Delta R_{3c})$ = 2 (12.3-9.8) = +5.0 m	$\varepsilon_1' = \varepsilon_1 + \Delta R_{1T}$ = +5.0 +12.3 = +17.3 m
	X		X	$\varepsilon_2 = E_{2.4} - \Delta R_{1c}$ = +5.0 -31.9 = -26.9 m	$\varepsilon_2' = \varepsilon_2 + \Delta R_{1T}$ = -26.9 +12.3 = -14.6 m
X			X	$\varepsilon_3 = E_{2.4} - \Delta R_{2c}$ = +5.0 -45.3 = -40.3 m	$\varepsilon_3' = \varepsilon_3 + \Delta R_{1T}$ = -40.3 +12.3 = -28.0 m
X		X		$\varepsilon_4 = E_{2.4} - \Delta R_{3c}$ = +5.0 -9.8 = -4.8 m	$\varepsilon_4' = \varepsilon_4 + \Delta R_{1T}$ = -4.8 +12.3 = +7.5 m

NOTE: 1. See tabulation of Test F3 results for computation of ΔR's.

2. For WICE: (Beacon only) = ε_1 = +7.5 m; (Beacon portion SK/BCN) = ε_3' = -28.0 m

TABLE 19

TABLE 20
TEST F4 DATA

(AN/FPS-16/BEACON #2)

(a) PREMISSION BEACON CALIBRATIONS

F4 CAL. STEP #	RADAR OPERATING MODE PULSEWIDTH	BANDWIDTH	RANGE READING (meters)
5	0.5 μSec	Narrow	10,195.73
6	1.0 μSec	Narrow	10,212.69
7	1.0 μSec	Wide	10,211.87
8	0.5 μSec	Wide	10,177.73

(b) POST MISSION BEACON CALIBRATIONS

5	0.5 μSec	Narrow	10,175.99
6	1.0 μSec	Narrow	10,212.93
7	1.0 μSec	Wide	10,211.38
8	0.5 μSec	Wide	10,176.60

(c) AVERAGE DIFFERENCES BETWEEN CALIBRATIONS

$\Delta R_{1c} = \bar{R}$ (Step 7) $-\bar{R}$ (Step 8) = +34.5 meters

$\Delta R_{2c} = \bar{R}$ (Step 6) $-\bar{R}$ (Step 8) = +35.6 meters

$\Delta R_{3c} = \bar{R}$ (Step 5) $-\bar{R}$ (Step 8) = -1.2 meters

(d) AVERAGE BEACON TRACK RANGE CHANGES

ΔR_{1T} (Bandwidth only switched) = $R_{Narrow} - R_{Wide}$ = -5.3 m

ΔR_{2T} (Pulsewidth only switched) = $R_{1.0} - R_{0.5}$ = +3.2 m

A comparison of the average differences between calibrations (c sections) for the AN/FPQ-6 and AN/FPS-16 radars will show that the AN/FPS-16 radar appears to be relatively insensitive to bandwidth changes (Δ R3c) as long as the pulsewidth is held constant. This apparent insensitivity of the AN/FPS-16 results from the availability of an additional beacon track delay adjustment within the ADRAN range tracker. The DIRAM used by the AN/FPQ-6 radar has only a single beacon track delay adjustment which can be used to zero set the radar for only one of the possible operating modes. The ADRAN equipped AN/FPS-17 contains two such adjustable lines so that proper zero set can be achieved for any two of the difficulty in analyzing the AN/FPS-16 tracking results. This factor plus the less well defined bandwidths make the AN/FPS-16 special test results somewhat suspect. The AN/FPQ-6, however, seems to follow the proposed mismatch error model quite well.

The (d) portions of the four tables contain the average range changes which were measured as the radar operating parameters were altered during the actual satellite track. Figures 24 through 25 provide plots of the data which were used to calculate these range differences. It can be seen that the parameters were varied numerous times during the missions so that the values given in the (d) portions of the tables are actually the averages of all the available range differences.

Reference to the mismatch models proposed in Section 3.6 will provide the reasoning behind the mismatch error computations which are given in Tables 15 and 19 for the AN/FPQ-6 radar and in 17 and 21 for the AN/FPS-16 radar.

AN/FPS-16 BANDWIDTH MISMATCH ERROR WHEN TRACKING

GEOS-II BEACON #2

CALIBRATION MODE				RADAR (BEACON #2 TRACK) BANDWIDTH MISMATCH ERROR	
NARROW B.W.	WIDE B.W.	0.5 μSec	1.0 μSec	TRACK MODE BANDWIDTH = WIDE	TRACK MODE BANDWIDTH = NARROW
	X	X		$\varepsilon_1 = 2(\Delta R_{1T} - \Delta R_{3c})$ $= 2[(-5.3) - (-1.2)] = -8.2$ m	$\varepsilon'_1 = \varepsilon_1 + \Delta R_{1T}$ $= (-8.2) + (-5.3) = -13.5$ m
	X		X	$\varepsilon_2 = \varepsilon_1 - \Delta R_{1c}$ $= (-8.2) - (+34.5) = -42.7$ m	$\varepsilon'_2 = \varepsilon_2 + \Delta R_{1T}$ $= (-42.7) + (-5.3) = -48.0$ m
X			X	$\varepsilon_3 = \varepsilon_2$	$\varepsilon'_3 = \varepsilon'_2$
X		X		$\varepsilon_4 = \varepsilon_1$	$\varepsilon'_4 = \varepsilon'_1$

NOTES: 1. See tabulation of Test F4 for computation of ΔR's.

TABLE 21

FIGURE 25

VARIATION OF PARAMETERS TEST FOR
AN/FPQ-6 TRACK OF BEACON #1

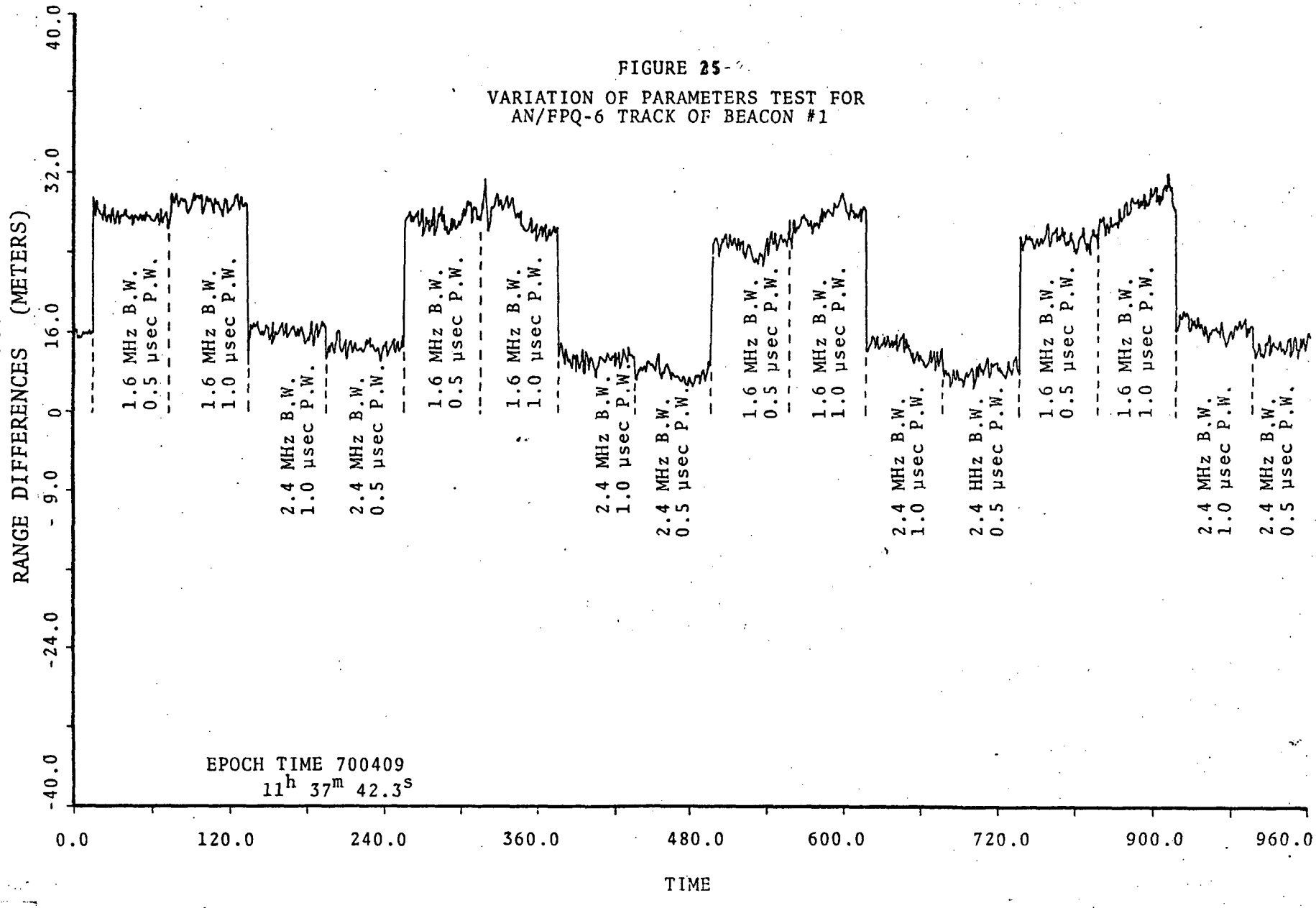

FIGURE 26
VARIATION OF PARAMETERS TEST
FOR AN/FPS-16 TRACK OF BEACON #1

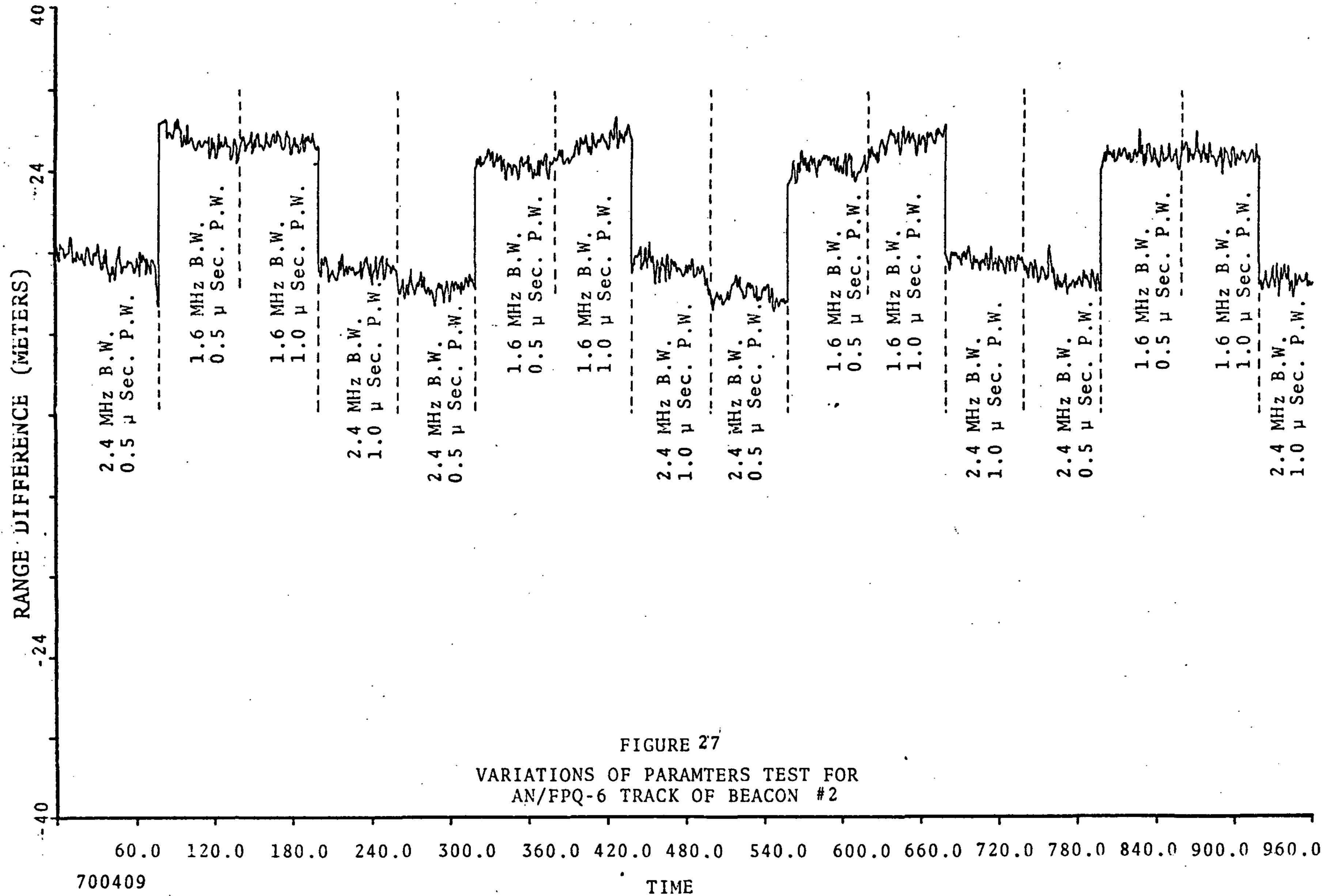

FIGURE 27

VARIATIONS OF PARAMTERS TEST FOR
AN/FPQ-6 TRACK OF BEACON #2

FIGURE 28
VARIATION OF PARAMETERS TEST FOR AN/FPS-16 TRACK OF BEAC

The AN/FPQ-6 data has been found to be very stable over quite a long time period. Results from parameter variation tests which were separated in time by over a year agree within a meter. This fact, plus the fact that bandwidth only dependent range changes were readily detectable, indicates that this type of test contains the necessary data for performing accurate mismatch error computations. A proper model which can correlate these range difference readings with mismatch error can certainly be developed once sufficient test data is available. The model preposed in Section 3.2.6 seems quite adequate for the AN/FPQ-6 radar/DIRAM combination. Unfortunately, existing Wallops Island AN/FPS-16 parameter variation test results do not agree with the expected mismatch errors as computed in Section 3. It is not presently known whether the inconsistencies between the AN/FPS-16 and AN/FPQ-6 data are due to design differences in the two types of radars or whether the proposed model is in error. Another possibility is that changes have occurred in the Wallops Island AN/FPS-16 radar since the WICE data were gathered. This latter possibility could, of course, be checked out by obtaining new simultaneous tracking data for the two Wallops radars and seeing if the recently computed mismatch corrections do indeed cause these new radar range residuals to agree.

The possibility of the mismatch model being applicable to only the FPQ-6/DIRAM combination can be evaluated once existing Bermuda parameter variations data is reduced. The Bermuda site contains both an AN/FPQ-6 radar which uses an ADRAN and an AN/FPS-16 with an ADRAN. Therefore, the data from this site should answer the design dependency question.

The final possibility, that the model is inadequate can be investigated by conducting a systematic test program where the range change is measured while the receiver bandwidth and received pulsewidth are varied in a prescribed fashion. Such a test could be performed using readily available boresight tower equipment.

In summary, it appears that the parameter variations test technique can provide the necessary data for computing accurate estimates of beacon track mismatch error. This has been proven for the Wallops Island AN/FPQ-6 radar but uncertainties still remain with respect to the Wallops Island AN/FPS-16 radar. Additional investigations into this technique should be carried out since it shows promise of providing easily computed mismatch corrections using only the radar itself as the test instrument.

5.0 GEOS RELATED DEVELOPMENT PROGRAMS

Based upon some of the early results of the GEOS-II C-Band systems project, several hardware oriented studies were performed which if the results are implemented should prove valuable on other NASA geodetic and earth sciences programs. Only the two independent efforts which were carried out solely by RCA are briefly discussed in this section.

Detailed discussions of the GEOS associated efforts which are summarized below can be found in Reference 23, (Laser/MIPIR Integration Study, Final Report) and 24 (Radar Enhancement Study, Final Report).

5.1 LASER/MIPIR INTEGRATION AND LOOP LASER TRACKER

It became apparent early in the GEOS C-Band project that the C-Band radars were providing range data with comparable quality to that obtained from the collocated NASA-GSFC Laser. In addition, it also became apparent that the AN/FPQ-6 radar was capable of providing accurate angular designation data which could be used to designate an open loop device such as the GSFC Laser mount in real time. Unfortunately, the advantages of direct radar designation (e.g.: longer tracks, elimination of cumbersome designation tapes and programs, etc.) could not be achieved during the collocation experiment due to the lack of suitable Radar/Laser interface hardware.

Once the ability of the radar to assist the Laser tracker became recognized, the concept of an integrated Laser/Radar system materialized.

As presently conceived, the integrated system consists of a Q-switched ruby Laser which is directly affixed to the elevation shaft of the AN/FPQ-6 radar. This Laser is identical in capabilities to that employed in the GSFC systems. The AN/FPQ-6 calibration optics which are also affixed to the same elevation shaft is being used (at least initially) as the receive optics for the Laser system. The detected Laser return signal is processed by means of a signal strength insensitive, tapped delay line detector and then transmitted through the pedestal slip-rings to the Laser Ranging System. This system which contains a dual (i.e. both time interval count and closed loop tracking) range measurement capability is located in the radar electronics area.

The ranging equipment being incorporated in the system has resulted from applying radar processing techniques to the Laser tracking problem. This system, conceived and designed by RCA M&SR Division in conjunction with the Radar Systems section of NASA Wallops Island, will provide both time interval count (TIC) or closed loop range tracking data with granularities of 0.1 nanosecond. Except for the extreme precision capabilities of the system, the TIC system's configuration is relatively straightforward. The novelty of the RCA approach lies in the use of type three range servo loop to accurately maintain a continuous measurement of the Laser derived range. This closed loop ranging system has several inherent advantages such as:

a) The continuous availability of range data permits an extremely narrow range gate to be generated (100 nanoseconds total width) and properly positioned in time for receipt of the Laser return.

b) The continuous availability of range data permits synchronous sampling of the Laser and radar range data.

c) The dynamic tracking loop contains a built-in memory which will enable track to be maintained on an orbiting target even though several Laser returns are missed.

d) Real time range data permits orbital computations to be made directly with the ranging data without the need for the auxiliary Laser firing time data which is normally needed for Q-switched Laser systems.

By interfacing the Laser range system with the radar's 4101 computer, the ranging data will become immediately available for either real time processing or for automatic recording on magnetic tape.

The technique of mounting the Laser directly onto the radar pedestal enables the radar to continuously position the Laser in angle throughout the radar track. This means that the existence of partially cloudy skies should not seriously impair the integrated systems ability to obtain accurate Laser data. The system can also be designated by computer control in cases where the radar cannot track.

Finally, the integrated Laser/Radar ranging system incorporates the capability of tracking either the Laser return of the radar video. This latter capabilitity means that, if desired, the system can become a "piggy-back" radar range tracker. In this mode of operation, either

simultaneous tracks of the same signal can be obtained by both systems or separate returns can be simultaneously tracked. A very useful application for the tracking of separate returns would be simultaneous tracking of skin and beacon radar returns. This technique would permit real time measurement of beacon delay errors.

In conclusion, the Wallops Island integrated Laser/ Radar system will combine the versatility and accuracy of a radar with the accuracy of a Laser. Thus, the advantages of each system will be available without the drawbacks associated with either individual system.

5.2 PASSIVE RADAR ENHANCEMENT DEVICES

The GEOS-II skin tracking data obtained by the C-Band radars was made possible by the inclusion of a passive Van Atta array as a part of the GEOS-II instrumentation. The ability of the C-Band radars to obtain skin tracking data was extremely important to the success of the program since it provided a method for proving the beacon track accuracies. The results obtained during skin tracks of the GEOS-II satellite show that a passive retroreflective device such as a Van Atta array can be a very reliable and useful method of enhancing the skin tracking capabilities of a radar.

The success of the GEOS-II Van Atta array led to a detailed investigation into the radar enhancement capabilities of these and similar passive retroreflective devices. This investigation which was conducted by RCA under the auspices of NASA-Wallops Island included studies of the achievable

cross section enhancement as a function of the device's size and weight. Various types of devices were investigated along with various configurations for each type of device. In addition to various shapes of Van Atta arrays, the study investigated square, circular, and triangular corner reflectors, and Luneberg lens approach.

As a result of this study effort, a spherical (3 dimensional) form of the Van Atta array was conceptually arrived at which would be light weight, collapsible for launch purposes, and relatively inexpensive to manufacture. The gain of the device would, of course, depend upon its physical size but the Van Atta array approach was found to be optimum from a gain versus size point of view.

Having established several feasible array configurations, the study next evaluated the potential uses of these devices. As a starting point, the physical size and shape of various satellites were reviewed. The satellites chosed are all scheduled for launch in the next several years. An estimate of each satellite's crossection was developed and, based upon its planned orbit, the skin tracking capabilities of the MIPIR radars were evaluated. Table 22 has been extracted from the final report[24] of this study. A review of the data presented in this table shows that most planned satellites would require some form of the radar tracking aid (active or passive) if radar tracking data is to be gathered. The use of a passive device such as a Van Atta array would, of course, be very attractive from a satellite power drain point of view.

The geodetic capabilities of C-Band radars have been established during the GEOS-II project. The inclusion of radar tracking aids aboard future NASA orbiting satellites

SATELLITE NAME, ALTITUDE, AND ENHANCER DIMENSIONS REQUIRED FOR ACQUISITION. EL = ELEVATION ANGLE; P_D = PROBABILITY OF LOCK-ON; "A" IS SIDE DIMENSION CIRCULAR CORNER REFLECTOR (CCR) OR RADIUS CIRCULAR VAN ATTA (CVA) IN FT.

SATELLITE	ALTITUDE OR APOGEE, NM	EL = 0°				EL = 10°				COMMENT*
		P_D = 0.5		P_D = 0.9		P_D = 0.5		P_D = 0.9		
		CCR "A" FT.	CVA FT.	CCR "A" FT.	CVA FT.	CCR "A" FT.	CVA. FT.	CCR "A" FT.	CVA. FT.	
ITOS B,C,D,E	790	2.3	1.1	4.0	1.3	1.0	<1	1.7	<1	ENHANCER REQUIRED
OSO-H	300	1.4	<1.0	2.3	<1.0	0.9	<1.0	1.5	<1.0	ENHANCER REQUIRED
ISIS-B	920	2.5	1.2	4.3	1.4	2.1	1.0	3.6	1.2	ENHANCER REQUIRED
GRS	1,705	3.7	1.8	6.3	2.1	3.2	1.5	5.5	1.8	ENHANCER REQUIRED
ESRO-1B	435	1.7	<1.0	2.9	1.0	1.2	<1.0	2.2	<1.0	RCS NOT AVAILABLE
RAE-B	3,240	5.3	2.6	9.0	3.1	5.0	2.3	8.5	2.7	ENHANCER REQUIRED
OFO-B	320	1.4	<1.0	2.3	<1.0	1.0	<1.0	1.7	<1.0	RCS NOT AVAILABLE
NIMBUS D, EIF	600	2.0	<1.0	3.4	<1.0	1.5	<1.0	2.6	<1.0	NO ESTIMATE OF RCS
AEROS	530	1.9	<1.0	3.3	<1.0	1.4	<1.0	2.4	<1.0	ENHANCER REQUIRED
OAO-B,C	395	1.8	<1.0	3.1	<1.0	1.1	<1.0	1.9	<1.0	NO ENHANCER REQUIRED ABOVE 10°
SOLARD C	300	1.4	<1.0	2.3	<1.0	0.9	<1.0	1.5	<1.0	ENHANCER REQUIRED
SAS A,B	300	1.4	1.0	2.3	1.0	0.9	1.0	1.5	1.0	ENHANCER REQUIRED
SSS-A	13,800	15.5	7.8	26.4	9.0	15	7.5	25	8.6	ENHANCER REQUIRED
NATO A,B	21,000	22.0	10.4	37.4	12.2	21.5	10.2	36.4	11.9	RCS NOT AVAILABLE
SKYNET B	21,000	22.0	10.4	37.4	12.2	21.5	10.2	36.4	11.9	RCS NOT AVAILABLE
INTEL SAT III- F-7	21,000	22.0	10.4	37.4	12.2	21.5	10.2	36.4	11.9	RCS NOT AVAILABLE

TABLE 22

SATELLITE CROSSECTION DATE

would introduce the possibility of obtaining very accurate orbit determination data with a minumum of support effort.

A second possible use for a passive radar enhancement device would be as separate space vehicles. A three dimensional array could be fabricated for use either as a separate satellite or as a part of an instrumented vehicle to which it could be tethered. The spherical passive array would offer a very inexpensive method of obtaining a geodetic vehicle which would require no gravity stabilization or active circuits. Once there are more C-Band radars equipped with doppler tracking capabilities, the existence of such a satellite would enable radar data to be obtained with a precision which is compatible with future NASA geodetic program requirements such as a possible continental drift experiment. C-Band doppler data combined with C-Band range data provides the geodetic community with a source of tracking data which is capable of meeting all presently planned mission tracking requirements. All that is needed is that a suitable satellite borne passive array or coherent C-Band transponder be included as a part of the future space vehicles.

6.0 SUMMARY AND RECOMMENDATIONS

This report has described in detail the radar oriented efforts which have been expended throughout the GEOS-II C-Band systems project. The following material provides not only a summary of these efforts but also lists recommendations for future efforts. The material in this section has been organized in the same sequence as in the previous sections of the report.

The pre-mission plans were found to be very adequate in all respects except one. In retrospect, it is obvious that the initial operating instructions should have been accompanied by a set of calibration instructions. This oversight was subsequently corrected and should be avoided on similar future projects.

The analysis which was performed to arrive at a single operating servo bandwidth also resulted in the recommendation that the existing AN/FPQ-6 real time data correction program be modified to make use of a more sophisticated from of error pattern calibration. This change, and an associated calibration change, are still recommended. This modification would make real-time correction of angle servo lag errors practical even under conditions of low tracking dynamics such as are encountered during satellite tracking missions. The ability to make accuracte lag corrections would in turn allow the use of lower angle servo bandwidths with the attendant improvement in thermal noise error.

An experiment should be conducted where the results of the angle error recovery efforts are used in real time to

minimize radar angle tracking errors. Such an experiment would require that several satellite tracks having varying geometries be carried out while making real time use of the recovered angle error coefficients. The result would prove useful in verifying the validity of the orbital calibration techniques.

Some of the data from the special tests has never been fully analyzed. This analysis should be completed. In particular, the tracking data from the plunge-normal tracking test should be analyzed to determine the accuracy with which this test can establish the radar's elevation droop error coefficient.

A technique for automatic pedestal mislevel error calibration and correction was suggested which, if implemented, would significantly reduce the effects of this angle error. This recommendation involves inserting the automatically digitized measurements of the leveling error sensor directly into the radar's computer. This automatic operation would make pre and post mission mislevel-calibration practical from a scheduling point of view. A mission by mission mislevel calibration capability would minimize the presently large pedestal mislevel errors.

The harmful effects of very high signal strengths during range calibrations should be investigated. Some method should be found for obtaining reasonably low reference target return signal strengths for use by radars which do not contain receive R.F. attenuators. One possible solution is a modified form ofthe Frequency Shift Reflectors presently in use at many of the radar sites.

The effects of beacon track mismatch range errors must be more fully investigated. These effects are felt to be the dominant source of beacon track range errors. It is recommended that the interrelated effects of pulsewidth and bandwidth changes be measured by means of a purely ground based experiment. The resulting data should then be used in conjunction with parameter variation tests to remove the effects of this beacon tracking error from all radars in any future multi-station network.

An automatic method of measuring the beacon delay error will shortly be available at Wallops Island. The inclusion of the laser ranging equipment will result in a radar having two independent range trackers. These instruments can provide simultaneous skin and beacon range tracking data. Since synchronous operation is possible, the simple subtraction of these two sets of range data would provide the desired beacon delay error.

The above mentioned possibility of obtaining simultaneous skin and beacon range data is but one of many potential uses for the new laser range tracker. As indicated above, the instrument is actually a general purpose range tracker which can also be used to obtain accurate range measurements when used with a Laser. The unique capability of obtaining simultaneous Radar-skin/Laser, Radar-beacon/Laser, Radar-skin/Radar-beacon, etc., tracks will make the Wallops Island AN/FPQ-6 an entirely new of instrument. The capabilities of this new and highly versatile instrument must be carefully and thoroughly investigated.

The C-Band doppler experiments which have been conducted to date have shown that the accuracy and precision of the C-Band range data are at least as good as the data which can be obtained from other presently available measurement systems. Thus, it is difficult to place limit upon just how "good" this data is. The usefulness of the range rate data is greatly enhanced by the availability of simultaneous radar range data. Efforts have been initiated during the GEOS project which investigated a straightforward integration of the range rate data into "doppler ranges". These efforts should be continued and expanded. The future availability of simultaneous Laser range data will provide Wallops Island with a new source of initializing range data for range rate integration purposes.

The proven ability of C-Band radars to provide accurate tracking data for orbital determination purposes should be applied to future near earth satellite programs. The inclusion of a simple radar retroreflective device aboard these satellites (e.g., a GEOS-II type of Van Atta array) would make the accuracy and versatility of the radar immediately available for use either as an orbit keeping measurement device, or as an active participant in the scientific experiment.

BIBLIOGRAPHY

1) Dempsey, D.J.; "Error Model for the Wallops Island AN/FPQ-6 Instrumentation Radar System"; Presented at the GEOS-IIC-Band Project Technical Conference Held at NASA/GSFC Greenbelt, Md.; June 1969.

2) "Pre-Processing of Wallops Station AN/FPQ-6 GEOS-II Data"; R.L. Brooks and J.R. Vetter; Wolf Research and Development Corp. Report for NASA Contracts NAS6-1467 and NAS6-1628; February 1970; NASA-CR-62076.

3) "AN/FPQ-6 Operation Procedures"; NASA Wallops Station; August 1969.

4) "AN/FPS-16 Operation Procedures"; NASA Wallops Station; January 1969.

5) "GEOS-B C-Band Range Operations Requirements"; Revision 2, 23 October 1968; NASA/WS HK-720(OR).

6) "Final Report, Measurements and Analysis of Performance of MIPIR," RCA Missile and Surface Radar Division Report for Department of the Navy, Bureau of Naval Weapons; December 1964; Contract NOw61-0428d.

7) Final Report Addendum, Measurements and Analysis of Performance of MIPIR"; RCA M&SR Division Report for Department of the Navy Bureau of Naval Weapons; March 1965; Contract NOw61-0428d.

8) "Analysis of Wallops Island AN/FPQ-6 Leveling Data"; D.J. Dempsey; RCA M&SR Report for WOLF R&D; May 1968.

9) "Antenna Pedestal Level-Tilt Error in Elevation and Azimuth for the AN/FPQ-6 Radar at Wallops Island, Virginia; W.E. Flood, RCA Service Company Report to NASA Wallops Island; April 1968.

10) Roy, N.A.; "Wallops FPQ-6 Mislevel Analysis"; Presented at GEOS-II C-Band Project Working Group Meeting, Held at the AF/ETR Patrick Air Force Base, Florida; 26 and 27 June 1968.

11) Wells, W.T. and Martin, C.F.; "Comments on AN/FPQ-6 Pedestal Mislevel Errors"; Presented at GEOS-II C-Band Project Technical Conference, Held at the AF/WTR Vandenberg Air Force Base, California; 19 and 20 August 1968.

12) GEOS-B Engineering Services Program Monthly Activity Report No. 13; RCA M&SR Division for WOLF R&D Corp.; May 1970.

13) Beckett, W.H. and Dempsey, D.J.; "Investigation of Dynamic Lag Error Upon the AN/FPQ-6 Radar's GEOS-B Azimuth Track Data," Presented to GEOS-II C-Band Project Technical Conference, Held at NASA/GSFC Greenbelt, Md., June 1969.

14) "Evaluation of the AN/FPQ-6 Radar Angle Lag Error Calibration as Carried Out for the GEOS-B C-Band Radar Experiment"; D.J. Dempsey; RCA M&SR Division Report, Prepared for WOLF R&D Corp.; August 1968.

15) "Error Sensitivity Function Catalog"; C.F. Martin and J.R. Vetter; WOLF R&D Corp. Report, Prepared for NASA Wallops Station; March 1970; Contract NAS6-1467; NASA CR-1511.

16) "Recovery of Azimuth Secant Bias for the Wallops AN/FPQ-6 Radar"; R.L. Brooks; WOLF R&D Report, prepared for NASA Wallops Station; April 1969; Contract NAS6-1628.

17) R.L. Brooks and H.R. Stanley; "Global C-Band Radar Network Calibration Utilizing GEOS-II Satellite," Presented at GEOS-II Review Conference, NASA/GSFC, Greenbelt, Md.; June 1970.

18) "Calibration and Evaluation of the Wallops AN/FPQ-6 Radar Utilizing the GEOS-II Satellite, A Status Report"; Prepared by the GEOS-B C-Band System Project Group; August 1968; NASA X-16-68-1.

19) Dempsey, D.J.; "Calibration of Instrumentation Radars to Obtain Accurate Real-Time Tracking Data"; Presented at AIAA Guidance, Control, and Flight Mechanics Conference; Princeton, N.J., August 1969; AIAA Paper No. 69-872.

20) Berbert, J.H. and Parker, H.C.; "Comparison of C-Band, Secor, and TRANET with a Collocated Laser on 19 Tracks of GEOS-II; Presented at GEOS-II C-Band Project Meeting Held at AF-WTR Vandenberg Air Force Base, California; November 1968.

21) Mitchell, R.D., Wells, W.T., and McGoogan, J.T.,; "Some Remarks on the FPQ-6 Pulse Doppler System"; Presented at GEOS-II C-Band Project Technical Conference; Held at AF-WTR Vandenberg AFB, California; November 1968.

22) McGoogan, J.T., Mitchell, R.D., and Wells, W.T.; "Further Results on Coherent Signal Processor Range Measurements"; presented at GEOS-II C-Band Project Technical Conference Held at NASA GSFC, Greenblet, Md.; June 1969.

23) "Final Report on the LASER/MIPIR Integration Study Program"; RCA M&SR Division Report for NASA Wallops Island Station; July 1969; NAS6-1625.

24) "Passive Radar Enhancement Devices; Final Report"; RCA M&SR Division Report for NASA Wallops Station; June 1970; NAS6-1788.

25) Leitao, C.D. and Brooks, R.L.; "C-Band Radar Range Measurements, An Assessment of Accuracy"; Presented at International Symposium on Electromagnetic Distance Measurement and Atmospheric Refraction; Boulder, Colorado; June 1969.

APPENDIX A

SPECIAL RADAR TEST PROCEDURES

1.0 TRANSPONDER SWITCHING TEST/TEST A

1.1 TEST OBJECTIVE

To obtain measurements on the relative effects of the two transponders upon the C-Band tracking data.

1.2 TEST PROCEDURE

1) Standard (for skin/beacon mission) GEOS-II Pre and Post Mission calibrations should be performed.

2) Acquire and beacon track the GEOS-II satellite with both radars.

3) Upon receipt of a sufficiently strong echo return, transfer the AN/FPQ-6 into the skin-track mode.

4) Approximately 30 seconds after track mode transfer has occurred, the GEOS-II telemetry control site should be requested to turn-off the beacon which was tracked in 3). In addition, the telemetry should activate (place into stand-by) the alternate beacon.

5) The AN/FPQ-6 and AN/FPS-16 shall continue to transmit their beacon interrogation code throughout the skin-track portion of the mission. (The AN/FPS-16 should be designated by the AN/FPQ-6 during the beacon down time.) Approximately 42 seconds after activation, the alternate beacon will begin to respond to these interrogations. The AN/FPS-16 should acquire this beacon signal as soon as possible.

The AN/FPQ-6 should, if possible, temporarily remain in the skin track mode. After obtaining 15 to 30 seconds of overlapping (FPS-16 beacon and FPQ-6 skin) tracking data, the AN/FPQ-6 should be switched to the beacon track mode.

6) Both radars should continue to beacon track the satellite throughout the remainder of the mission.

2.0 POLARIZATION TEST/TEST B1 AND B2

2.1 TEST OBJECTIVE

Evaluate the dependency of the AN/FPQ-6 GEOS-II tracking data upon the polarization of the transmit/receive signal.

2.2 TEST PROCEDURE

1) Normal GEOS-II Pre- and Post-Mission Calibrations should be carried out. In addition to the standard checks, it will be necessary that a receiver gain calibration be carried out. The results of this test should be printed out on the flexowriter for later use. The radar's analog recorder should also be calibrated.

2) The radar should be set up in a manner which in consistent with past GEOS-II skin/beacon tracks.

3) After acquisition of the satellite by both radars and prior to the start of skin-track, the polarization of the AN/FPQ-6 should be switched back-and-forth between linear vertical and circular polarization (tracking data should be obtained which spans 30 sec to 60 sec in each polarization during each switchover). The AN/FPS-16 radar should carry out a standard GEOS-II beacon track with no variations made to its normal tracking procedures.

4) As PCA is approached, the radar should be placed into the linear polarization mode and no further

polarization switching should be carried out until after the radar has been transferred over to the skin-track mode.

5) Step 3 shall be repeated while the radar is skin-tracking the satellite.

6) When the echo return signal strength becomes low, the radar should be switched back to beacon track mode and step 3 should be repeated until the culmination of the mission.

3.0 ANGLE CALIBRATION TRACKING TESTS/TEST C

3.1 TEST OBJECTIVE

To obtain tracking data which may help to identify the source of the large azimuth residual errors whcih have appeared in the short arc solutions for high elevation passes.

3.2 TEST PROCEDURE

1) Pre-and Post-Mission Tests - The basic intent of this test is to eliminate pedestal mislevel as a potential cause of the azimuth residual errors. This will be accomplished by performing a pre and a post mission pedestal mislevel calibration. The availability of these calibration data will permit the real-time pedestal mislevel error to be estimated and eliminated during post-mission data reduction. It is desirable that the leveling calibration be performed as near the track times as possible. Also, it is not necessary that the leveling data be immediately analyzed for new K_2 and K_3 error coefficients. Instead, the level error coefficients presently in the 4101 computer can be left in the system. The resulting real-time level correction will be removed from the track data during the data reduction process and a new correction will be computed and applied based upon the pre- and post-mission calibration data.

   A receiver gain/error pattern calibration for lag angle correction should also be performed sometime

prior to the angle calibration mission. The resulting data should be printed out on the flexowriter and submitted as a part of the mission data package. The calibration data should be manually scanned to ensure that the calibration was properly performed. Finally, range bias and normal-plunge calibrations must be performed on a pre- and post-mission basis.

2) Tracking Mission - A fairly high (>70°) elevation GEOS pass should be chosen for this test. The radar should be set-up as for a standard GEOS-II beacon tracking mission. The tracking data should cover as large a portion of the pass as is possible (i.e.: constant track between 10° elevation points, if possible). No unusual operating procedures are required and the normal GEOS-II data package plus the leveling, lag angle, and normal-plunge calibration data are all that is necessary.

4.0 LAG ANGLE ERROR CORRECTION TEST (TEST D)

4.1 TEST OBJECTIVES

This test is divided into two main sections:

The first section requires only the change of angle servo bandwidth switch settings for a high elevation pass. This test will serve two functions as follows:

1) Servo bandwidth #4 will be used which, for a high elevation GEOS track, should introduce noticable dynamic lag errors into the data if corrections are not applied. It is proposed that this data be reduced initially (short arc solution) without applying lag corrections. Having performed this reduction, the lag corrections should be applied and a second short arc reduction should be performed. A comparison of the range residuals from these two reductions should help to resolve the question of whether or not large angle residual errors can noticeably affect the calculated short-arc orbit.

2) A short-arc solution should be carried out using simultaneous tracking data obtained by the AN/FPS-16 radar. The AN/FPQ-6 residual angle errors should be computed and plotted based upon this independent orbit for both cases of corrected and uncorrected (lag error) AN/FPQ-6 data. The results of this reduction when coupled with the

results of 1) should provide at least a crude measure of the lag error correction capabilities of the AN/FPQ-6 radar.

The second section of the test will require that the existing 4101 software programming (error pattern calibration program) be modified so as to compute the linear fit coefficients over a reduced offset angle range about the boresight null ($\pm$1.0 MIL). In addition, the automatic offset steps built into the program should be changed so that the same number of calibration points are obtained over the reduced offset range.

Having accomplished these changes, a new set of receiver gain and error pattern calibrations should be performed followed by a tracking mission which is performed in a similar manner to that described above. Similar data reductions should also be carried out. It is hoped that the results of this test will demonstrate that the reduced calibration range has resulted in more accurate lag angle corrections. (It may also be desirable to perform a third track using standard GEOS-II servo bandwidths and with the more precise lag error corrections being applied to the data.

4.2 TEST PROCEDURES

The above discussion is felt to be quite explanatory and no repeat discussion will be given here. The test requirements are as follows:

1) Pre Soft-Ware Change Test:

   a) Perform a receiver gain and error pattern calibration together with other standard GEOS-II pre mission calibrations.

b) Perform a high elevation beacon track of the GEOS-II satellite with the angle servo bandwiths both set to switch position #4.

c) Perform the standard GEOS-II mission calibrations.

2) Post Soft-Ware Change Test:

Repeat a) after 4101 calibration program changes have been carried out.

5.0 NORMAL-PLUNGE TRACK (TEST E)

5.1 PURPOSE OF TEST

This test will attempt to directly utilize the GEOS satellite as a calibration aid to obtain measurements of the elevation bias and the droop error coefficient for the AN/FPQ-6 radar.

5.2 TEST PROCEDURE

5.2.1 General

This test will require simultaneous tracks of the GEOS-II satellite by both the Wallops Island AN/FPS-16 and AN/FPQ-6 radars. The AN/FPS-16 radar will perform a standard GEOS-II beacon track and its tracking data will be recorded and also utilized in real-time to provide designation data to the AN/FPQ-6 radar. The AN/FPQ-6 radar will also perform a beacon track on the GEOS satellite but will periodically switch between normal track mode and plunge track mode. The AN/FPQ-6 track should cover as wide a range of elevation angles as possible. Therefore, it is necessary that initial lock on occur at a low elevation angle and that a GEOS-II pass be chosen which has a high elevation angle at PCA ($70° \leq E \leq 84°$). The switching over between track modes (plunge & normal) should be performed as often as is possible.

5.2.2 Detailed Test Description

5.2.2.1 Pre-Mission Tests/Set-Up Procedures

a) Perform standard GEOS-II pre mission calibrations including a plunge-normal boresight tower calibration.

b) Repeat the standard plunge-normal test with the value of the droop error coefficient (K_o) in the 4101 computer set to zero.

c) Leave the droop error coefficients set at zero for the remainder of this test.

5.2.2.2 Tracking Test

Perform a beacon track of the GEOS satellite as discussed in Paragraph 5.2.1 above.

5.2.2.3 Post Mission Tests

a) Perform a plunge-normal boresight tower calibration with the value of the droop error coefficient remaining at zero.

b) Insert the previously used number for the droop error coefficient into the 4101 computer and repeat the plunge-normal calibration.

6.0 PARAMETERS VARIATION (TEST E)

6.1 OBJECT

The object of this procedure is to obtain both calibration and track data which describes the effects of varying the radar's operating parameters. It should be noted that even partial response to this procedure is of some use. For example, calibration data without track data would be useful as would pre-mission calibration and track data without post-mission calibration data. Complete response is, of course, desired.

6.2 PROCEDURE

a) Record surveyed range to range target and describe the object being used as a reference target.

b) Describe, in writing the radar set up procedure used during range zero-set for normal GEOS-II tracking missions (e.g. "The radar was set to read surveyed range in skin gate with 0.5 μsec P.W., 2.4 MHz BW, and 160 PRF; next, the beacon coder was turned on with proper coding and the beacon delay was adjusted to the proper value with all operating parameters remaining as described above.")

c) Perform the pre-mission calibration test steps as called for in Table 1(A) or 2(A) as applicable. Note, manually record the time at which the various calibration tests were started/stopped and include this record in mission data package. A manual recording of range readout (100 sample average) would also be desirable if automatic data handling capabilities are available for use.

d) Perform the track test steps as called for in Table 1(B) or 2(B) as applicalbe. The times of transfer between steps of the procedure should be noted and the data should be allowed to stabilize for at least 1/2 minute before proceeding to the next step.

e) Repeat the range calibration tests of Table 1 (A) or 2 (A) as a part of the post-mission test procedures.

TABLE 1
AN/FPS-16 TEST FOR EACH TRANSPONDER

TABLE 1(A)
PRE AND POST MISSION CALIBRATION TESTS

Test #	Gate	PRF	Receiver Bandwidth	Pulse Width
1	Skin	160	Wide	0.5 usec.
2	Skin	160	Wide	1.0 usec.
3	Skin	160	Narrow	1.0 usec.
4	Skin	160	Narrow	0.5 usec.
5	Beacon*	160	Narrow	0.5 usec.
6	Beacon*	160	Narrow	1.0 usec.
7	Beacon*	160	Wide	1.0 usec.
8	Beacon*	160	Wide	0.5 usec.

*NOTE: Beacon track calibrations should be performed with the beacon code generator turned on and set up in the same fashion as will be used to interrogate the GEOS transponder during track.

TABLE 1(B) TRACK TESTS

Track Test #	Gate	PRF	Receiver Bandwidth	Pulse Width
1	Beacon	160	Wide	0.5 usec.
2	Beacon	160	Narrow	0.5 usec.
3	Beacon	160	Narrow	1.0 usec.
4	Beacon	160	Wide	1.0 usec.
5	Beacon	160	Wide	0.5 usec.

Repeat above until end of track.

TABLE 2
AN/FPQ-6 TEST FOR EACH TRANSPONDER

TABLE 2(A)
PRE AND POST MISSION CALIBRATION TESTS

Test #	Gate	PRF	Receiver Bandwidth	Pulse Width
1	Skin	160	2.4 MHz	0.5 usec.
2	Skin	640	2.4 MHz	0.5 usec.
3	Skin	640	2.4 MHz	1.0 usec.
4	Skin	640	1.6 MHz	1.0 usec.
5	Skin	640	1.6 MHz	2.4 usec.
6	Skin	640	0.6 MHz	2.4 usec.
7	Skin	160	0.6 MHz	2.4 usec.
8	Skin	160	2.4 MHz	0.5 usec.
9	Beacon	160	2.4 MHz	0.5 usec.
10	Beacon	160	2.4 MHz	1.0 usec.
11	Beacon	160	1.6 MHz	1.0 usec.
12	Beacon	160	1.6 MHz	0.5 usec.
13	Beacon	160	2.4 MHz	0.5 usec.

NOTE: Only tests 8 through 13 need be carried out on those radars which track GEOS only in the beacon track mode.

TABLE 2(B) AN/FPQ-6 TRACK TESTS

Test #	Gate	PRF	Receiver Bandwidth	Pulse Width
1	Beacon	160	2.4 MHz	0.5 usec.
2	Beacon	160	1.6 MHz	0.5 usec.
3	Beacon	160	1.6 MHz	1.0 usec.
4	Beacon	160	2.4 MHz	1.0 usec.
5	Beacon	160	2.4 MHz	0.5 usec.
	Repeat until satellite range permits switchover to skin track at which time track should be switched to skin gate.			
*6	Skin	640	0.6 MHz	2.4 usec.
7	Skin	160	0.6 MHz	2.4 usec.
8	Skin	640	0.6 MHz	2.4 usec.
	Repeat until signal strength requires return to beacon track mode and repeat steps 1 through 5.			

*NOTE: It is recognized that immediate transfer from step 5 to step 6 cannot be carried out. Intermediate steps as may be required are permitted.